REMARKS

Status of the Claims

Claims 1, 2, 5 and 9-11 are currently pending in the application. Claims 1, 2, 4, 5 and 8-11 stand rejected. Claims 1 has been amended. Claims 4 and 8 have been cancelled. All amendments and cancellations are made without prejudice or disclaimer. No new matter has been added by way of the present amendments. Specifically, the amendment to claim 1 is to remove the compound of formula (9), i.e. [Ka 9], from the claim. Reconsideration is respectfully requested.

Rejections Under 35 U.S.C. § 112, First Paragraph

Written Description

Claims 4 and 8-11 stand rejected under 35 U.S.C. § 112, first paragraph, for failing to comply with the written description requirement. (*See*, Office Action of April 1, 2008, at pages 2-3, hereinafter, "Office Action"). Claims 4 and 8 have been cancelled, thereby obviating the rejection of these claims. Applicants traverse the rejection as to the remaining claims.

The Examiner states that new claim 9 is not supported by paragraph [0032] and claims 10 and 11 are not supported by paragraph [0042], as stated in the previous amendment.

In the Amendment of December 20, 2007, we referred to paragraphs [0032] and [0042] for support of new claims 8-11. However, these paragraphs refer to the published specification, not the as-filed specification. The paragraphs in the as-filed specification are [0026], [0032]-[0034] and [0042]. Therefore, Applicants believe that the new claims 9-11 are fully supported by the as-filed specification at least at paragraphs [0026], [0032]-[0034] and [0042].

Reconsideration and withdrawal of the written description rejection of claims 9-11 are respectfully requested.

Enablement

Claims 4 and 8-11 stand rejected under 35 U.S.C. § 112, first paragraph, for failing to comply with the enablement requirement. (*See*, Office Action, at pages 3-8). Claims 4 and 8 have been cancelled, thereby obviating the rejection of these claims. Applicants traverse the rejection as to the remaining claims.

The Examiner states that there is no "known prior art that broadly teaches applicability of the compounds for treating all the recited diseases and inhibition of aldose reductase." The Examiner also states that to perform the method (presumably of claim 10) would require that in every instance the gene for aldose reductase be sequenced and after patients are treated, assays be performed on each to determine if treatment is successful. Furthermore, the Examiner states that due to unpredictability in the art, one of skill in the art could not determine which prodrug encompassed by the claims might be effective and possess the required activity and which prodrug would be ineffective. The Examiner further states that the claims encompass treatment of all forms of cancer and all forms of infection. The Examiner states that Applicants have not provided sufficient disclosure to enable one of skill in the art to practice the claimed invention. Finally, the Examiner alleges that the diseases disclosed in the specification at pages 12-13 as being directly linked to aldose reductase activity are unsupported. That is, the Examiner alleges that there is no proof or scientific evidence linking these diseases to aldose reductase activity.

However, the present claims are not directed to nucleic acid or amino acid sequences of aldose reductase or determining the sequence of aldose reductase. Although such determinations would certainly be routine in the art, the present claims do not encompass these steps and there is no need to perform them to carry out the claimed method. Normal and abnormal levels of the enzyme gene or protein need not be determined because Applicants have clearly shown that their compounds inhibit the activity of the enzyme.

Furthermore, determination of an effective dose of the claimed chemicals is within the capabilities of one of skill in the art, since such determinations typically require only routine experimentation. Applicants have also shown in Examples 10 and 11 that the claimed compounds have the activity claimed. Formulations and dosages for the claimed compositions are provided at paragraphs [0042] to [0045] of the specification.

Applicants wish to clarify for the Examiner that although the therapeutic effects of the compounds of the presently claimed invention may in one embodiment be exhibited by aldose reductase enhancement, which is caused by an induction of mutation(s) into the aldose reductase gene, there are additional activities of the claimed compounds, such as direct binding and inhibition of the aldose reductase enzyme.

Regarding the diabetic complications which are among the diseases recited in claim 10 (such as cataracts, peripheral nerve disease, nephritic disease, infections caused by lowering of phagocytotic action of leukocytes, diabetic coma and arteriosclerosis caused by atheromatous degeneration in the great vessel wall), the method of treatment of the presently claimed invention is based on the finding that the presently claimed compounds inhibit aldose reductase enzyme activity. Thus, the action of the presently claimed compounds does not relate to enhancement of

the expression of the aldose reductase enzyme or mutation of the aldose reductase gene. (*See*, for example, the specification at least at paragraph [0035]). The inhibitory action for aldose reductase by the compound of claim 1 is disclosed in the specification at, for instance, Example 10.

The Examiner believes that the biochemical or physiological relationship between aldose reductase enzyme activity, and the diseases to be treated by the method of claim 10, are not disclosed by the present specification. However, it was well known to a person of skill in the art on the effective filing date of the present application that inhibition of aldose reductase enzyme is effective for treating diabetic complications.

Furthermore, the biochemical mechanism of aldose reductase inhibition as it relates to diabetic complications was well-known as of the effective filing date of the present application. As evidence of the level of knowledge of one of skill in the art at the time the present application was filed, Applicants attach hereto a copy of Yabe-Nishimura, *Pharmacol. Rev.*, 1998, 50(1):21-33 as Exhibit A. Yabe-Nishimura discloses, for example, at page 22, the left column, lines 3-6, that aldose reductase inhibitors were developed as possible therapeutic agents for diabetic complications. Accordingly, one of ordinary skill in the art at the time the present application was filed knew that compounds which inhibit aldose reductase enzyme activity were effective for treating diabetic complications.

Further, the Examiner asserts that claim 10, encompassing the treatment of all categories of cancers and all inflammatory responses, is not enabled by the present specification. However, the presently claimed invention, encompassing the treatment of cancerous diseases and inflammatory responses, is accomplished by administering the compound of claim 1 which

suppresses NO production. (*See*, for instance, the present specification at paragraph [0033] and Example 11). Example 11 of the present specification shows that the compounds of claim 1 suppress NO production.

Suppression of NO production results in the suppression of vascularization of tissue, which thereby inhibits production of cancerous cells and metastasis of cancer. This therapeutic effect on cancer, caused by suppression of vascularization, is not limited to any specific cancer and is applicable to all cancers in general.

As proof of the knowledge of one of skill in the art at the time the present application was filed, Applicants attach hereto as Exhibit B a publication disclosing the biochemical mechanism which directly links suppression of NO production to inhibition of cancer growth. (*See*, Gallo et al., *J. Natl. Cancer Inst.*, 1998, 90(8):587-96, a copy of which is attached hereto as Exhibit B). Gallo et al. disclose, for example, at page 592, the left column, line 9 to line 4 from the bottom, that inhibition of NO synthase causes inhibition of angiogenesis in all implanted tumor samples.

Furthermore, one of ordinary skill in the art, at the time the present application was filed, knew that NO levels are directly linked to general inflammatory diseases. Thus, the method of treatment of the presently claimed invention is clearly enabled for application in general to inflammatory diseases. That is, it was well known to a person of skill in the art that suppression of NO production is effective for treating inflammatory diseases. This is evidenced by the disclosure of Salvemini et al., *Br. J. Pharmacol.*, 1996, 118(4):829-38, a copy of which is attached hereto as Exhibit C. Salvemini et al. disclose, for example, at page 837, right column, lines 19-22, that NO synthase inhibitors exert anti-inflammatory effects. Additionally, Salvemini

et al., at page 836, Figure 9, disclose the mechanism(s) of action of NO on the inflammatory response.

Thus, as evidenced by the cited disclosures, Exhibits A-C, one of skill in the art knew of the underlying biochemical mechanisms of the various diseases such as diabetes complications, cancer, and inflammation. Applicants believe that all of the subject matter encompassed by claims 9-11 are fully enabled by the present specification, i.e. at least Examples 10 and 11, and the knowledge of one of skill in the art.

The Examiner is respectfully reminded that, "As long as the specification discloses at least one method for making and using the claimed invention that bears a reasonable correlation to the entire scope of the claim, then the enablement requirement of 35 U.S.C. 112 is satisfied." (*See, In re Fisher*, 427 F.2d 833, 839, 166 U.S.P.Q. 18, 24 (CCPA 1970)). Furthermore, Applicants point out that a "patent need not teach, and preferably omits, what is well known in the art." (*See, Spectra-Physics, Inc. v. Coherent, Inc.*, 827 F.2d 1524, 1534 (Fed. Cir. 1987)).

Reconsideration and withdrawal of the enablement rejection of claims 9-11 are respectfully requested.

Rejections Under 35 U.S.C. § 112, Second Paragraph

Claims 4, 8 and 9 stand rejected under 35 U.S.C. § 112, second paragraph, for failing to particularly point out and distinctly claim the subject matter which Applicants regard as the invention. (*See*, Office Action, at page 8). Claims 4 and 8 have been cancelled, thereby obviating the rejection of claims 4 and 8. Applicants traverse the rejection as to claim 9.

The Examiner states that the term "hydrolyzable prodrug" is indefinite in claims 8 and 9. However, claim 9 does not recite the term "hydrolyzable prodrug." Claim 9 recites, in part, "hydrolyzable glycoside, or a salt thereof." Applicants believe this term is sufficiently clear to one of skill in the art. That is, one of skill in the art knows what hydrolyzable means and knows what the term glycoside encompasses. Glycosides are a very well known and well characterized group of chemical compounds.

Reconsideration and withdrawal of the indefiniteness rejection of claim 9 are respectfully requested.

Rejections Under 35 U.S.C. § 102(a)

Enoki et al., WO 2004/096198

Claims 1, 2, 4, 5, 10 and 11 stand rejected under 35 U.S.C. § 102(a) as being anticipated by Enoki et al., WO 2004/096198, hereinafter referred to as "Enoki et al." (*See*, Office Action, at page 9). Claim 4 has been cancelled, thereby obviating the rejection of claim 4. Applicants traverse the rejection as to the remaining claims.

The Examiner states that compound "Ka9" disclosed in Enoki et al. anticipates the presently claimed compounds.

Although Applicants do not agree that the claims are anticipated by the disclosure of Enoki et al., to expedite prosecution, claim 1 has been amended to remove the compound of formula (9), i.e. [Ka 9]. Therefore, since Enoki et al. does not disclose all of the limitations of the presently claimed invention, Applicants believe the Enoki et al. cannot anticipate the presently claimed invention. Anticipation requires that "each and every element as set forth in

the claim is found, either expressly or inherently described, in a single prior art reference." (*See*, *In re Robertson*, 169 F.3d 743, 745, 49 U.S.P.Q.2d 1949 (Fed. Cir. 1990), quoting *Verdegaal Bros., Inc. v. Union Oil Co.*, 814 F.2d 628, 631, 2 U.S.P.Q.2d 1051, 1053 (Fed. Cir. 1987)).

Dependent claims 2, 5, 10 and 11 are not anticipated as, *inter alia*, depending from a non-anticipated base claim, amended claim 1.

Reconsideration and withdrawal of the anticipation rejection of claims 1, 2, 5, 10 and 11 are respectfully requested.

JP 64-13019

Claims 1, 2, 4, 5 and 8-11 stand rejected under 35 U.S.C. § 102(a) as being anticipated by JP 64-13019, published in 1989. (*See*, Office Action, at page 9). Claims 4 and 8 have been cancelled, thereby obviating the rejection of these claims. Applicants traverse the rejection as to the remaining claims.

The Examiner comments that the rejection is based on the International Search Report (ISR) which states that the reference is a novelty-destroying reference.

Applicants attach hereto as Exhibit D a copy of the International Preliminary Report on Patentability (IPER) corresponding to International Patent Application No. PCT/JP2004/017887, to which the present application claims priority. As shown therein, JP 64-13019 is cited because the compound Ka 9 is disclosed.

Although Applicants do not agree that the claims are anticipated by the disclosure of JP 64-13019, to expedite prosecution, claim 1 has been amended to remove the compound of formula (9), i.e. [Ka 9]. Therefore, since JP 64-13019 does not disclose all of the limitations of

the presently claimed invention, Applicants believe the JP 64-13019 cannot anticipate the presently claimed invention. (*See*, *In re Robertson*, 169 F.3d at 745).

Dependent claims 2, 5 and 9-11 are not anticipated as, *inter alia*, depending from a non-anticipated base claim, amended claim 1.

Reconsideration and withdrawal of the anticipation rejection of claims 1, 2, 5 and 9-11 are respectfully requested.

Rejections Under 35 U.S.C. § 102(b)

Claims 8-11 stand rejected under 35 U.S.C. § 102(b) as being anticipated by Ohnogi et al., WO 2001/54682, hereinafter referred to as "Ohnogi et al." (*See*, Office Action, at page 9). Claim 8 has been cancelled, thereby obviating the rejection of claim 8. Applicants traverse the rejection as to the remaining claims.

Applicants note that independent claim 1 is not rejected as being anticipated by the disclosure of Ohnogi et al. Therefore, dependent claims 9-11 cannot be anticipated by Ohnogi et al. because, *inter alia*, they depend from a non-anticipated base claim, claim 1. Applicants further note that compounds 26 and 27 of Ohnogi et al. do not correspond in structure to any of the compounds recited in claim 1. Furthermore, compounds 26 and 27 of Ohnogi et al., even if considered to be a glycosidic hydrolyzable prodrug, still do not correspond in any way to any of the compounds recited in claim 1. That is, the base compounds disclosed in Ohnogi et al. must disclose every atom and bond recited in the presently claimed compounds to be anticipatory. Since the Ohnogi et al. compounds fail this test, the Ohnogi et al. compounds cannot anticipate the presently claimed invention.

Therefore, reconsideration and withdrawal of the anticipation rejection of claims 9-11 are respectfully requested.

CONCLUSION

If the Examiner has any questions or comments, please contact Thomas J. Siepmann, Ph.D., Registration No 57,374, at the offices of Birch, Stewart, Kolasch & Birch, LLP.

If necessary, the Commissioner is hereby authorized in this, concurrent, and future replies, to charge payment or credit any overpayment to our Deposit Account No. 02-2448 for any additional fees required under 37 C.F.R. § 1.16 or under § 1.17; particularly, extension of time fees.

Dated: July 1, 2008

Respectfully submitted,

By _____

Marc S. Weiner
Registration No.: 32,181
BIRCH, STEWART, KOLASCH & BIRCH, LLP
8110 Gatehouse Road
Suite 100 East
P.O. Box 747
Falls Church, Virginia 22040-0747
(703) 205-8000
Attorney for Applicants

Attachments: Exhibit A - Copy of Yabe-Nishimura, *Pharmacol. Rev.*, 1998, 50(1):21-33;
Exhibit B – Copy of Gallo et al., *J. Natl. Cancer Inst.*, 1998, 90(8):587-96;
Exhibit C – Copy of Salvemini et al., *Br. J. Pharmacol.*, 1996, 118(4):829-38;
Exhibit D – Copy of the IPER issued in PCT/JP2004/017887

EXHIBIT A

0031-6997/98/5001-0021$03.00/0
PHARMACOLOGICAL REVIEWS
Vol. 50, No. 1
Printed in U.S.A.

Aldose Reductase in Glucose Toxicity: A Potential Target for the Prevention of Diabetic Complications

CHIHIRO YABE-NISHIMURA[a]

Department of Pharmacology, Kyoto Prefectural University of Medicine, Kyoto, Japan

I. Introduction

Recent data obtained from the Diabetes Control and Complications Trial clearly indicate that intensive insulin treatment effectively delays the onset and slows the progression of longterm diabetic complications in patients with insulin-dependent diabetes mellitus (IDDM)[b] (Diabetes Control and Complications Trial Research Group, 1993). Nevertheless, even with the best clinical management available at present, it is practically impossible to maintain normoglycemia at all times throughout the life of diabetic individuals. Accordingly, chemical agents that effectively halt the hyperglycemic injury in diabetic patients would be of great clinical importance.

[a] Address for correspondence: Chihiro Yabe-Nishimura, Department of Pharmacology, Kyoto Prefectural University of Medicine, Kawaramachi-Hirokoji, Kamikyoku, Kyoto 602, Japan.

[b] Abbreviations: cDNA, complementary deoxyribonucleic acid; DAG, diacylglycerol; FR-1, fibroblast-growth-factor-1-regulated protein; HbA_{1c}, glycosylated hemoglobin; IDDM, insulin-dependent diabetes mellitus; mRNA, messenger ribonucleic acid; MVDP, mouse vas deferens protein; NAD^+, nicotinamide adenine dinucleotide; NADPH, reduced nicotinamide adenine dinucleotide phosphate; NIDDM, non-insulin-dependent diabetes mellitus; NO, nitric oxide.

Under normoglycemia, most of the cellular glucose is phosphorylated into glucose 6-phosphate by hexokinase. A minor part of nonphosphorylated glucose enters the so-called polyol pathway, the alternate route of glucose metabolism. The rate-limiting step of this polyol pathway is the reduction of glucose to sorbitol catalyzed by aldose reductase (EC 1.1.1.21). Sorbitol is subsequently converted to fructose by sorbitol dehydrogenase, thus constituting the polyol (sorbitol) pathway (fig. 1). Under hyperglycemia, because of the saturation of hexokinase with ambient glucose, the increased flux of glucose through the polyol pathway accounts for as much as one-third of the total glucose turnover (González et al., 1984). This leads to overflow of the products of the polyol pathway along with depletion in reduced nicotinamide adenine dinucleotide phosphate (NADPH) and the oxidized form of nicotinamide adenine dinucleotide (NAD^+), the cofactors used in the pathway. The acceleration of the polyol pathway thus elicits various metabolic imbalances in those tissues that undergo insulin-independent uptake of glucose. Such metabolic perturbation provokes the early tissue damage in the "target" organs of diabetic complications, such as ocular

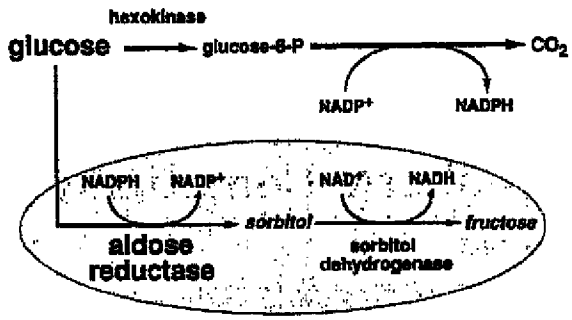

FIG. 1. Polyol (sorbitol) pathway; glucose-6-P, glucose 6-phosphate.

lens, retina, peripheral nerve, and renal glomerulus (Kinoshita and Nishimura, 1988; Pugliese et al., 1991).

These observations led to the development of numerous aldose reductase inhibitors of diverse chemical structures as possible therapeutic agents for diabetic complications. Sorbinil, ponalrestat, and tolrestat were among the most studied inhibitors to prevent cataracts, retinal capillary basement membrane thickening, and nerve conduction velocity deficits in experimental diabetic animal models. Until now, however, the clinical efficacy of these inhibitors in diabetic patients has not been fully proved to meet the standards of the Food and Drug Administration (Pfeifer et al., 1996).

In this review, recent advances in the understanding of the pathophysiological significance of aldose reductase are presented that would be relevant to the efficacy of the enzyme inhibitors in clinical intervention trials of diabetic complications. An extensive review on the pathogenesis of diabetic complications is outside the scope of this review. For this topic, the reader is encouraged to refer to other excellent reviews published elsewhere (Pugliese et al., 1991; Greene et al., 1993; Cameron and Cotter, 1994; Yagihashi, 1995).

II. Aldose Reductase and Aldo-Keto Reductase Superfamily

A. Aldose Reductase as a Member of the Aldo-Keto Reductase Superfamily

Aldose reductase is a small monomeric protein composed of 315 amino acid residues. The primary structure, first determined on rat lens aldose reductase (Carper et al., 1987, 1989), demonstrated high similarities to another NADPH-dependent oxidoreductase, human liver aldehyde reductase (EC 1.1.1.2) (Wermuth et al., 1987) and to ρ-crystallin, a major structural component of the lens of frog *Rana pipiens* (Tamarev et al., 1984). The degree of similarity clearly suggests that these proteins belong to the same family, namely aldo-keto reductase superfamily, with related structures and evolutionary origins. Subsequently, complementary deoxyribonucleic acid (cDNA) clones of human placenta, retina, and muscle aldose reductase were isolated (Bohren et al., 1989; Chung and LaMendola, 1989; Nishimura et al., 1990). As the coding sequences of these cDNAs originating from different tissues turned out to be essentially identical, the existence of tissue-specific isoforms for human aldose reductase has yet to be verified. The identification of amino acid sequences of aldose reductase from different species revealed a relatively low sequence identity (82–85%) conserved among human, rat, and other animal species. This could account for the species' differences in the sensitivity of aldose reductase to some of the inhibitors. For screening the potency and efficacy of the newly designed inhibitors, human enzyme preparations may be preferable and can be readily obtained by the recent recombinant technique (Nishimura et al., 1991).

In the past few years, molecular cloning techniques have identified many amino acid sequences for cellular proteins and a recent search of a database of these sequences identified as many as 39 proteins as members of the aldo-keto reductase superfamily (Jez et al., 1996). A wide variety of proteins from various species constitute this family, including aldehyde and xylose reductases from plants, yeast, and bacteria, as well as bovine and rat *Shaker* K^+ channel β-subunit (Rettig et al., 1994). Nonetheless, the majority of this family is represented by mammalian aldehyde reductases, aldose reductases, and hydroxysteroid dehydrogenases. Approximately 50% of the amino acid sequences are conserved between aldose reductase and these mammalian enzymes from various species and tissues. For instance, among the members coexisting in human liver are aldehyde reductase (Bohren et al., 1989), hepatic bile acid-binding protein (Stolz et al., 1993), Δ^4-3-oxosteroid 5β-reductase (Kondo et al., 1994), type I 3α-hydroxysteroid dehydrogenase, also referred to as chlordecone reductase (Winters et al., 1990), and type II 3α-hydroxysteroid dehydrogenase (Khanna et al., 1995).

B. A Closely Related Subgroup in the Aldo-Keto Reductase Superfamily

Interestingly, a unique subgroup was recently demonstrated in this superfamily. Cloning and determination of the amino acid sequence of mouse aldose reductase cDNA revealed the presence of closely related proteins with high sequence similarities in mouse (Gui et al., 1995). These are mouse vas deferens protein (MVDP) (Pailhoux et al., 1990) and fibroblast-growth-factor-1-regulated protein (FR-1) (Donohue et al., 1994), that respectively manifest as much as 69% identity to mouse aldose reductase. The identity between MVDP and FR-1 is nearly 82%. These three murine proteins therefore constitute a new subgroup within the aldo-keto reductase superfamily (fig. 2). Between rat and mouse aldose reductases, approximately 97% of the amino acid sequence is conserved. Analogously, one of the tumor-associated variants of protein detected in rat liver exhibited high sequence similarity to rat aldose reductase and to MVDP (Zeindl-Eberhart et al., 1994). This protein variant possibly belongs to the above subgroup of the

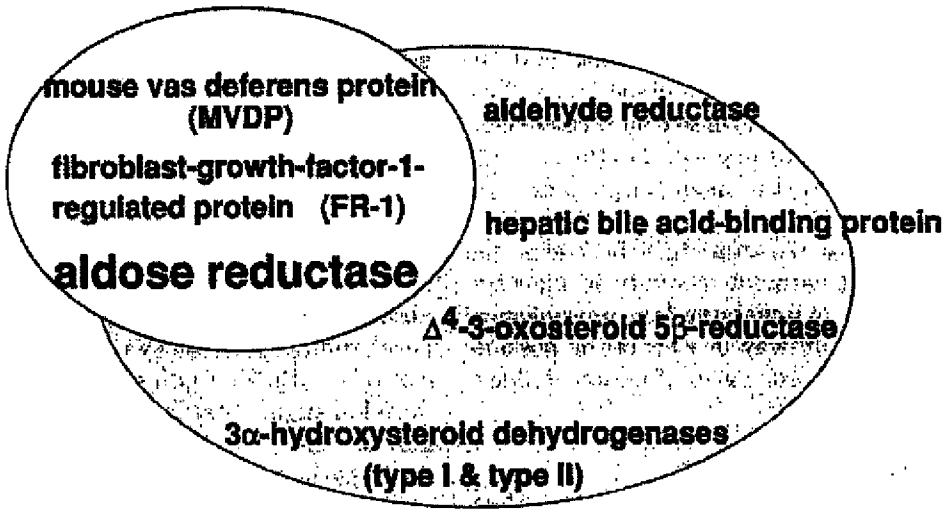

FIG. 2. Members of aldo-keto reductase superfamily identified in human and a closely related subfamily demonstrated in mouse (MVDP and FR-1).

aldo-keto reductase family as well. In view of these findings, the existence of hitherto unidentified proteins closely related to aldose reductase in humans can be speculated.

As the enzyme inhibitor zopolrestat was shown to bind and inhibit the action of mouse FR-1 to catalyze the reduction of DL-glyceraldehyde (Wilson et al., 1995), it is conceivable that the human counterpart of such related proteins may bind and prevent the action of inhibitors of aldose reductase. In fact, some aldose reductase inhibitors are known to equally interact with aldehyde reductase, a member of the aldo-keto reductase family that coexists with aldose reductase in most tissues (Sato and Kador, 1990). A widely used inhibitor like sorbinil inhibits aldose and aldehyde reductases with comparable IC_{50} values, whereas zopolrestat has higher specificity for aldose reductase as compared with aldehyde reductase (Barski et al., 1995).

C. Tertiary Structure of Aldose Reductase

Crystallographic structures have been determined for pig (Rondeau et al., 1992) and human aldose reductases (Borhani et al., 1992; Wilson et al., 1992). The enzyme molecule contains a $(\beta/\alpha)_8$ barrel structural motif with a large hydrophobic active site. The cofactor NADPH binds in an extended conformation to the bottom of the active site, located at the center of the barrel. The holoenzyme structure complexed with the enzyme inhibitor zopolrestat further demonstrated that the inhibitor binds to the active site on top of the nicotinamide ring of the NADPH (Wilson et al., 1993). When zopolrestat was complexed with the holoenzyme, however, it perturbed the position of two loops in the protein and changed the shape of the active site pocket. When the enzyme was complexed with another inhibitor sorbinil, the inhibitor simply occupied the active site pocket and did not induce further conformational change in the enzyme molecule (Urzhumtsev et al., 1997). These findings suggest that many compounds with diverse chemical structures can interact with the enzyme in different conformations. This illustrates the dangers of using theoretical approaches to predict the rigid inhibitor binding site of aldose reductase, as the enzyme apparently retained considerable flexibility in its tertiary structure (Wilson et al., 1996).

As mentioned above, there are marked differences in the selectivity toward aldose and aldehyde reductases among the known enzyme inhibitors. Such selectivity has been attributed to the interaction of the inhibitors with the enzyme molecule, depending upon whether the enzyme opens a 'specificity' pocket. This pocket binds inhibitors that are more effective against aldose reductase than against aldehyde reductase (Urzhumtsev et al., 1997). In this regard, identification and characterization of as yet unknown members of the aldo-keto reductase subfamily in humans seem essential. To effectively block the enhanced flux of glucose through polyol pathway, the inhibitor needs to be specific for aldose reductase and devoid of intercalating into other structurally related proteins coexisting in the "target" organs of diabetic complications.

III. Physiological Significance of Aldose Reductase

A. Polyol Pathway First Identified in the Seminal Vesicle

At present, physiological functions of aldose reductase have not been entirely clarified. Aldose reductase is a cytosolic enzyme present in most of the mammalian cells, although the distribution of the enzyme is not uniform among tissues. Nearly forty years ago the polyol pathway was first identified in the seminal vesicle by Hers (Hers, 1956), who demonstrated the conversion of blood glucose into fructose, an energy source of sperm cells. Later Van Heyningen reported the presence of

sorbitol in diabetic rat lens (Van Heyningen, 1959), and her work provided an opening for new research concerning the pathological role of aldose reductase and the polyol pathway in the development of diabetic complications. In fact aldose reductase messenger ribonucleic acid (mRNA) in rat was highly expressed in the lens, the retina, and the sciatic nerve, the major "target" organs of diabetic complications (Nishimura et al., 1988). Ever since, inhibitors for aldose reductase have been expected to become a potential treatment modality in diabetes. However, it is necessary to understand the physiological relevance of the polyol pathway in view of the possible side effects arising from a prolonged inhibition of aldose reductase in diabetic patients.

B. Osmoregulatory Role in the Kidney

In the previous decade, elevated extracellular NaCl was demonstrated to elicit marked increase in aldose reductase expression and accumulation of intracellular sorbitol in the cultured cell line from rabbit renal papilla (Bagnasco et al., 1987). In the kidney, aldose reductase mRNA was abundantly expressed in the medulla compared with relatively low expression in the cortex (Nishimura et al., 1988). These findings were confirmed by biochemical and immunohistochemical analyses of rat and human kidneys (Terubayashi et al., 1989). Sorbitol is one of the organic osmolytes that balance the osmotic pressure of extracellular NaCl, fluctuating in accord with urine osmolality (Burg, 1995). These findings, therefore, suggest the osmoregulatory role of aldose reductase in the renal homeostasis. The increased expression of aldose reductase under hyperosmotic stress was subsequently reported in a variety of cells of nonrenal origin, such as Chinese hamster ovary cells (Kaneko et al., 1990), cultured human retinal pigment epithelial cells (Henry et al., 1993), and human embryonic epithelial cells (Ferraretto et al., 1993). Transient transfection studies with luciferase or chloramphenicol acetyltransferase reporter constructs, containing various 5′-flanking regions of aldose reductase gene, identified the osmotic response element mediating this hyperosmotic stress-induced increase in transcription of aldose reductase gene (Ferraris et al., 1996; Daoudal et al., 1997; Ko et al., 1997). Studies on the factors that interact with these response elements and augment the transcription of aldose reductase gene are now in progress and may provide insight into the regulatory mechanisms of the gene expression. Nevertheless, physiological implications of the osmoregulatory role for aldose reductase in nonrenal cells is still unknown.

C. Unique Tissue Distribution Pattern of Aldose Reductase

Recent investigations disclosed the unexpected distribution pattern of aldose reductase not only in different species but in tissues other than "target" organs of diabetic complications. In mouse, aldose reductase mRNA was most abundantly expressed in the testis, whereas a very low level of the transcript was detected in the sciatic nerve and lens (Gui et al., 1995). These results suggest that mouse aldose reductase may possess a significant role in the testicular metabolism. On the other hand, the low expression of the enzyme in the nerve and lens was in marked contrast with the findings in rat, which indicated the localization of the enzyme transcript in these "target" organs of diabetic complications (Nishimura et al., 1988). Consistent with these findings is the absence of cataract formation during the course of hyperglycemia in mouse (Varma and Kinoshita, 1974), in contrast with the finding in rat, the first experimental model of sugar cataract formation (Kinoshita and Nishimura, 1988). Immunoblot and immunohistochemical analyses in rat tissues further showed high levels of aldose reductase protein in the adrenal gland and various reproductive organs, including the granulosa cells of rat ovary (Iwata et al., 1990). Of particular interest is the fact that cyclic changes in the expression and localization of aldose reductase were observed in rat ovary during the estrous cycle (Iwata et al., 1996). These changes in the enzyme expression were indicated to be under hormonal control, and the study suggests another functional role of aldose reductase in the female reproductive organ, which can be deranged under diabetic conditions.

D. Diverse Substrates for Aldose Reductase

Other lines of investigation have demonstrated that aldose reductase exhibits broad substrate specificity for both hydrophilic and hydrophobic aldehydes. Aldose reductase and the structurally related enzyme in the aldo-keto reductase family, aldehyde reductase, both catalyze the reduction of biogenic aldehydes derived from the catabolism of the catecholamines and serotonin by the action of monoamine oxidase (Turner and Tipton, 1972; Tabakoff et al., 1973; Wermuth et al., 1982). These two enzymes also catalyze the reduction of isocorticosteroids, intermediates in the catabolism of the corticosteroid hormones (Wermuth and Monder, 1983). Recently, aldose reductase in the adrenal gland was reported to be a major reductase for isocaproaldehyde, a product of sidechain cleavage of cholesterol (Matsuura et al., 1996).

Apart from these findings, molecular cloning of bovine testicular 20α-hydroxysteroid dehydrogenase cDNA incidentally revealed that the deduced amino acid sequence of the enzyme is identical with bovine lens aldose reductase (Warren et al., 1993). The result implies that a biologically active progesterone as well as 17α-hydroxyprogesterone, a major precursor of the androgens, estrogens, and glucocorticoids, are endogenous substrates for bovine aldose reductase. To examine whether this finding is also applicable to mouse aldose reductase, we tested various steroids as substrates in the kinetic analysis of purified recombinant enzyme. Although progesterone and 17α-hydroxyprogesterone potently com-

peted with the substrate binding, the mouse enzyme did not show any steroid dehydrogenase activity (Gui et al., 1995). The lack of catalytic activity for the steroid substrate in mouse aldose reductase could be attributed to a subtle difference in the amino acid residues constituting the active site, whereas low inhibition constants for these steroids introduced the possibility that availability of glucose to mouse enzyme may be significantly affected in the tissues containing high levels of endogenous steroids. By contrast, human aldose reductase was recently reported to exhibit the reductase activity for 17α-hydroxyprogesterone with the similar kinetic parameters to bovine enzyme (Petrash et al., 1996). It can therefore be postulated that the functional or physiological roles of aldose reductase differ considerably among animal species as well as among tissues.

In a series of aldehyde substrates for human aldose reductase investigated, isocorticosteroids (Wermuth and Monder, 1983) and isocaproaldehyde (Matsuura et al., 1996), both with K_M values of approximately 1 μM or less, are the best physiological substrates known to date. The next preferred substrates for aldose reductase may be aldehydes derived from biogenic amines (Turner and Tipton, 1972; Tabakoff et al., 1973) and methylglyoxal, a toxic aldehyde produced nonenzymatically from triose phosphate and enzymatically from acetone/acetol metabolism (Vander Jagt et al., 1992). 17α-hydroxyprogesterone (Petrash et al., 1996) and 4-hydroxynonenal (Vander Jagt et al., 1995), a reactive aldehyde produced by oxidative damage to unsaturated fatty acids, are also excellent substrates for the enzyme with K_M values of 20–30 μM. Another line of study demonstrated that 3-deoxyglucosone, one of the crosslinking agents formed as intermediates in nonenzymatic glycation, is a good substrate for aldose reductase (Feather et al., 1995). Aldose reductase also catalyzes the reduction of acrolein, a highly reactive and mutagenic molecule generated during lipid peroxidation and as a metabolic by-product of cyclophosphamide (Kolb et al., 1994). Both 3-deoxyglucosone and acrolein exhibited a similar range of K_M values (40–80 μM) in the kinetic analysis (Vander Jagt et al., 1996). Whereas glucose is one of the endogenous substrates for aldose reductase, comparison with other endogenous aldehydes unequivocally indicates that glucose is a rather poor substrate with a K_M value of 70 mM (Vander Jagt et al., 1990). The interpretation of these findings is that aldose reductase in the adrenal gland and reproductive organs may normally participate in the synthesis and catabolism of steroid hormones, whereas it is involved in the metabolism of biogenic amines in the central nervous system. The enzyme may also act as extrahepatic detoxification enzyme in various tissues (fig. 3). Thus the significance of aldose reductase in the polyol pathway may be quite limited under nondiabetic conditions: it provides an osmolyte sorbitol in the renal medulla and supplies fructose as an energy source of sperm in the seminal vesicle.

Recent studies hence illustrate the diversity in biological significance of aldose reductase in different tissues and in different animal species. The interactions of the inhibitors with aldose reductase in various organs along with other structurally related proteins in aldo-keto reductase family, may become a potential source of their ineffectiveness and/or side effects when drugs are administered to diabetic patients for a prolonged period of time. Experimental data on the efficacy and side effects of inhibitors obtained from animal models should be cautiously interpreted, as significant species-specific dif-

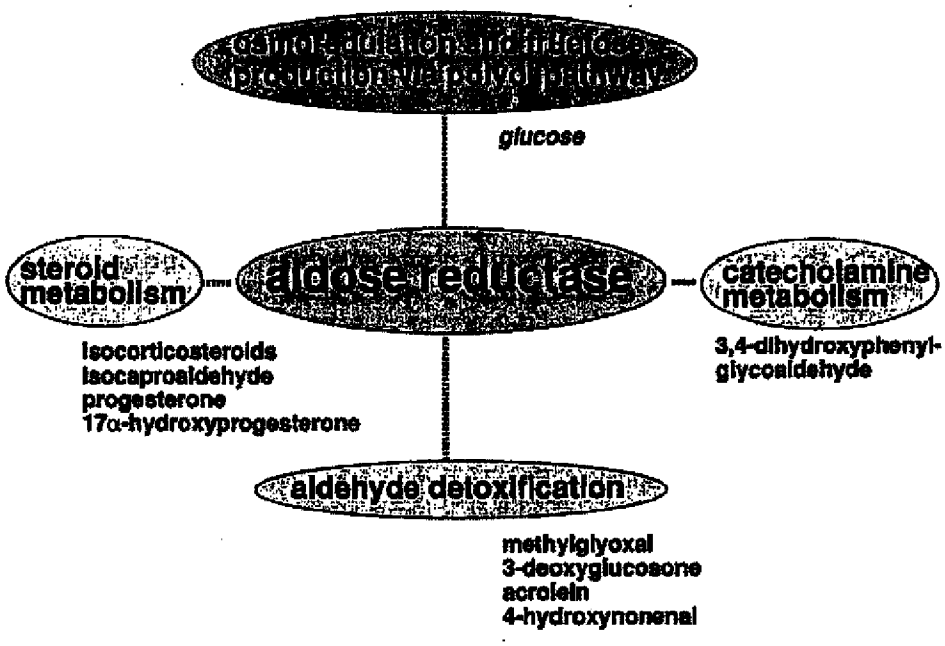

FIG. 3. A diversity of substrates and putative physiological roles of aldose reductase. See Section III for further detail.

ferences in the localization and in physiological functions of aldose reductase were noted. Nevertheless, it should be appended that aldose reductase is not the only enzyme participating in most of the above-mentioned pathways of endogenous aldehyde metabolism. The suppression of aldose reductase activity with enzyme inhibitors may thus have moderate effects on such aldehyde metabolism aside from polyol pathway.

IV. Aldose Reductase in Glucose Toxicity

A. Effect of Accelerated Polyol Pathway

For the past 4 decades, a wealth of experimental data has been accumulated on the role of accelerated polyol pathway in the process leading to the early tissue damage observed under hyperglycemia (Kinoshita and Nishimura, 1988). In the ocular lens, the accumulation of polyol induces hyperosmotic swelling and deranges the cell membrane, resulting in the leakage of amino acids, glutathione, and myoinositol to provoke cataract formation (Nagata et al., 1989). In other "target" organs of diabetic complications, however, such osmotic stress is currently considered to play a minor role in the tissue damage. Instead, depletion of cofactors used in the pathway by accelerated flux of glucose is postulated to elicit various metabolic disturbances in those tissues. Under normoglycemic conditions, polyol pathway accounts for approximately 3% of glucose utilization (Morrison et al., 1970), whereas more than 30% of glucose is metabolized through this pathway under hyperglycemia (González et al., 1984). The increased flux of glucose through this pathway and consequent expenditure of cofactors for aldose reductase (NADPH) and sorbitol dehydrogenase (NAD^+) lead to a redox state change and a cascade of interrelated metabolic imbalances. Substantially affected are activities of glutathione reductase and nitric oxide (NO) synthase because of the depletion of the cofactor NADPH. As glutathione reductase is an antioxidative enzyme that maintains the level of tissue glutathione, the overall effect would be the increased susceptibility to oxidative stress under diabetic conditions. Indeed increased susceptibility to H_2O_2 along with a reduced level of glutathione was reported in the endothelial cells cultured in high glucose medium (Kashiwagi et al., 1994). Similarly, the production of NO from L-arginine by NO synthase is suppressed resulting from the depletion of NADPH, thereby reducing the release of NO to elicit microvascular derangement and the slowing of nerve conduction (Cameron et al., 1993; Stevens et al., 1994).

In the retina of experimental diabetic animal models, the early lesion emerges in vascular component. Consistent with this observation, the localization of aldose reductase in retinal microvessels was demonstrated in various animal species including human trypsin-digested retina (Akagi et al., 1983; Kennedy et al., 1983; Hohman et al., 1989). Treatment with aldose reductase inhibitors was shown to prevent capillary basement membrane thickening, the early structural lesion observed in the retina (Frank et al., 1983; Robison et al., 1983, 1989; Chakrabarti and Sima, 1989). By contrast, whether perturbation in the vasculature or metabolic disturbance in the neural cells contributes primarily to the development of diabetic neuropathy has long been controversial. In 1959, Fagerberg first described the vascular involvement in the process leading to the structural lesion observed in diabetic neuropathy (Fagerberg, 1959). Later, however, most investigators in the field turned their attention to metabolic disturbances and ensuing neurochemical alterations in diabetic nerve. Effects of hyperglycemia on the polyol pathway activity and associated neurochemical derangement have been extensively studied in the peripheral nerve of experimental animals (Tomlinson et al., 1984; Greene et al., 1987; Nishimura et al., 1987). In fact, aldose reductase immunoreactivity was found in the paranodal cytoplasm of Schwann cells as well as in pericytes and endothelial cells of endoneurial capillaries (Chakrabarti et al., 1987).

B. Transgenic Animal Model

To investigate the effect of enhanced polyol pathway activity on the process leading to early tissue damage in diabetes, we made a transgenic animal model expressing human aldose reductase (Yamaoka et al., 1995; Yagihashi et al., 1996). As the transgene was driven by the murine major histocompatibility complex class I antigen, H-$2K^d$ gene promoter, a broad expression of human aldose reductase was demonstrated in most of the mouse tissues examined. In the sciatic nerve, immunohistochemical analysis using antibody, specific for human enzyme, indicated that aldose reductase was localized in Schwann cells, axons, and endothelial cells of endoneurial microvessels in the transgenic mice (Yagihashi, 1995). When these mice were fed with the diet containing 30% galactose, a significant level of galactitol was accumulated in the nerve. In this experiment, galactose feeding was substituted for induction of hyperglycemia so as to evaluate the direct effect of aldose reductase activity overexpressed in transgenic mice. This is because galactose is a better substrate for aldose reductase and galactitol is not further metabolized by sorbitol dehydrogenase (Hayman and Kinoshita, 1965). The level of galactitol in nerves of galactose-fed transgenic mice was 10 times higher than that in galactose-fed nontransgenic littermate mice, indicating the functional expression of the transgene integrated in the nerve tissue. The biochemical derangement in galactose-fed transgenic mice was accompanied by a significant delay in motor nerve conduction velocity, as well as significant atrophy in the myelinated fiber as was determined by morphometric analysis. Our transgenic mouse work, therefore, suggests the primary role of the augmented aldose reductase activity in the development of functional and

structural abnormalities in the peripheral nerve of the diabetic animal model.

C. Hemodynamic Abnormalities in Diabetic Neuropathy

On the other hand, renewed attention has recently been paid to the vascular involvement in the pathogenesis of diabetic neuropathy. Systemic investigation of the distribution of myelinated fiber loss from proximal to distal levels of the lower limb nerves in diabetic patients indicated the involvement of ischemia in the process leading to these morphological changes (Dyck et al., 1986). In fact, endoneurial hypoxia resulting from reduced nerve perfusion was demonstrated in diabetic rat (Tuck et al., 1984) and later in diabetic patients with neuropathy (Newrick et al., 1986). Of particular interest is the fact that administration of an aldose reductase inhibitor significantly improved the blood flow in the nerve tissue measured by laser-Doppler flowmetry, and a strong correlation between inhibitor-mediated improvement in the blood flow and in nerve conduction velocity was observed (Cameron et al., 1994). The possible link between metabolic disturbances elicited by hyperglycemia and such hemodynamic abnormalities in the nerve tissue of diabetic animals is the accelerated polyol pathway flux in the vascular cells. Enhanced polyol pathway activity would provoke impaired production of NO and other bioactive molecules in vascular endothelial cells. Experimental data also indicate that the deficit in NO release was prevented by aldose reductase inhibitor in the aorta of diabetic rats (Cameron and Cotter, 1992).

Intriguingly, however, there emerged unexpected data on the dose-response relationships for aldose reductase inhibition and various experimental findings in these animal experiments. Poor agreement was demonstrated between functional deficits and biochemical changes in the nerve of diabetic rats (Cameron et al., 1994). Compared with the dosage of aldose reductase inhibitor to correct the biochemical changes in the nerve, nearly 10 times higher dosage was necessary to correct the blood flow and conduction velocity of diabetic rat nerves. Thus, nerve conduction velocity is much less sensitive to the inhibitor treatment, and the improvement in nerve conduction does not correlate with the improvement in polyol pathway metabolites in the nerve. In this context, it should be noted that the levels of polyol pathway metabolites reflect the mass derived from axons and Schwann cells, the dominant components in the peripheral nerve. The mechanisms underlying this significant disparity in the inhibitor effects are still unknown. In any case, such difference in the sensitivity may at least partly explain the modest effect of aldose reductase inhibitors on nerve conduction velocity deficits reported in clinical trials. The involvement of aldose reductase in diabetic vascular abnormalities has been a matter of recent attention, and much remains to be clarified on the discrepancy in the dose-response relationship of inhibitors between neural and vascular components of the peripheral nerve. It should be noted, however, that the above provocative findings on dose-response relationships of aldose reductase inhibitors for corrections of the blood flow and nerve conduction velocity have not been verified by other laboratories.

D. Aldose Reductase and Other Factors in Glucose Toxicity

Along with the increased flux of glucose through the polyol pathway, there are other putative mechanisms that may take part in the toxic effects of hyperglycemia (fig. 4). Among the well-documented factors are activation of protein kinase C (Lee et al., 1989; Williams, 1995), enhanced nonenzymatic glycation (Brownlee et al., 1984), and augmentation of oxidative stress (Sato et al., 1979; Hunt et al., 1993). Some of these are postulated to be correlated with each other. Activation of protein kinase C was reported in vascular smooth muscle and endothelial cells after the exposure to hyperglycemia. Increased incorporation of [^{14}C]glucose into diacylglycerol (DAG) indicated that the enzyme activation was elicited by increased de novo synthesis of DAG through glycolytic pathway (Craven et al., 1990). The rise in NADH/NAD$^+$ ratio via enhanced polyol pathway may also facilitate the DAG synthesis by increasing the availability of dihydroxyacetone phosphate as well as favoring its reduction to *sn*-glycerol 3-phosphate, the intermediates of DAG synthesis (Pugliese et al., 1991). The increased protein kinase C activity would attenuate contractile responses of aortic vascular smooth muscle cells to such pressor hormones as angiotensin II and arginine vasopressin. The activation of protein kinase C increases sodium-proton antiport activity that regulates intracellular pH, cell growth, and differentiation and also augments expression of various matrix proteins such as fibronectin, type IV collagen, and laminin (Williams, 1995). All these biochemical changes could be relevant to diabetes-induced vascular dysfunction. This phenomenon was demonstrated in several tissues including retina, aorta, and renal glomeruli. Recently a specific inhibitor for the β isoform of protein kinase C was shown to ameliorate vascular dysfunctions in diabetic rats (Ishii et al., 1996). In peripheral nerve, however, the DAG level was reduced in diabetic rats (Zhu and Eichberg, 1993; Ido et al., 1994) and an activation of protein kinase C has not been reported in diabetic nerves. The underlying mechanisms of this tissue specific activation of protein kinase C have to be further elucidated. Although the new protein kinase C inhibitor can be another candidate drug for therapeutic usage, such difference in the activation pattern among the "target" organs and localization of the enzyme β isoform in tissues other than "target" organs of diabetic complications may hinder its general application to diabetic individuals.

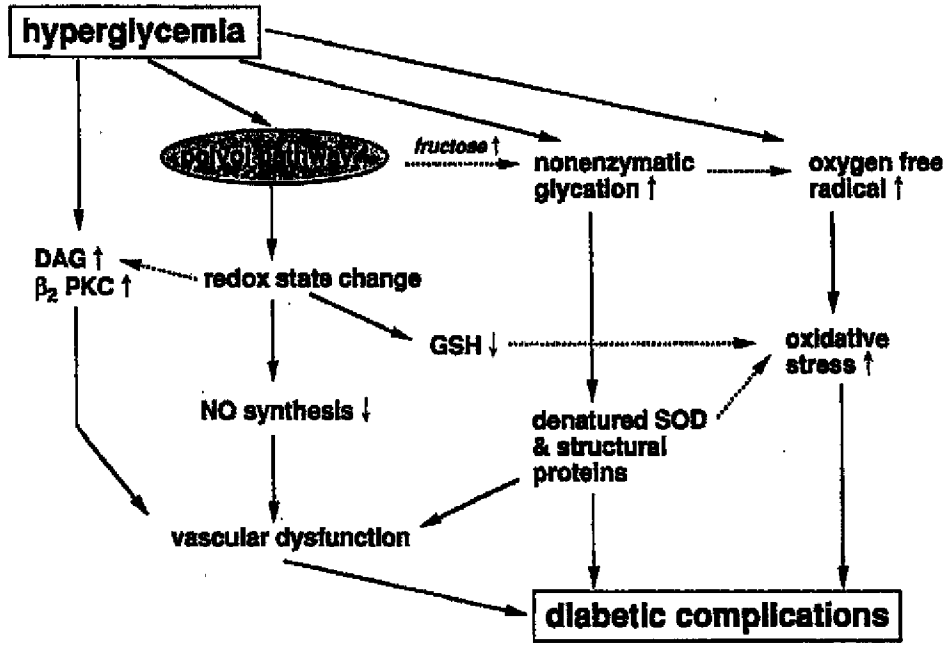

FIG. 4. A schematic diagram of possible interactions among factors involved in the pathogenesis of diabetic complications. (DAG), diacylglycerol; (β2 PKC), β_2 isoform of protein kinase C; (NO), nitric oxide; (GSH), glutathione; (SOD), superoxide dismutase.

Under hyperglycemic conditions, nonenzymatic glycation of structural proteins is enhanced, and advanced glycation end-products accumulate in diabetic tissues. As a glycation agent, fructose is more potent than glucose (Stevens et al., 1977), and the formation of fructose is augmented because of the accelerated flux of glucose through the polyol pathway. Increased nonenzymatic glycation has been shown to alter the structure and function of various macromolecules in the tissue, causing basement membrane thickening, demyelination, and impaired axonal transport as a result of the glycation of myelin, tubulin, and neurofilaments (Brownlee et al., 1988). Longterm treatment with aminoguanidine, an inhibitor of the glycation process, was effective in retaining the functional and structural integrity in the vascular and peripheral nerve tissues in diabetic rats (Hammes et al., 1991; Yagihashi et al., 1992). However, interpretation of these data is not straightforward, as aminoguanidine was later shown to inhibit the NO synthase (Corbett et al., 1992).

Various mechanisms are postulated to account for augmented oxidative stress in diabetes. A generation of oxygen free radicals was enhanced because of auto-oxidation of glucose. The protection against oxidative stress was attenuated because of reduced glutathione availability and inactivation of superoxide dismutase. Vascular dysfunction and resulting derangement in tissue perfusion under diabetic conditions would induce ischemia and reperfusion process, which further generate oxygen free radicals (McCord, 1985). On the other hand, it has been generally accepted that advanced glycation participates in the production of oxygen free radicals (Hunt et al., 1993). Inactivation of superoxide dismutase in diabetes was demonstrated to result from glycation of the two lysine residues on the enzyme protein (Arai et al., 1987). The polyol pathway may act upon this enhanced glycation process, supplying a reactive glycation agent fructose. Reduced glutathione availability under hyperglycemia is attributed to the accelerated polyol pathway flux, depleting the cofactor NADPH for glutathione reductase (fig. 1).

In this context, most of the putative mechanisms implicated in the toxic effects of hyperglycemia can be interrelated to each other and linked to enhanced polyol pathway activity. The crucial question yet left unanswered is as to what extent the polyol pathway participates in such an interrelated process leading to diabetic complications.

V. A Potential Target for the Prevention of Diabetic Complications

A. Clinical Trials of Aldose Reductase Inhibitors

A promising effect of aldose reductase inhibitor on nerve conduction velocity was reported more than a decade ago. When diabetic patients without any symptomatic neuropathy were treated with the aldose reductase inhibitor sorbinil, significant improvement in the conduction velocity was observed in all three nerves tested: the peroneal motor nerve, the median motor nerve, and the median sensory nerve (Judzewitsch et al., 1983). Subsequently, numerous clinical studies were carried out to evaluate the efficacy of sorbinil. However, the overall effect turned out to be disappointingly modest, possibly because of the difference in the study design, subjects with various degrees of symptomatic neu-

ropathy, and neurophysiological parameters examined as study endpoints (Fagius et al., 1985; O'Hare et al., 1988; Sima et al., 1988). The major adverse reaction of sorbinil was a hypersensitivity reaction in the early weeks of therapy, which is similar to that seen with other hydantoins. Although no clinically important adverse reaction was observed with ponalrestat, the succeeding aldose reductase inhibitor of a different chemical structure, its beneficial effect failed to be proved in randomized controlled study (Krentz et al., 1992). After the clinical trials, however, it was shown that ponalrestat did not penetrate the human nerve at doses sufficient to decrease the nerve sorbitol levels (Greene and Sima, 1993). The efficacy of another class of inhibitor, tolrestat, was modest in diabetic patients already symptomatic of neuropathy (Boulton et al., 1990), although the progress of mild diabetic autonomic and peripheral neuropathy could be halted (Giugliano et al., 1993, 1995). The only adverse reaction reported on tolrestat was an increase in serum levels of alanine aminotransferase or aspartate aminotransferase, although some patients in the placebo group also exhibited similar clinical findings during the study (Nicolucci et al., 1996). Because of the inability to demonstrate efficacy on the nerve conduction velocity in the multicenter double-blind studies on diabetic neuropathy, however, the clinical development of tolrestat was eventually withdrawn.

B. Variable Levels of Aldose Reductase in Diabetic Patients

Substantial variations in the levels of aldose reductase expression in various tissues exist among individuals with or without diabetes. Marked variability in aldose reductase activity was reported for enzyme preparations isolated from human placentas (Vander Jagt et al., 1990). Aldose reductase purified from erythrocytes exhibited a nearly three-fold variation in activity among diabetic patients (Hamada et al., 1991). Such differences in the activity of aldose reductase may influence the susceptibility of patients to glucose toxicity via acceleration of polyol pathway when these individuals are maintained under equivalent glycemic control. To test this hypothesis, it is necessary to determine the levels of aldose reductase in numerous diabetic subjects. In the previous studies, investigators examined variations in aldose reductase by isolating the enzyme from placenta or erythrocytes and assaying its activity (Vander Jagt et al., 1990; Hamada et al., 1991). The isolation of the enzyme was necessary because of the presence of other structurally related members of aldo-keto reductase family, particularly aldehyde reductase, in crude tissue preparations. These enzymes share overlapping substrate specificity with aldose reductase. Determination of the enzyme activity in human subjects was therefore quite laborious. Moreover, the tedious isolation procedures have problems of possible variations in enzyme recovery when the activity is to be compared among a group of individuals. By contrast, our newly developed immunoassay method using a specific antibody against aldose reductase could circumvent such difficulties (Nishimura et al., 1993). The amount of the enzyme determined by the immunoassay highly correlates with the activity of aldose reductase isolated from the erythrocytes of the same individuals (Nishimura et al., 1994a).

By using this assay method, we investigated the association between the aldose reductase level in the erythrocyte, and various clinical parameters determined in patients with non-insulin-dependent diabetes mellitus (NIDDM). Several-fold difference in the erythrocyte enzyme level was depicted among diabetic patients, whereas no significant difference in the mean enzyme level was demonstrated between the healthy and diabetic individuals. The enzyme level did not correlate with age, duration of diabetes, fasting blood glucose, or glycosylated hemoglobin (HbA_{1c}) levels, which represent glycemic control of the patient. However, data obtained from two different groups of diabetic subjects suggest that a high level of erythrocyte aldose reductase may affect the susceptibility and prognosis of diabetic retinopathy (Nishimura et al., 1994b, 1997). In another study group, 95 NIDDM patients were classified according to the results of seven nerve function tests, and the association between the enzyme level and the clinical findings was investigated (Ito et al., 1997). The erythrocyte aldose reductase level was significantly higher in those patients showing overt neuropathy compared with those without demonstrable neuropathy (fig. 5). Multivariate logistic regression analysis identified that a higher level of aldose reductase is one of the independent risk factors for overt neuropathy. Accordingly, these results support our earlier hypothesis that a difference in the level of aldose reductase is responsible for the susceptibility of diabetic patients to toxic effects of glucose. Along with our findings, the activity of aldose reductase fractionated from the erythrocytes was reported to be significantly higher in IDDM patients with complications compared with those showing no sign of complications (Hamada et al., 1993). Recently, increased levels of aldose reductase protein were also demonstrated by immunoblot analysis in the mononuclear cells isolated from IDDM patients with apparent diabetic complications (Ratliff et al., 1996).

The question as to what is responsible for high or low expression of aldose reductase in human tissue is not only of scientific, but also of great clinical significance when targeting the enzyme for therapeutic intervention of diabetic complications. The level of aldose reductase expressed in the erythrocyte seems to be stable, as no apparent alteration in the enzyme level was observed during the follow-up period of 12 months in the studied patients (Ito et al., 1997). In this study, the enzyme level remained unchanged irrespective of improved or stably high HbA_{1c} levels during the follow-up period. These

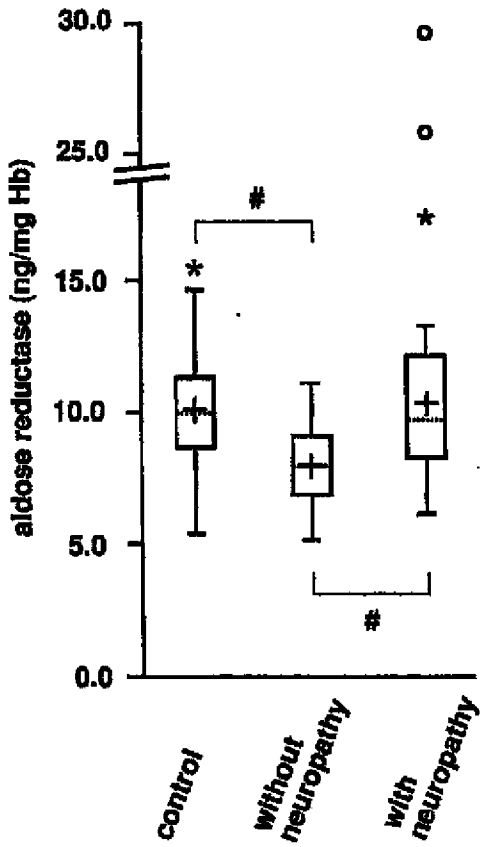

FIG. 5. Box-plots of erythrocyte aldose reductase levels in 76 healthy individuals (control) and 95 non-insulin-dependent diabetes mellitus patients determined by immunoassay. Based on the results of nerve function tests, patients were classified into those without demonstrable neuropathy (without neuropathy; $n = 45$) and those with overt neuropathy (with neuropathy; $n = 50$). The mean enzyme levels expressed per mg of hemoglobin (Hb) are represented by + in the plots. # $p < 0.01$, by Bonferroni t-tests, whether the 3 extreme values in "with neuropathy" group were excluded or included. No statistical difference was demonstrated between the healthy controls and the total diabetic patients. Modified from Ito T, Nishimura C, Takahashi Y, Saito T, and Omori Y (1997) The level of erythrocyte aldose reductase: a risk factor for diabetic neuropathy? *Diabetes Res Clin Pract* 36:161–167. With permission from Elsevier Science Ireland Ltd, Bay 15K, Shannon Industrial Estate, Co. Clare, Ireland.

findings indicate that the expression of the erythrocyte enzyme is unaffected by the glycemic control of the patients. It can, therefore, be speculated that different levels of aldose reductase observed in diabetic patients may be genetically determined. To explore this possibility, we examined two regions on the aldose reductase gene relevant to the enzyme expression: the promoter region containing a TATA box (Wang et al., 1993), and the region containing the recently identified osmotic response sequences (Ko et al., 1997). However, in the DNA sampled from 700 NIDDM patients with different enzyme levels in the erythrocyte, we found no change in either of these regions associated with differences in the expression of aldose reductase levels (Nishimura, unpublished observations). Thus the reason for the variable expression of aldose reductase in human subjects has yet to be elucidated. The understanding of the mechanisms defining the expression levels in the targeted tissues may lead to new avenues of preventive therapy for diabetic complications.

A hypothesis as to whether the high enzyme level predisposes the patients to the development of complications has to be further tested by the prospective study carried out through the prolonged time course of diabetes. Also to be considered is the relevance of the aldose reductase level in the erythrocyte in predicting the enzyme level in the "target" tissues of diabetic complications. Whether a high level of enzyme expression in the erythrocyte reflects the level in the different cell lineage has to be determined. It will take some time before all the data become available; nonetheless, a high level of aldose reductase in the erythrocyte was demonstrated to be a risk factor for vascular and neural derangement observed in diabetic patients. Identification of a subset of patients who have a high level of aldose reductase expression, and thereby are more susceptible to toxic effects of glucose, may enable us to target these patients for clinical intervention trial by use of new aldose reductase inhibitors. The data on the enzyme levels may also aid in the optimization of administration of the inhibitors to match the extent of enzyme suppression when exploring their efficacy in diabetic individuals.

VI. Conclusions

Recent progress in the understanding of biochemical correlates of aldose reductase has paved the way for designing and screening specific inhibitors of this enzyme that can be used as therapeutic agents for diabetic complications. The tertiary structure of aldose reductase, including the active site and the interaction with inhibitors of diverse chemical structures has been resolved. Abundant amounts of purified human enzyme are now available by recombinant technique. Nevertheless, much still remains to be elucidated regarding the pathophysiological significance of the enzyme and the regulatory mechanisms of aldose reductase expression in various human tissues.

In diabetic animal models, promising effects of aldose reductase inhibitors were demonstrated. Most of the clinical trials carried out so far, however, produced rather modest or disappointing effects of the inhibitors on the functional and morphological improvements in diabetic neuropathy. There could be several reasons that account for the disparity in the inhibitor effects observed between animal and clinical studies. Possible explanations include the chronic nature of diabetes in human subjects and the ensuing loss of ability to reconstitute the structural derangement once triggered under hyperglycemia. High variability in the neurological measurements as endpoints for the inhibitor effects should be considered as well. Yet there may be other reasons for disappointing results observed with clinical trials. For example, other structurally related members of aldo-keto reductase family, coexisting in the "target" tissues, may have interfered with the action of inhibitors,

quenching their action against aldose reductase. We still do not know the relative abundance of the aldo-keto reductase family, such as aldehyde reductase. These enzymes are colocalized in human tissues and the latter may interfere with the action of inhibitors to suppress aldose reductase.

Moreover, inappropriate dosage of inhibitors may have been used resulting in a failure to observe improvements in the endpoint of these clinical studies, as the dosage to correct the nerve conduction velocity may be significantly higher than that to substantially reduce polyol pathway metabolites in neuronal tissues. Whether nearly 100% inhibition of the polyol pathway metabolites is required for an improvement of nerve conduction velocity or if there are hitherto unknown reasons needs to be elucidated. Species difference in the structure and distribution of the enzyme and ensuing differences in sensitivity to inhibitors may also contribute to the disappointing clinical results obtained with inhibitors that have marked effects in animal studies. Lastly, the efficacy of aldose reductase inhibitors may depend on the enzyme level expressed in diabetic individuals. The variable levels of the enzyme expressed in the "target" tissues may affect the extent of involvement of the polyol pathway in the pathogenetic mechanisms of diabetic complications. If multiple mechanisms are involved in the pathogenesis of diabetic complications, the extent of the effectiveness of aldose reductase inhibitors is likely to be determined by the extent of the polyol pathway involvement in the toxic effects of hyperglycemia. This extent is likely to be variable among individuals having different levels of aldose reductase in "target" tissues.

REFERENCES

Akagi Y, Kador P, Kuwabara T, and Kinoshita J (1983) Aldose reductase localization in human retinal mural cells. *Invest Opthalmol & Visual Sci* 24:1516–1519.

Arai K, Maguchi S, Fujii S, Ishibashi H, Oikawa K, and Taniguchi N (1987) Glycation and inactivation of human Cu-Zn-superoxide dismutase. Identification of the *in vitro* glycated sites. *J Biol Chem* 262:16969–16972.

Bagnasco SM, Uchida S, Balaban RS, Kador PF, and Burg MB (1987) Induction of aldose reductase and sorbitol in renal inner medullary cells by elevated extracellular NaCl. *Proc Natl Acad Sci USA* 84:1718–1720.

Barski OA, Gabbay KH, Grimshaw CE, and Bohren KM (1995) Mechanism of human aldehyde reductase: characterization of the active site pocket. *Biochemistry* 34: 11264–11275.

Bohren KM, Bullock B, Wermuth B, and Gabbay KH (1989) The aldo-keto reductase superfamily. cDNAs and deduced amino acid sequences of human aldehyde and aldose reductases. *J Biol Chem* 264:9547–9551.

Borhani DW, Harter TM, and Petrash JM (1992) The crystal structure of the aldose reductase: NADPH binary complex. *J Biol Chem* 267:24841–24847.

Boulton AJ, Levin S, and Comstock J (1990) A multicentre trial of the aldose-reductase inhibitor, tolrestat, in patients with symptomatic diabetic neuropathy. *Diabetologia* 33:431–437.

Brownlee M, Cerami A, and Vlassara H (1988) Advanced products of nonenzymatic glycosylation and the pathogenesis of diabetic vascular diseases. *Diabetes Metab Rev* 4:437–451.

Brownlee M, Vlassara H, and Cerami A (1984) Nonenzymatic glycosylation and the pathogenesis of diabetic complications. *Ann Intern Med* 101:527–537.

Burg MB (1995) Molecular basis of osmotic regulation. *Am J Physiol* 268: F983–996.

Cameron NE and Cotter MA (1992) Impaired contraction and relaxation in aorta from streptozotocin-diabetic rats: role of polyol pathway activity. *Diabetologia* 35:1011–1019.

Cameron NE and Cotter MA (1994) The relationship of vascular changes to metabolic factors in diabetes mellitus and their role in the development of peripheral nerve complications. *Diabetes Metab Rev* 10:189–224.

Cameron NE, Cotter MA, Dines KC, and Maxfield EK (1993) Pharmacological manipulation of vascular endothelium function in non-diabetic and streptozotocin-diabetic rats: effects on nerve conduction, hypoxic resistance and endoneurial capillarization. *Diabetologia* 36:516–522.

Cameron NE, Cotter MA, Dines KC, Maxfield EK, Carey F, and Mirrlees DJ (1994) Aldose reductase inhibition, nerve perfusion, oxygenation and function in streptozotocin-diabetic rats: dose-response considerations and independence from a myo-inositol mechanism. *Diabetologia* 37:651–663.

Carper D, Nishimura C, Shinohara T, Dietzchold B, Wistow G, Craft C, Kador P, and Kinoshita JH (1987) Aldose reductase and ρ-crystallin belong to the same protein superfamily as aldehyde reductase. *FEBS Lett* 220:209–213.

Carper DA, Wistow G, Nishimura C, Graham C, Watanabe K, Fujii Y, Hayashi H, and Hayashi O (1989) A superfamily of NADPH-dependent reductases in eukaryotes and prokaryotes. *Exp Eye Res* 49:377–388.

Chakrabarti S and Sima AA (1989) Effect of aldose reductase inhibition and insulin treatment on retinal capillary basement membrane thickening in BB rats. *Diabetes* 38:1181–1186.

Chakrabarti S, Sima AA, Nakajima T, Yagihashi S, and Greene DA (1987) Aldose reductase in the BB rat: isolation, immunological identification and localization in the retina and peripheral nerve. *Diabetologia* 30:244–251.

Chung S and LaMendola J (1989) Cloning and sequence determination of human placental aldose reductase gene. *J Biol Chem* 264:14775–14777.

Corbett JA, Tilton RG, Chang K, Hasan KS, Ido Y, Wang JL, Sweetland MA, Lancaster JRJ, Williamson JR, and McDaniel ML (1992) Aminoguanidine, a novel inhibitor of nitric oxide formation, prevents diabetic vascular dysfunction. *Diabetes* 41:552–556.

Craven PA, Davidson CM, and DeRubertis FR (1990) Increase in diacylglycerol mass in isolated glomeruli by glucose from *de novo* synthesis of glycerolipids. *Diabetes* 39:667–674.

Daoudal S, Tournaire C, Halere A, VeyssiOere G, and Jean C (1997) Isolation of the mouse aldose reductase promoter and identification of a tonicity-responsive element. *J Biol Chem* 272:2615–2619.

Diabetes Control and Complications Trial Research Group (1993) The effect of intensive treatment of diabetes on the development and progression of long-term complications in insulin-dependent diabetes mellitus. *N Engl J Med* 329:977–986.

Donohue PJ, Alberts GF, Hampton BS, and Winkles JA (1994) A delayed-early gene activated by fibroblast growth factor-1 encodes a protein related to aldose reductase. *J Biol Chem* 269:8604–8609.

Dyck PJ, Karnes JL, O'Brien P, Okazaki H, Lais A, and Engelstad J (1986) The spatial distribution of fiber loss in diabetic polyneuropathy suggests ischemia. *Ann Neurol* 19:440–449.

Fagerberg SE (1959) Diabetic neuropathy: a clinical and histologic study on the significance of vascular affections. *Acta Med Scand* 164:1–80.

Fagius J, Brattberg A, Jameson S, and Berne C (1985) Limited benefit of treatment of diabetic polyneuropathy with an aldose reductase inhibitor: a 24-week controlled trial. *Diabetologia* 28:323–329.

Feather MS, Flynn TG, Munro KA, Kubisaki TJ, and Walton DJ (1995) Catalysis of reduction of carbohydrate 2-oxoaldehydes (osones) by mammalian aldose reductase and aldehyde reductase. *Biochim Biophys Acta* 1244:10–16.

Ferraretto A, Negri A, Giuliani A, De GL, Fuhrman CAM, and Ronchi S (1993) Aldose reductase is involved in long-term adaptation of EUE cells to hyperosmotic stress. *Biochim Biophys Acta* 1175:283–288.

Ferraris JD, Williams CK, Jung KY, Bedford JJ, Burg MB, and Garcia-Perez A (1996) ORE, a eukaryotic minimal essential osmotic response element. The aldose reductase gene in hyperosmotic stress. *J Biol Chem* 271:18318–18321.

Frank RN, Keirn RJ, Kennedy A, and Frank KW (1983) Galactose-induced retinal capillary basement membrane thickening: prevention by Sorbinil. *Invest Opthalmol & Visual Sci* 24:1519–1524.

Giugliano D, Marfella R, Quatraro A, De RN, Salvatore T, Cozzolino D, Ceriello A, and Torella R (1993) Tolrestat for mild diabetic neuropathy. A 52-week, randomized, placebo-controlled trial. *Ann Intern Med* 118:7–11.

Giugliano D, Misso L, and Acampora R (1995) Tolrestat in the primary prevention of diabetic neuropathy. *Diabetes Care* 18:536–541.

González RG, Barnett P, Aguayo J, Cheng HM, and Chylack LTJ (1984) Direct measurement of polyol pathway activity in the ocular lens. *Diabetes* 33:196–199.

Greene DA and Sima AAF (1993) Effects of aldose reductase inhibitors on the progression of nerve damage. *Diabetic Med* 10:318–328.

Greene DA, Lattimer SA, and Sima AA (1987) Sorbitol, phosphoinositides, and sodium-potassium-ATPase in the pathogenesis of diabetic complications. *N Engl J Med* 316:599–606.

Greene DA, Sima AA, Stevens MJ, Feldman EL, Killen PD, Henry DN, Thomas T, Dananberg J, and Lattimer SA (1993) Aldose reductase inhibitors: an approach to the treatment of diabetic nerve damage. *Diabetes Metab Rev* 9:189–217.

Gui T, Tanimoto T, Kokai Y, and Nishimura C (1995) Presence of a closely related subgroup in the aldo-ketoreductase family of the mouse. *Eur J Biochem* 227:448–453.

Hamada Y, Kitoh R, and Raskin P (1991) Crucial role of aldose reductase activity and plasma glucose level in sorbitol accumulation in erythrocytes from diabetic patients. *Diabetes* 40:1233–1240.

Hamada Y, Kitoh R, and Raskin P (1993) Association of erythrocyte aldose reductase activity with diabetic complications in type 1 diabetes. *Diabetic Med* 10:33–38.

Hammes HP, Martin S, Federlin K, Geisen K, and Brownlee M (1991) Aminoguanidine treatment inhibits the development of experimental diabetic retinopathy. *Proc Natl Acad Sci USA* 88:11555–11558.

Hayman S and Kinoshita JH (1965) Isolation and properties of lens aldose reductase. *J Biol Chem* 240:877–882.

Henry DN, Del MM, Greene DA, and Killen PD (1993) Altered aldose reductase gene regulation in cultured human retinal pigment epithelial cells. *J Clin Invest* 92: 617–623.

Hers HG (1956) Le Mechanisme de la transformation de glucose en fructose par les vesicules seminales. *Biochim Biophys Acta* 22:202–203.

Hohman TC, Nishimura C, and Robison WG, Jr (1989) Aldose reductase and polyol in cultured pericytes of human retinal capillaries. *Exp Eye Res* 48:55–60.

Hunt JV, Bottoms MA, and Mitchinson MJ (1993) Oxidative alterations in the experimental glycation model of diabetes mellitus are due to protein-glucose

adduct oxidation. Some fundamental differences in proposed mechanisms of glucose oxidation and oxidant production. *Biochem J* 291:529–535.
Ido Y, McHowat J, Chang KC, Arrigoni-Martelli E, Orfalian Z, Kilo C, Corr PB, and Williamson JR (1994) Neural dysfunction and metabolic imbalances in diabetic rats. Prevention by acetyl-L-carnitine. *Diabetes* 43:1469–1477.
Ishii H, Jirousek MR, Koya D, Takagi C, Xia P, Clermont A, Bursell S-E, Kern TS, Ballas LM, Heath WF, Stramm LE, Feener EP, and King GL (1996) Amelioration of vascular dysfunctions in diabetic rats by an oral PKC β inhibitor. *Science* 272:728–731.
Ito T, Nishimura C, Takahashi Y, Saito T, and Omori Y (1997) The level of erythrocyte aldose reductase: a risk factor for diabetic neuropathy? *Diabetes Res Clin Pract* 36:161–167.
Iwata N, Hara S, Nishimura C, Takahashi M, Mukai T, Takayama M, and Endo T (1996) Hormonal regulation of aldose reductase in rat ovary during the estrous cycle. *Eur J Biochem* 235:444–448.
Iwata N, Inano N, and Satoh T (1990) The purification and properties of aldose reductase from rat ovary. *Arch Biochem Biophys* 282:70–77.
Jez JM, Flynn GF, and Penning TM (1996) A nomenclature system for the aldo-keto reductase superfamily, in *Enzymology and Molecular Biology of Carbonyl Metabolism 6* (Weiner H, Lindahl R, Crabb DW, and Flynn TG, eds) pp 579–589, Plenum Press, New York.
Judzewitsch RG, Jaspan JB, Polonsky KS, Weinberg CR, Halter JB, Halar E, Pfeifer MA, Vukadinovic C, Bernstein L, Schneider M, Liang KY, Gabbay KH, Rubenstein AH, and Porte D, Jr (1983) Aldose reductase inhibition improves nerve conduction velocity in diabetic patients. *N Engl J Med* 308:119–125.
Kaneko M, Carper D, Nishimura C, Millen J, Bock M, and Hohman TC (1990) Induction of aldose reductase expression in rat kidney mesangial cells and Chinese hamster ovary cells under hypertonic conditions. *Exp Cell Res* 188:135–140.
Kashiwagi A, Asahina T, Ikebuchi M, Tanaka Y, Takagi Y, Nishio Y, Kikkawa R, and Shigeta Y (1994) Abnormal glutathione metabolism and increased cytotoxicity caused by H_2O_2 in human umbilical vein endothelial cells cultured in high glucose medium. *Diabetologia* 37:264–269.
Kennedy A, Frank RN, and Varma SD (1983) Aldose reductase activity in retinal and cerebral microvessels and cultured vascular cells. *Invest Opthalmol & Visual Sci* 24:1250–1258.
Khanna M, Qin K-N, Wang RW, and Cheng K-C (1995) Substrate specificity, gene structure, and tissue-specific distribution of multiple human 3α-hydroxysteroid dehydrogenase. *J Biol Chem* 270:20162–20168.
Kinoshita JH and Nishimura C (1988) The involvement of aldose reductase in diabetic complications. *Diabetes Metab Rev* 4:323–337.
Ko BCB, Ruepp B, Bohren KM, and Gabbay KH (1997) Identification and characterization of multiple osmotic response sequences in the human aldose reductase gene. *J Biol Chem* 272:16431–16437.
Kolb NS, Hunsaker LA, and Vander Jagt DL (1994) Aldose reductase-catalyzed reduction of acrolein: implications in cyclophosphamide toxicity. *Mol Pharmacol* 45:797–801.
Kondo KH, Kai MH, Setoguchi Y, Eggertsen G, Sjoblom P, Setoguchi T, Okuda KI, and Bjorkhem I (1994) Cloning and expression of cDNA of human delta 4-3-oxosteroid 5 beta-reductase and substrate specificity of the expressed enzyme. *Eur J Biochem* 219:357–363.
Krentz AJ, Honigsberger L, Ellis SH, Hardman M, and Nattrass M (1992) A 12-month randomized controlled study of the aldose reductase inhibitor penalrestat in patients with chronic symptomatic diabetic neuropathy. *Diabetic Med* 9:463–468.
Lee T-S, Saltsman KA, Ohashi H, and King GL (1989) Activation of protein kinase C by elevation of glucose concentration: proposal for a mechanism in the development of diabetic vascular complications. *Proc Natl Acad Sci USA* 86:5141–5145.
Matsuura K, Deyashiki Y, Bunai Y, Ohya I, and Hara A (1996) Aldose reductase is a major reductase for isocaproaldehyde, a product of side-chain cleavage of cholesterol, in human and animal adrenal glands. *Arch Biochem Biophys* 328:265–271.
McCord JM (1985) Oxygen-derived free radicals in postischemic tissue injury. *N Engl J Med* 312:159–163.
Morrison AD, Clements RS, Travis SB, Oski F, and Winegrad AI (1970) Glucose utilization by the polyol pathway in human erythrocytes. *Biochem Biophys Res Commun* 40:199–205.
Nagata M, Hohman TC, Nishimura C, Drea CM, Oliver C, and Robison WG, Jr (1989) Polyol and vacuole formation in cultured canine lens epithelial cells. *Exp Eye Res* 48:667–677.
Newrick PG, Wilson AJ, Jakubowski J, Boulton AJM, and Ward JD (1986) Sural nerve oxygen tension in diabetes. *Br Med J* 293:1053–1054.
Nicolucci A, Carinci F, Graepel JG, Hohman TC, Ferris F, and Lachin JM (1996) The efficacy of tolrestat in the treatment of diabetic peripheral neuropathy. A meta-analysis of individual patient data. *Diabetes Care* 19:1091–1096.
Nishimura C, Furue M, Ito T, Omori Y, and Tanimoto T (1993) Quantitative determination of human aldose reductase by enzyme-linked immunosorbent assay. Immunoassay of human aldose reductase. *Biochem Pharmacol* 46:21–28.
Nishimura C, Graham C, Hohman TC, Nagata M, Robison WG, Jr, and Carper D (1988) Characterization of mRNA and genes for aldose reductase in rat. *Biochem Biophys Res Commun* 153:1051–1059.
Nishimura C, Hamada Y, Tachikawa T, Ishikawa T, Gui T, Tsubouchi J, Hotta N, Tanimoto T, and Urakami T (1994a) Enzyme immunoassay for erythrocyte aldose reductase. *Clin Chem* 40:889–894.
Nishimura C, Hotta Y, Gui T, Seko A, Fujimaki T, Ishikawa T, Hayakawa M, Kansi A, and Saito T (1997) The level of erythrocyte aldose reductase is associated with the severity of diabetic retinopathy. *Diabetes Res Clin Pract* 37:173–177.
Nishimura C, Lou MF, and Kinoshita JH (1987) Depletion of myo-inositol and amino acids in galactosemic neuropathy. *J Neurochem* 49:290–295.
Nishimura C, Matsuura Y, Kokai Y, Akera T, Carper D, Morjana N, Lyons C, and Flynn TG (1990) Cloning and expression of human aldose reductase. *J Biol Chem* 265:9788–9792.
Nishimura C, Saito T, Ito T, Omori Y, and Tanimoto T (1994b) High levels of erythrocyte aldose reductase and diabetic retinopathy in NIDDM patients. *Diabetologia* 37:328–330.
Nishimura C, Yamaoka T, Mizutani M, Yamashita K, Akera T, and Tanimoto T (1991) Purification and characterization of the recombinant human aldose reductase expressed in baculovirus system. *Biochim Biophys Acta* 1078:171–178.
O'Hare JP, Morgan MH, Alden P, Chissel S, O'Brien IA, and Corrall RJ (1988) Aldose reductase inhibition in diabetic neuropathy: clinical and neurophysiological studies of one year's treatment with sorbinil. *Diabetic Med* 5:537–542.
Pailhoux EA, Martinez A, Veyssiere GM, and Jean CG (1990) Androgen-dependent protein from mouse vas deferens. cDNA cloning and protein homology with the aldo-keto reductase superfamily. *J Biol Chem* 265:19932–19936.
Petrash JM, Harter TM, and Murdock GL (1996) A potential role for aldose reductase in steroid metabolism, in *Enzymology and Molecular Biology of Carbonyl Metabolism 6* (Weiner H, Lindahl R, Crabb DW, and Flynn TG, eds) pp 465–473, Plenum Press, New York.
Pfeifer MA, Schumer MP, and Gelber DA (1996) Aldose reductase inhibitors: the end of an era or the need for different trial designs? *Diabetes* 45:S82–S89.
Pugliese G, Tilton GT, and Williamson JR (1991) Glucose-induced metabolic imbalances in the pathogenesis of diabetic vascular disease. *Diabetes Metab Rev* 7:35–59.
Ratliff DM, Vander Jagt DJ, Eaton RP, and Vander Jagt DL (1996) Increased levels of methylglyoxal-metabolizing enzymes in mononuclear and polymorphonuclear cells from insulin-dependent diabetic patients with diabetic complications: aldose reductase, glyoxalase I, and glyoxalase II—a clinical research center study. *J Clin Endocrinol & Metab* 81:488–492.
Rettig J, Heinemann SH, Wunder F, Lorra C, Parcej CN, Dolly JO, and Pongs O (1994) Inactivation properties of voltage-gated K^+ channels altered by presence of beta subunit. *Nature* 369:289–294.
Robison WG, Jr, Kador PF and Kinoshita JH (1983) Retinal capillaries: basement membrane thickening by galactosemia prevented with aldose reductase inhibitor. *Science* 221:1177–1179.
Robison WG, Jr, Nagata M, Laver N, Hohman TC, and Kinoshita JH (1989) Diabetic-like retinopathy in rats prevented with an aldose reductase inhibitor. *Invest Opthalmol & Visual Sci* 30:2285–2292.
Rondeau JM, Tete F, F., Podjarny A, Reymann JM, Barth P, Biellmann JF, and Moras D (1992) Novel NADPH-binding domain revealed by the crystal structure of aldose reductase. *Nature* 355:469–472.
Sato S and Kador PF (1990) Inhibition of aldehyde reductase by aldose reductase inhibitors. *Biochem Pharmacol* 40:1033–1042.
Sato Y, Hotta N, Sakamoto N, Matsuoka S, Ohishi N, and Yagi K (1979) Lipid peroxide level in plasma of diabetic patients. *Biochem Med* 21:104–107.
Sima AA, Bril V, Nathaniel V, McEwan TA, Brown MB, Lattimer SA, and Greene DA (1988) Regeneration and repair of myelinated fibers in sural-nerve biopsy specimens from patients with diabetic neuropathy treated with sorbinil. *N Engl J Med* 319:548–555.
Stevens MJ, Dananberg J, Feldman EL, Lattimer SA, Kamijo M, Thomas TP, Shindo H, Sima AA, and Greene DA (1994) The linked roles of nitric oxide, aldose reductase and, (Na^+,K^+)-ATPase in the slowing of nerve conduction in the streptozotocin diabetic rat. *J Clin Invest* 94:552–559.
Stevens VJ, Vlassara H, Abati A, and Cerami A (1977) Nonenzymatic glycosylation of hemoglobin. *J Biol Chem* 252:2998–3002.
Stolz A, Hammond L, Lou H, Takikawa H, Rank M, and Shively JE (1993) cDNA Cloning and expression of the human hepatic bile acid-binding protein. *J Biol Chem* 268:10448–10457.
Tabakoff B, Anderson R, and Alivisatos SGA (1973) Enzymatic reduction of "biogenic" aldehydes in brain. *Mol Pharmacol* 9:428–437.
Tamarev AS, Zinovieva RD, Dolgilevich SM, Luchin SD, Krayev AS, Skryabin KG, and Gause GGJ (1984) A novel type of crystallin in the frog eye lens. 35-kDa polypeptide is not homologous to any of the major classes of lens crystallins. *FEBS Lett* 171:297–302.
Terubayashi H, Sato S, Nishimura C, Kador PF, and Kinoshita JH (1989) Localization of aldose and aldehyde reductase in the kidney. *Kidney Int* 36:843–851.
Tomlinson DR, Moriarty BJ, and Mayer JH (1984) Prevention and reversal of defective axonal transport and motor nerve conduction velocity in rats with experimental diabetes by treatment with the aldose reductase inhibitor Sorbinil. *Diabetes* 33:470–476.
Tuck RR, Schmelzer JD, and Low PA (1984) Endoneurial blood flow and oxygen tension in the sciatic nerve of rats with experimental diabetic neuropathy. *Brain* 107:935–950.
Turner AJ and Tipton KF (1972) The characterization of two reduced nicotinamide-adenine dinucleotide phosphate-linked aldehyde reductases from pig brain. *Biochem J* 130:765–772.
Urzhumtsev A, Tête-Favier F, Mitschler A, Barbanton J, Barth P, Urzhumtseva L, Biellmann J-F, Podjarny AD, and Moras D (1997) A 'specificity' pocket inferred from the crystal structures of the complexes of aldose reductase with the pharmaceutically important inhibitors tolrestat and sorbinil. *Structure* 5:601–612.
van Heyningen R (1959) Formation of polyols by the lens of the rat with 'sugar' cataract. *Nature* 468:194–195.
Vander Jagt DL, Hunsaker LA, Robinson B, Stangebye LA, and Deck LM (1990) Aldehyde and aldose reductases from human placenta. Heterogeneous expression of multiple enzyme forms. *J Biol Chem* 265:10912–10918.
Vander Jagt DL, Kolb NS, Vander Jagt TJ, Chino J, Martinez FJ, Hunsaker LA, and Royer RE (1995) Substrate specificity of human aldose reductase: identification of 4-hydroxynonenal as an endogenous substrate. *Biochim Biophys Acta* 1249:117–126.
Vander Jagt DL, Robinson B, Taylor KK, and Hunsaker LA (1992) Reduction of trioses by NADPH-dependent aldo-keto reductases. Aldose reductase, methylglyoxal, and diabetic complications. *J Biol Chem* 267:4364–4369.
Vander Jagt DL, Torres JE, Hunsaker LA, Deck LM, and Royer RE (1996) Physiological substrates of human aldose and aldehyde reductases, in *Enzymology and*

Molecular Biology of Carbonyl Metabolism 6 (Weiner H, Lindahl R, Crabb DW, and Flynn TG, eds) pp 491–497, Plenum Press, New York.

Varma SD and Kinoshita JH (1974) The absence of cataracts in mice with congenital hyperglycemia. *Exp Eye Res* 19:577–582.

Wang K, Bohren KM, and Gabbay KH (1993) Characterization of the human aldose reductase gene promotor. *J Biol Chem* 268:16052–16058.

Warren JC, Murdock GL, Ma Y, Goodman SR, and Zimmer WE (1993) Molecular cloning of testicular 20 alpha-hydroxysteroid dehydrogenase: identity with aldose reductase. *Biochemistry* 32:1401–1406.

Wermuth B and Monder C (1983) Aldose and aldehyde reductase exhibit isocorticosteroid reductase activity. *Eur J Biochem* 131:423–426.

Wermuth B, Burgisser H, Bohren K, and von Wartburg J-P (1982) Purification and characterization of human brain aldose reductase. *Eur J Biochem* 127:279–284.

Wermuth B, Omar A, Forster A, di Francesco C, Wolf M, von Wartburg JP, Bullock B, and Gabbay KH (1987) Primary structure of aldehyde reductase from human liver, in *Enzymology and Molecular Biology of Carbonyl Metabolism: Aldehyde Dehydrogenase, Aldo-Keto Reductase, and Alcohol Dehydrogenase* (Weiner H and Flynn TG, eds) pp 297–307, Alan R. Liss, New York.

Williams B (1995) Glucose-induced vascular smooth muscle dysfunction: the role of protein kinase C. *J Hypertens* 13:477–486.

Wilson DK, Bohren KM, Gabbay KH, and Quiocho FA (1992) An unlikely sugar substrate site in the 1.65 Å structure of the human aldose reductase holoenzyme implicated in diabetic complications. *Science* 257:81–84.

Wilson DK, Nakano T, Petrash JM, and Quiocho FA (1995) 1.7 Å structure of FR-1, a fibroblast growth factor-induced member of the aldo-keto reductase family, complexed with coenzyme and inhibitor. *Biochemistry* 34:14323–14330.

Wilson DK, Nakano T, Petrash JM, and Quiocho FA (1996) Structure studies of aldo-keto reductase inhibition, in *Enzymology and Molecular Biology of Carbonyl Metabolism 6* (Weiner H, Lindahl R, Crabb DW, and Flynn TG, eds) pp 435–442, Plenum Press, New York.

Wilson DK, Tarle I, Petrash JM, and Quiocho FA (1993) Refined 1.8 Å structure of human aldose reductase complexed with the potent inhibitor zopolrestat. *Proc Natl Acad Sci USA* 90:9847–9851.

Winters CJ, Molowa DT, and Guzelian PS (1990) Isolation and characterization of cloned cDNAs encoding human liver chlordecone reductase. *Biochemistry* 29: 1080–1087.

Yagihashi S (1995) Pathology and pathogenetic mechanisms of diabetic neuropathy. *Diabetes Metab Rev* 11:193–225.

Yagihashi S, Kamijo M, Baba M, Yagihashi N, and Nagai K (1992) Effect of aminoguanidine on functional and structural abnormalities in peripheral nerve of STZ-induced diabetic rats. *Diabetes* 41:47–52.

Yagihashi S, Yamagishi S, Wada R, Sugimoto K, Baba M, Wong HG, Fujimoto J, Nishimura C, and Kokai Y (1996) Galactosemic neuropathy in transgenic mice for human aldose reductase. *Diabetes* 45:56–59.

Yamaoka T, Nishimura C, Yamashita K, Itakura M, Yamada T, Fujimoto J, and Kokai Y (1995) Acute onset of diabetic pathological changes in transgenic mice with human aldose reductase cDNA. *Diabetologia* 38:255–261.

Zeindl-Eberhart E, Jungblut PR, Otto A, and Rabes HM (1994) Identification of tumor-associated protein variants during rat hepatocarcinogenesis. Aldose reductase. *J Biol Chem* 269:14589–14594.

Zhu X and Eichberg J (1993) Molecular species composition of glycerophospholipids in rat sciatic nerve and its alteration in streptozotocin-induced diabetes. *Biochim Biophys Acta* 1168:1–12.

EXHIBIT B

Role of Nitric Oxide in Angiogenesis and Tumor Progression in Head and Neck Cancer

*Oreste Gallo, Emanuela Masini, Lucia Morbidelli, Alessandro Franchi, Isabella Fini-Storchi, William A. Vergari, Marina Ziche**

Background: **Angiogenesis (formation of new blood vessels) is associated with tumor growth and metastasis in patients with solid tumors, including those of the head and neck. Nitric oxide (NO) production may contribute to these processes. We assessed the role of the NO pathway in angiogenesis and tumor progression in patients with head and neck cancer.** ***Methods:*** **Biochemical assays were used to measure NO synthase (NOS) activity and cyclic guanosine monophosphate (cGMP) levels in specimens of tumor and normal mucosa obtained from 27 patients. Microvessels in tumor specimens were identified by CD-31-specific immunohistochemical staining. Associations between microvessel densities, levels of NOS, and cGMP were examined by use of two-sided statistical tests. Tumor specimens and human squamous carcinoma A-431 cells were grown as explants on the corneas of rabbits, and the effect of the NOS inhibitor N^{ω}-nitro-L-arginine-methyl ester (L-NAME) was tested.** ***Results:*** **Levels of total NOS, inducible NOS, and cGMP were higher in tumor specimens than in specimens of normal mucosa (all $P<.0001$). Tumor specimens from patients with lymph node metastases presented a higher total NOS activity ($P = .005$) and were markedly more vascularized than tumor specimens from patients with no lymph node involvement ($P = .0002$). Microvessel density at the tumor edge was an independent predictor of metastasis for this series of patients (odds ratio = 1.19; 95% confidence interval = 1.07–2.89; $P = .04$). A-431 cells and tumor specimens exhibiting high levels of NOS activity induced angiogenesis in the rabbit cornea assay; when NO production was blocked, tumor angiogenesis and growth were repressed.** ***Conclusions:*** **The NO pathway appears to play a key role in tumor angiogenesis and spread in patients with head and neck cancer. [J Natl Cancer Inst 1998;90:587–96]**

Squamous cell carcinoma of the head and neck is among the most common human cancers and remains a major cause of mortality and morbidity throughout the world *(1)*. The most

**Affiliations of authors:* O. Gallo, I. Fini-Storchi, W. A. Vergari (Institute of Otolaryngology Head and Neck Surgery), E. Masini, L. Morbidelli, M. Ziche (Department of Preclinical and Clinical Pharmacology), A. Franchi (Institute of Anatomic Pathology), University of Florence, Italy.

Correspondence to: Marina Ziche, M.D., Department of Pharmacology, University of Florence, Viale Morgagni 65, 50134 Florence, Italy. E-mail: ziche@stat.ds.unifi.it

See "Notes" following "References."

important prognostic factor in patients with head and neck cancer is the presence of lymph node metastasis that correlates with locoregional recurrence, distant metastatic spread, and survival *(2)*. As documented in both clinical and experimental studies [reviewed in *(3)*], the ability of tumor cells to induce new blood vessel growth (angiogenesis) is a critical factor in determining tumor size as well as regional and distant tumor spread. If tumor angiogenesis is limited or prevented, tumor cells are much more likely to undergo programmed cell death (apoptosis) and tumor growth is strongly reduced. On the basis of the hypothesis that inhibition of angiogenesis results in a reduction of tumor size and metastases, several antiangiogenic drugs are presently under investigation as new therapeutic strategies in cancer treatment *(4,5)*.

Head and neck squamous cell carcinomas have been found to promote microvascular growth *in vivo*. Culture supernatants from head and neck squamous cell carcinoma cell lines grown *in vitro* have also been found to promote microvascular growth in the chorioallantoic membrane (angiogenesis) assay *(6,7)*. The density of microvessels in head and neck tumors has consistently been found to correlate with metastatic spread and prognosis *(8–10)*. However, no information is available to date regarding the nature of the angiogenic mediator implicated.

Immunohistochemical studies *(11–13)* have indicated that nitric oxide (NO) synthase (NOS) is present at higher levels in solid tumors, including those of the head and neck, compared with normal tissue *(11–13)*; however, no definite explanation for the role of NO in tumor growth has been provided *(14)*. NO functions as a mediator in the vascular, nervous, and immune systems by regulating vasodilation, vascular permeability, platelet adhesion and aggregation, and tumor blood flow *(15–17)*. We recently reported *(18,19)* that NO plays a central role in the angiogenic cascade by demonstrating that vascular endothelial growth factor (VEGF), released as a purified protein or produced by tumor cells, requires a functioning NO/cyclic guanosine monophosphate (cGMP) pathway within the endothelial compartment to promote neovascular growth.

We pursued the hypothesis that the NO pathway could control the sequential steps responsible for the neovascularization in head and neck cancer and thus influence tumor cell dissemination. To this aim, we have assessed the status of the NOS/cGMP pathway and its association with microvessel density in a series of 27 head and neck cancer patients distributed according to lymph node status. The ability to directly stimulate angiogenesis by head and neck cancer was assessed *in vivo* in the avascular cornea of albino rabbits. The role of NO in controlling angiogenesis was evaluated *in vivo* in rabbits receiving pharmacologic inhibition of NOS pathway produced by N^{ω}-nitro-L-arginine-methyl ester (L-NAME). The effect of the treatment was evaluated for its ability to prevent angiogenesis and to produce its regression in animals implanted with tumor tissue and with a squamous cell carcinoma cell line.

Materials and Methods

Patients and Tissue Collection

We studied 27 consecutive head and neck cancer patients who underwent surgical treatment of the primary tumor and of the neck at the Institute of Otolaryngology Head and Neck Surgery, University of Florence, during the period from April 1996 through April 1997. Clinical, epidemiologic, and histopathologic characteristics of these patients are shown in Table 1. All tumors were histologically confirmed to be squamous cell carcinomas and were graded as well differentiated, moderately differentiated, and poorly differentiated *(20,21)*.

Samples of the tumor core, the invasive edge of the tumor (tumor edge), and macroscopically healthy mucosa (control) were obtained from surgical specimens taken from each patient for NO analysis and angiogenesis assay. The portion of primary tumor was obtained by superficial biopsy of either the tumor bulk or the edge of the malignant ulcer for more infiltrative cancers. Samples of tissue identified as tumor edge were taken at the tumor periphery, whereas samples of control mucosa were obtained from a macroscopically uninvolved area 2–5 cm away from the tumor.

Cell Line and Culture Conditions

Human epidermoid carcinoma A-431 cells were obtained from the American Type Culture Collection (Rockville, MD). Cells were maintained in culture in Dulbecco's modified Eagle medium supplemented with 4500 g/L glucose, 2 m*M* L-glutamine, antibiotics (100 U/mL penicillin and 100 μg/mL streptomycin) (Sigma Chemical Co., St. Louis, MO), and 10% fetal calf serum (FCS) (Hyclone Laboratories, Inc., Logan, UT). Cells were split 1 : 5 twice a week.

Assay for NOS Activity

Fragments of tissues were homogenized at 0–4 °C in buffer containing 0.32 *M* sucrose, 20 m*M* HEPES (pH 7.2), 0.5 *M* EDTA, and 1 m*M* dithiothreitol. The homogenates were then processed, and the total NOS (tNOS) activity was measured as previously described *(22)*. The activity of the calcium-calmodulin-independent isoform (inducible NOS [iNOS]) was identified in tumor homogenates by measuring the enzymatic activity in buffer containing 1 m*M* EGTA and the calmodulin inhibitor trifluoperazine (100 μ*M*) (but no calcium) as previously reported *(22)*. For the evaluation of NOS activity in A-431 cells, the cells in 60-mm-diameter culture dishes were stimulated with 10 μg/mL lipopolysaccharide (LPS) for 24 hours and treated as described *(23)*. All determinations were performed in duplicate. NOS activity is expressed as picomoles of [^{3}H]citrulline formed per minute per milligram protein.

Measurement of cGMP Content

The levels of cGMP were measured in the aqueous phase of tissue homogenates extracted from 10% trichloroacetic acid with 0.5 *M* tri-*n*-octylamine dis-

Table 1. Clinical, epidemiologic, and histologic characteristics of 27 patients with squamous cell carcinoma of the head and neck

Characteristic	No. (%)
Total No. of patients	27 (100)
Age, y	
Median: 64	
Range: 43–75	
Sex	
Male	23 (85.1)
Female	4 (14.9)
Tumor stage *(20)*	
I	4 (14.9)
II	5 (18.5)
III	7 (25.9)
IV	9 (33.3)
Recurrences	2 (7.4)
Tumor site	
Larynx	18 (66.7)
Oral cavity	6 (22.2)
Oropharynx	3 (11.1)
Lymph node status	
Negative (N–)	16 (59.3)
Positive (N+)	11 (40.7)
Tumor grade *(21)*	
Well-differentiated	9 (33.3)
Moderately differentiated	12 (44.5)
Poorly differentiated	6 (22.2)

solved in 1,1,2-trichlorotrifluoroethane *(22)*. cGMP was measured with the use of a radioimmunoassay kit and ^{125}I-labeled cGMP (Amersham, Buckinghamshire, England) after acetylation of the samples with acetic anhydride. All determinations were performed in duplicate. Values are expressed as femtomoles of cGMP per milligram protein.

Immunofluorescence Analysis of Inducible Form of NOS

Tissue samples were frozen by immersion in liquid nitrogen, and 7-μm-thick sections were cut with the use of a cryostat. A-431 cells were grown on multichamber glass slides coated with gelatin. Both the sections and the cell specimens were fixed in 4% formaldehyde in phosphate-buffered saline (PBS) for 10 minutes at room temperature, washed thoroughly in PBS, and then immunolabeled with rabbit polyclonal anti-iNOS antibodies (Calbiochem, Inalco, Milan, Italy; working dilution 1 : 25). The immune reaction was detected with fluorescein isothiocyanate-labeled goat anti-rabbit serum (Sigma Chemical Co.; working dilution 1 : 40). The immunostained sections were mounted in Gel-mount (Biomeda, Foster City, CA) and then observed and photographed under an Axioskop UV light microscope (Zeiss, Oberkochen, Germany).

Microvessel Density Determination

Microvessels were identified in formalin-fixed, paraffin-embedded tumor tissue sections by use of an immunohistochemical method. A monoclonal antibody against CD-31 (JC/70; Dako, Glostrup, Denmark) diluted at 1 : 20 in PBS was employed. Incubation was carried out for 30 minutes, after digestion of the tissue sections with protease XIV (Sigma Chemical Co.) for 3 minutes at 37 °C. Sections were stained with use of a standard streptavidin–avidin–biotin technique (LSAB kit; Dako) with diaminobenzidine as chromogen and hematoxylin as counterstain. Microvessel density was determined by use of the procedure proposed by Weidner et al. *(24)*. The tumor area with the highest concentration of stained microvessels was identified at scanning magnification (×40), and microvessels were counted in a blinded manner by two independent operators at ×200 magnification (field area, 0.73 mm^2). Results are expressed as the highest number of microvessels identified within a ×200 field.

Rabbit Cornea Assay for Angiogenesis

Corneal assays for angiogenesis were performed in New Zealand white rabbits (Charles River, Calco, Como, Italy) as described *(25)* and in accordance with the guidelines of the European Economic Community (EEC) for animal care and welfare (EEC law No. 86/609). Tumor fragments (2–3 mg each) or cell suspensions (2.5 × 10^5 cells) were implanted into surgically produced corneal micropockets. The angiogenic response was assessed in a blinded manner by two independent operators, who did not perform the surgery, by use of a slit lamp stereomicroscope, and capillary progression was scored daily as previously reported *(26)*. The number of tissue samples inducing angiogenesis over the total number of implants performed was recorded during each observation. Implants that failed to produce a neovascular growth within 10 days were considered negative, while implants showing an inflammatory reaction were discarded. The potency of angiogenic activity (angiogenic score) was determined on the basis of the number and growth rate of newly formed capillaries and calculated as vessel density × distance from the limbus *(19,27)*. Corneas were removed at the end of the experiment as well as at defined intervals after surgery and/or treatment and were fixed in formalin for histologic examination.

To evaluate the effect of NOS inhibition on tumor angiogenesis, we administered L-NAME in the drinking water. L-NAME solutions (1 g/L) were freshly prepared every day. Water intake was approximately 200 mL/day per animal in the treated animals and was not different from that in animals in the control group. After 14 days of treatment and after 5 days from the end of treatment, rabbits were killed and autopsied. L-NAME was shown to have effectively inhibited NOS activity in the rabbits by evaluation of the contractility of the aortic rings *(27)*.

Differential Reverse Transcription–Polymerase Chain Reaction Analysis of NOS Expression

A-431 cells at 90% confluence were stimulated for 24 hours with test substances in the presence of 1% FCS. Total RNA from cells was isolated by the standard guanidinium thiocyanate-phenol-chloroform extraction *(28)*. Complementary DNA (cDNA) was synthesized as described *(29)*. Differential reverse transcription–polymerase chain reaction (RT–PCR) *(29)* for NOS isoforms was carried out by use of 5 μL of cDNA and specific primers with sequences as follows: for endothelial NOS (eNOS), sense 5′-GTG ATG GCG AAG CGA GTG AAG-3′, antisense 5′-CCG AGC CCG AAC ACA CAG AAC-3′; for iNOS, sense 5′-TCC GAG GCA AAC AGC ACA TTC A-3′, antisense 5′-GGG TTG GGG GTG TGG TGA TGT-3′ *(30)*. Calibration was performed by coamplification of the same cDNA sample with primers for glyceraldehyde 3-phosphate dehydrogenase (GAPDH) as internal standard, with sequences as described *(29)*. The PCR cycles were 1 minute at 94 °C, 1 minute at 60 °C, and 1.5 minutes at 72 °C for eNOS and iNOS. After 35 cycles of amplification, aliquots of each sample product (20 μL) were subjected to electrophoresis on a 3% agarose gel and stained with ethidium bromide. The size of the amplification products were 196 base pairs (bp) for GAPDH, 422 bp for eNOS, and 462 bp for iNOS. Image processing and analysis of the intensity of the bands were performed as described *(29)*. The results were analyzed as the ratio between the optical densities of the bands related to the amplification products of the target genes (eNOS and iNOS) and GAPDH.

Statistical Analysis

Statistical analysis was performed with use of Stata Statistic Software (release 5.0; Stata Corporation, College Station, TX) and Number Cruncher Statistical System (version 5.03; J. L. Hintze, Kaysville, UT). Data are reported as median and range for NOS/cGMP values and microvessel density and as means with 95% confidence intervals (CIs) for the angiogenesis score.

Within different tissue samples, NOS activity and cGMP levels were compared by use of a paired-value Wilcoxon test. The Wilcoxon rank sum test for unpaired data was used to assess the differences between NOS activity and cGMP levels in different tissues as well as microvessel density (CD-31 staining) according to lymph node status.

The relationships between the microvessel count and NOS activity and cGMP levels are reported as Spearman product-moment correlation coefficient (r_S). Moreover, differences among microvessel density according to tumor stage and tumor grade were analyzed by the use of the Kruskal–Wallis test.

A multivariate logistic regression analysis was performed to explore the effects of several possible prognostic factors (age, sex, tumor grade, tumor stage, tumor location, microvessel density, NOS activity, and cGMP levels) in predicting the risk of lymph node metastases. The final results of these analyses are the odds ratios (ORs) and their 95% CIs. The Wald statistic was used to test the following hypothesis: OR = 1.00.

For the angiogenesis data, multiple comparisons were performed by analysis of variance (ANOVA), and individual differences during each day of observation were tested by Fisher's test after the demonstration of significant intergroup differences by ANOVA.

All P values resulted from use of two-sided statistical tests. P values less than .05 were considered to indicate statistically significant differences.

Results

NOS Activity in Normal and Neoplastic Tissues of the Upper Aerodigestive Tract: Correlation With Lymph Node Metastasis

The activities of tNOS and iNOS were measured in biopsy specimens obtained from the tumor core, the invasive edge of the tumor (tumor edge), and normal mucosa in 27 patients who underwent surgery for head and neck cancer.

In specimens from unaffected mucosa, we detected a median baseline activity of tNOS and iNOS of 1.37 (range, 0.64–3.50) and 0.95 (range, 0.59–2.93) pmol/minute per mg protein, respectively. In tumor tissue, tNOS and iNOS levels were elevated to 4.08 (range, 2.03–8.78) and 3.67 (range, 1.94–6.85) pmol/minute per mg protein, respectively (paired-value Wilcoxon test, P<.0001 in all cases compared with normal control mucosa). The localization of NOS enzyme within the tumor cell population was assessed by immunofluorescence analysis on tumor sections by the use of polyclonal anti-iNOS antibodies. The strongest immunoreactivity was detected in cancer cells rather than in stromal cells. In normal control mucosa, the iNOS im-

munostaining was prevalent in the epithelial cells of the basal layer (Fig. 1, A and B).

The extent of NOS activity increment was significantly different according to the site of sampling within the tumor mass. The specimens at the invasive edge of the tumor exhibited the highest NOS activity. In tumor core samples, the median value was 4.08 (range, 2.03–8.78) pmol/minute per mg protein for tNOS and 3.67 (range, 1.94–6.85) pmol/minute per mg protein for iNOS; in samples from the tumor edge, the values were 5.36 (range, 2.73–23.74) pmol/minute per mg protein for tNOS and 4.06 (range, 2.04–21.83) pmol/minute per mg protein for iNOS (paired-value Wilcoxon test, tumor core versus tumor edge: P = .0003 for tNOS and P = .004 for iNOS activity, respectively).

We then analyzed NOS activity in tumor specimens from patients in the cohort according to tumor stage and metastatic behavior. Eleven patients had histologically confirmed cervical lymph node metastases (N+), whereas the remaining 16 patients had no clinical and histopathologic evidence of neck disease (N−). The levels of NOS in specimens from N+ patients were higher in each tissue sample examined compared with the specimens sampled from patients with histologically negative (i.e., no detectable cancer) lymph nodes (Fig. 2, A and B).

Accordingly, the specimens sampled at the periphery of the tumor had significantly higher tNOS and iNOS activities in more advanced disease (stage III or IV) *(20)* when compared with those from early stage lesions (stage I or II) (P = .016 and P = .04, respectively). No difference in the levels of tNOS and iNOS activities in specimens was found according to tumor grade.

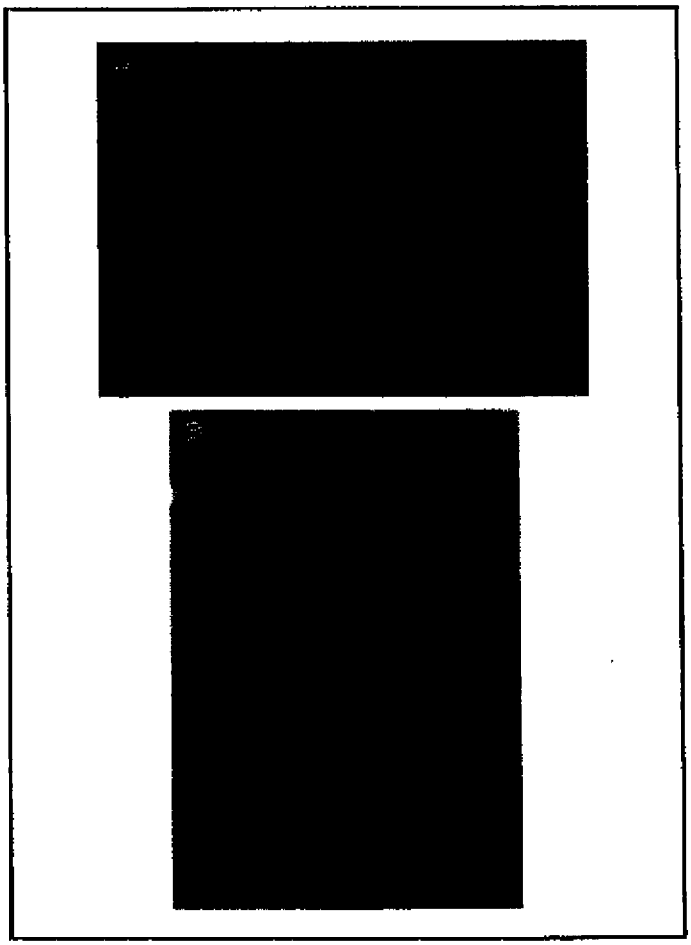

Fig. 1. Nitric oxide synthase (NOS) expression in tumor samples and normal mucosa from head and neck cancer patients. A representative picture is shown of immunofluorescence detection of inducible NOS in cancer tissue (**A**) and in normal control mucosa (**B**). Tissues were obtained from patients who underwent surgery for head and neck cancer (original magnification ×500; bar = 20 μm).

cGMP Determination in Normal Mucosa and Tumor Tissue: Correlation With Lymph Node Metastasis

cGMP is known to be the mediator of the response of the cells to NO *(31)*. To ascertain whether cGMP undergoes changes in head and neck cancers, we next measured cGMP levels in the aqueous phase of 10% trichloroacetic acid extracts of head and neck cancer tissues. Increased cGMP levels were detected in the tumor core and the tumor edge (median values of 5.39 [range, 3.35–7.93] and 6.37 [range, 3.84–16.81] fmol/mg protein, respectively) compared with normal control tissues (2.97 [range, 1.87–4.96] fmol/mg protein) (paired-value Wilcoxon test, P<.0001). The increment of cGMP levels in the tumor edge was significantly higher than in the tumor core (paired-value Wilcoxon test, P = .0001). When cGMP levels in tissues from N+ patients were compared with those from N− patients, a statistically significant difference was demonstrated only in the tumor edge (unpaired-value Wilcoxon test, P = .005) but not in unaffected control mucosa (P = .805) or in the tumor core (P = .621) (Fig. 2, C).

A progressive increase in cGMP was also detected from stage I to IV tumors only in peritumoral samples, although this finding was not statistically significant (P = .156). No difference in cGMP levels was found according to tumor grade.

Correlation of Microvessel Density With NOS Activity, cGMP Levels, Lymph Node Status, Tumor Grade, and Tumor Stage: Multivariate Analysis

We then assessed the extent of vascularization in our series of head and neck cancer patients. Immunohistochemical expression of CD-31 and Ki-67 was detected as previously described *(32)*. Microvessel counts in cancers from different patients and also within different areas of the same carcinoma were heterogeneous. The highest density of microvessels was observed at the invasive edge of the tumor and was associated with an increased proliferative activity of tumor cells (Fig. 3). According to tumor grade, we found a statistically significant increase in the microvessel counts passing from well-differentiated to poorly differentiated carcinomas (Spearman coefficient r_S = .435; P = .03), as well as from early stage cancers to more advanced cancers (r_S = .599; P = .001). N+ patients had a significantly higher median microvessel count in tumor specimens than N− patients (unpaired-value Wilcoxon test, P = .0002) (Fig. 3).

When we correlated tNOS and iNOS activities with microvessel density in the tumor core and tumor edge samples, we found that the increased tumor vascularization was statistically associated with an increased NOS activity (both tNOS and iNOS) (r_S = .468 and P = .016 and r_S = .434 and P = .027 in tumor core, respectively; r_S = .571 and P = .002 and r_S = .498 and P = .010 in tumor edge, respectively). A suggestive correlation between cGMP activity and CD-31 density was ob-

served only in samples from the tumor periphery (r_S = .352; P = .078). Furthermore, analysis indicated that there was a statistically significant association between vascular density and tumor stage (Kruskal–Wallis test; P = .018).

Thus, increased NOS activity and cGMP levels in both the tumor core and the tumor-front areas, high microvessel density, and poor histologic differentiation of cancers were significantly correlated with the presence of lymph node metastasis. Multivariate stepwise logistic regression analysis confirmed that microvessel count (CD-31 expression) was the most important and independent predictor of lymph node metastasis in our series (OR = 1.19; 95% CI = 1.07–2.89; Wald statistic = 3.79; P = .04), whereas cGMP levels were strongly suggestive (OR = 1.39; 95% CI = 0.97–1.99; Wald statistic = 1.79; P = .06).

Angiogenesis Produced by Head and Neck Cancer Tissue: Blockage by NOS Inhibitor

To assess whether the tumor expression of NOS activity could be directly correlated with an increased angiogenic potential, we assayed tumor specimens of head and neck cancer for angiogenesis in an *in vivo* experimental setting by use of the avascular rabbit cornea to monitor vascular growth. Fragments (2–3 mg) of tumor tissue and of unaffected control mucosa from 12 randomly selected patients with either positive (five patients) or negative (seven patients) lymph nodes were sampled and implanted in the corneal stroma. For each specimen, at least two fragments were tested. Within 5 days from the implant, all tumor fragments induced a strong angiogenic response in all the re-

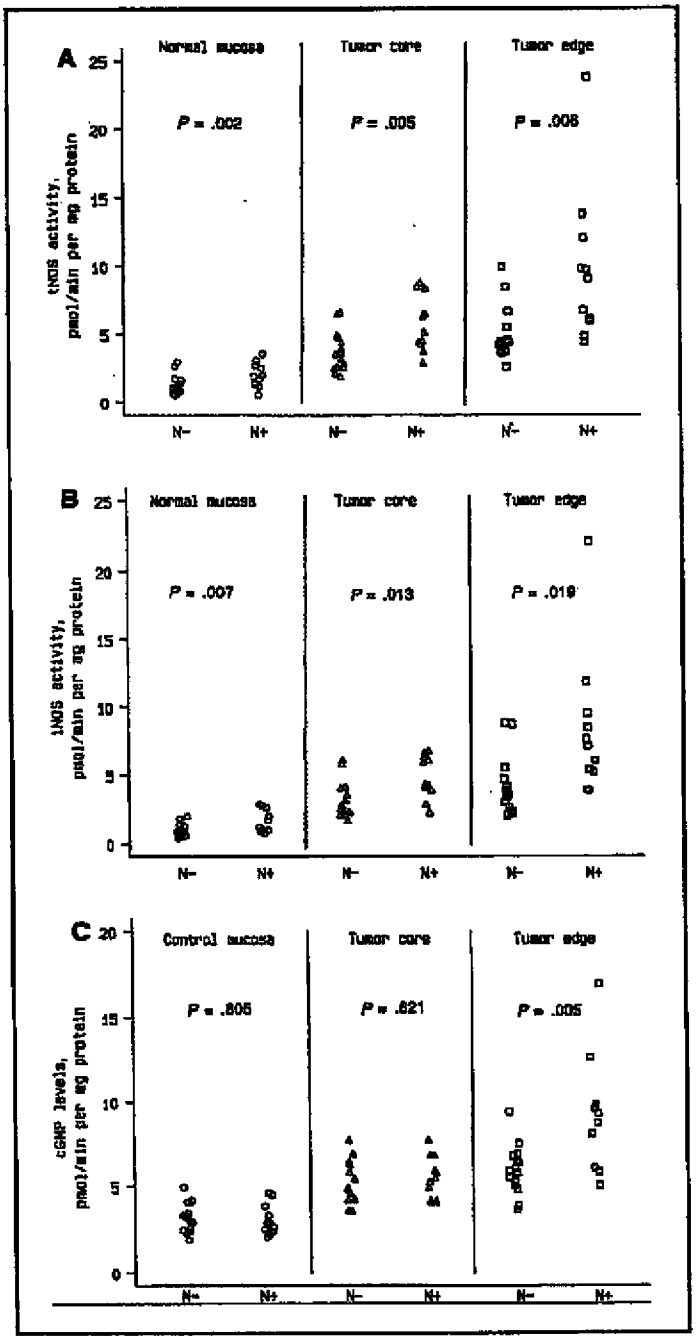

Fig. 2. Nitric oxide synthase (NOS) activity and cyclic guanosine monophosphate (cGMP) levels in tumor samples and normal mucosa from head and neck cancer patients. Total NOS (tNOS) (**A**) and inducible NOS (iNOS) (**B**) activities were measured in specimens selected from the tumor core, the invasive edge of the tumor (tumor edge), and normal mucosa (control). Data are expressed as pmol of [^{3}H]citrulline formed/minute per mg protein. tNOS and iNOS activities are sorted and compared according to lymph node status (11 lymph node-negative [N–] and 16 lymph node-positive [N+] patients). tNOS activities for control mucosa, tumor core, and tumor edge were 0.95 (range, 0.64–2.67), 3.62 (range, 2.03–6.54), and 4.37 (range, 2.73–9.72) pmol/minute per mg protein, respectively, for N– patients and 1.93 (range, 0.96–3.50), 4.96 (range, 2.79–8.78), and 8.97 (range, 4.61–23.74) pmol/minute per mg protein, respectively, for N+ patients. iNOS activities for control mucosa, tumor core, and tumor edge specimens were 0.81 (range, 0.59–2.16), 2.70 (range, 1.94–6.07), and 3.68 (range, 2.041–8.98) pmol/minute per mg protein, respectively, for N– patients and 1.10 (range, 0.63–2.93), 4.07 (range, 2.04–6.85), and 6.98 (range, 3.89–21.83) pmol/minute per mg protein, respectively, for N+ patients. **C)** cGMP levels were measured in the aqueous phase of tissue homogenates by radioimmunoassay. Data are expressed as fmol/mg of protein (11 N– and 16 N+ patients). cGMP levels in control mucosa, tumor core, and tumor edge were 3.01 (range, 2.02–4.96), 5.21 (range, 3.35–7.42), and 5.96 (range, 3.846–9.41) pmol/mg protein, respectively, for N– patients and 2.73 (range, 1.87–4.71), 5.63 (range, 3.91–7.93), and 8.52 (range, 4.96–16.81) pmol/mg protein, respectively, for N+ patients.

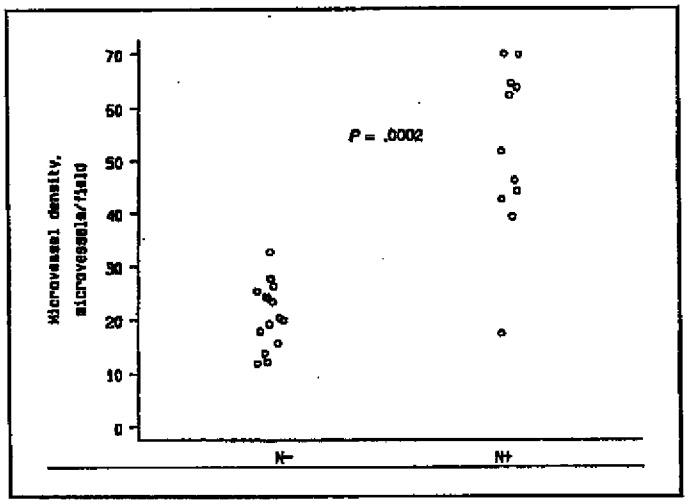

Fig. 3. Microvessel density in head and neck cancer according to lymph node status. The immunohistochemical staining was performed as described in the "Materials and Methods" section. Results are expressed as the highest number of microvessels identified within a ×200 field (11 lymph node-negative [N−] and 16 lymph node-positive [N+] patients). Median microvessel density was 21 microvessels per field (range, 12–32) and 52 microvessels per field (range, 18–70) for N− and N+ patients, respectively.

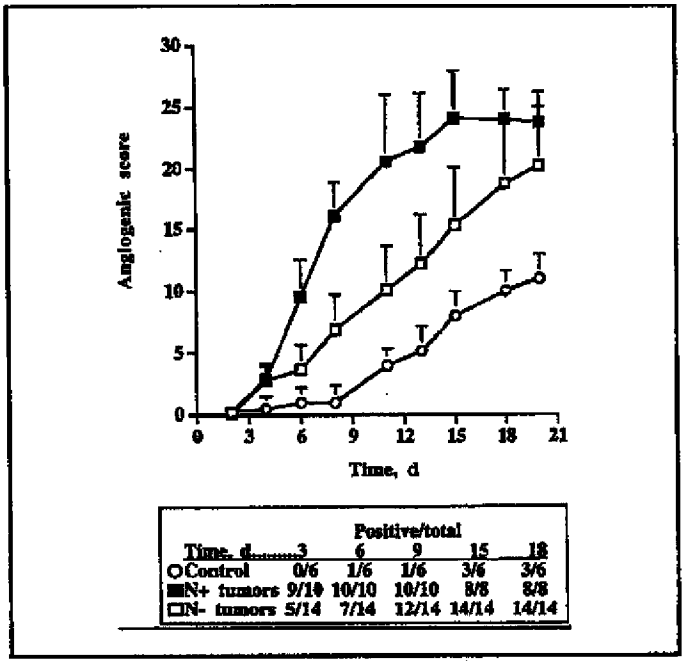

Time, d	3	6	9	15	18
	Positive/total				
○Control	0/6	1/6	1/6	3/6	3/6
■N+ tumors	9/10	10/10	10/10	8/8	8/8
□N− tumors	5/14	7/14	12/14	14/14	14/14

Fig. 4. Angiogenesis produced in the rabbit cornea by normal control mucosa and tumor specimens from head and neck cancer patients. Progression and efficiency over time of neovascular growth produced by nonpathologic mucosa and tumor tissue from head and neck cancer patients according to lymph node status. Angiogenesis is reported as angiogenic score (vessel length × vessel density) over time (days). In the inset is reported the number of tissue samples inducing angiogenesis over the total number of samples tested (positive/total). One animal bearing two samples was killed because of tumor overgrowth. The sample size consisted of six samples from three patients for normal mucosa, 14 samples from seven lymph node-negative (N−) patient tumors, and 10 samples (until day 10) from five lymph node-positive (N+) patient tumors. d = day.

cipient animals, whereas only a few of the implanted fragments elicited a modest angiogenic response (Fig. 4; Fig. 5, a). In the following days (days 12–15), angiogenesis induced by the tumors progressed; the newly formed capillaries reached the tumor implant, vascularized it, and produced an increase in the tumor size (Fig. 4; Fig. 5, a–c). Samples from N+ patients (14 fragments from seven patients) induced a more potent angiogenic response than samples from N− patients (50% increase in neovascularization, 10 fragments from five patients) (Fig. 4). Fisher's test after ANOVA analysis revealed a statistically relevant difference between the three groups from day 8 to day 18 of observation ($P = .01$).

To assess whether head and neck cancer-induced angiogenesis could be controlled by NOS inhibition, two experimental approaches were followed. In a first set of experiments, a group of animals received the NOS inhibitor L-NAME (1 g/L) in the drinking water once a consistent vascular network had been elicited by the tumor implant in the cornea (Fig. 5, c). By 24 hours after the administration of the NOS inhibitor, the diameters of the capillaries, measured by use of an ocular grid, were reduced by 50%, thus resulting in decreased tumor perfusion. In the following days, the vascular network started to regress (Fig. 6, A) (Fisher's test following ANOVA; $P = .05$), while the tumor size appeared grossly reduced (about 50% reduction) (Fig. 5, d–f; Fig. 6, A). Conversely, the tumor fragments in the control group did not change their size or vascular support.

In a second set of experiments, L-NAME treatment was given before the animals received the tumor implant. Under systemic inhibition of NOS activity in the host, angiogenesis was not produced by any implanted tumor samples (zero vascularized implants of eight performed in L-NAME-treated animals versus six of eight in untreated rabbits) (Fisher's test following ANOVA, $P = .01$ for days 8–18) (Fig. 6, B). When the treatment was interrupted, vascularization started from the 8th day after the suspension of treatment and progressed, reproducing the vascular pattern of untreated, implanted animals (Fig. 6, B).

Control by NO of Angiogenesis by Squamous Cell Carcinoma Cell Line A-431

To prove that the NO production by the neoplastic cell population triggered angiogenesis, we used the epidermoid cell line A-431 as an experimental tumor model. This cell line was characterized for NOS isoform activity and for NO production and was assessed in the rabbit cornea angiogenesis assay.

The extent of NO produced under basal conditions was approximately 3.8 (95% CI = 3.0–4.6) pmol/minute per mg protein. Immmunofluorescence analysis revealed a clear-cut cytoplasmic localization of iNOS immunostaining (data not shown). By differential RT–PCR, the constitutive presence of two NOS isoforms was shown, identifiable with the eNOS and the iNOS isoforms (mean ratios of 0.380 [95% CI = 0.351–0.409] and 0.341 [95% CI = 0.327–0.355] for eNOS and iNOS, respectively). NO production by A-431 cells could be modulated. Following a 24-hour stimulation with 10 μg/mL LPS, the NOS activity increased by approximately threefold (10.71 [95% CI = 9.45–11.97] pmol/minute per mg protein in LPS-treated cells [$P<.001$] versus basal control, Student's t test), an effect that could be specifically blocked by L-NAME (3.04 [95% CI = 2.56–3.52] pmol/minute per mg protein in cells treated with 2 mM L-NAME [$P<.01$] versus LPS alone, Student's t test).

A-431 cells treated *in vitro* for 24 hours with LPS (10 μg/mL) and then implanted in the cornea elicited angiogenesis within 5 days, and complete vascularization of the tumor cell implant

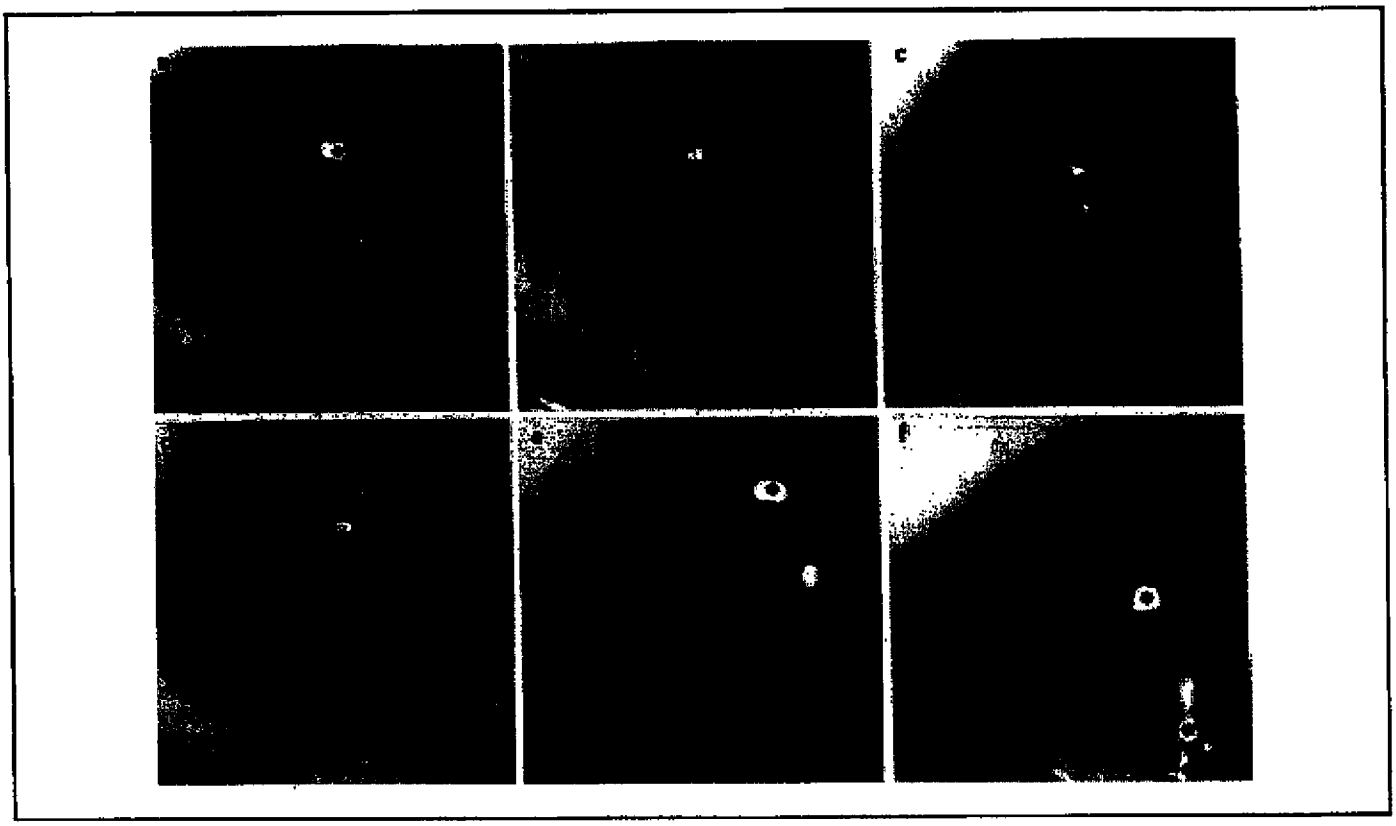

Fig. 5. Angiogenesis induced by tumor samples from head and neck cancer patients in the rabbit cornea: effect of the nitric oxide synthase (NOS) inhibitor N^{ω}-nitro-L-arginine-methyl ester (L-NAME). **Upper panels (a–c):** representative pictures taken at 6, 14, and 24 days, respectively, of neovascular growth produced by a tumor sample in the rabbit cornea. Within 5 days from the surgical implant, the tumor induced a strong neovascular outgrowth at the limbus (**a**, arrows). In the following days (day 14, **b**), angiogenesis induced by the tumor progressed and the newly formed capillaries reached the tumor implant and vascularized it, leading to an increase in the tumor size (day 24, **c**). **Lower panels:** The effect of L-NAME on tumor-induced angiogenesis is shown. L-NAME (1 g/L) was given in the drinking water for 1 week from day 26 after tumor implant. Pictures were taken at 2, 4, and 8 days from the beginning of the treatment. Within 2 days from systemic NOS inhibition, tumor vasculature consistently and progressively regressed (**d–f**) and the tumor size appeared grossly reduced (**e, f**).

occurred within 2 weeks from surgery (Fig. 7, open bars). In rabbits receiving L-NAME, the angiogenic response was reduced and delayed by 1 week (Fig. 7, hatched bars) (Fisher's test following ANOVA, $P = .01$ for days 13–15). When A-431 cells were treated *in vitro* with LPS in the presence of the NOS inhibitor, no angiogenesis was produced by the tumor cells, suggesting that NO production within the tumor cells was required for the angiogenic activity elicited by LPS treatment (Fig. 7, inset).

Discussion

In this study, we show that an increase in NOS activity is found in head and neck cancer, is associated with elevated cGMP levels, and correlates with tumor vascularization. Microvessel density and NOS activity correlate with lymph node metastases, indicating that an increased metastatic behavior is associated with a high NOS activity and angiogenesis. Animal studies demonstrate that transplant of tumor samples and a cell line from squamous cell carcinoma produce angiogenesis *in vivo* strictly linked to NO production, which is made to regress by treatment with NOS inhibitors. Taken together, these data suggest that, in head and neck cancer, the increased NOS activity can be regarded as a novel biologic marker for tumor progression related to angiogenesis and point to inhibitors of NOS as potential antiangiogenic drugs.

Head and neck cancer is a major cause of morbidity and mortality worldwide, representing 5% of all new cancers estimated in major Western countries per year *(1)*. The cure rate for head and neck cancer drops substantially when lymph nodes in the neck are involved *(2)*. Despite the continuous effort, no reliable prognostic markers for head and neck cancer exist. Angiogenesis is associated with regional and distant tumor spread in several solid tumors, including head and neck cancer *(8–10)*, thus predicting patient outcome. Although the microvessel count in tumor tissue correlates with tumor aggressiveness, little information is provided by this pathologic assessment about the biochemical pathway responsible for tumor angiogenesis.

NO has been shown to play a role in various phenomena involved in the angiogenic process. Observations that NOS expression is increased in fresh tumor tissue from gynecologic *(11)* and brain *(33)* neoplasms and that it can be generated *in vitro* by tumor cells *(34,35)* have suggested that NO may have a role in tumor growth and metastasis *(14)*. We have recently reported that NO controls angiogenesis by modulating the activity of angiogenic factor released by tumor cells as VEGF *(18,19)*.

NOS activity is normally present in the upper and lower airway epithelia, where it plays a major role in host airway

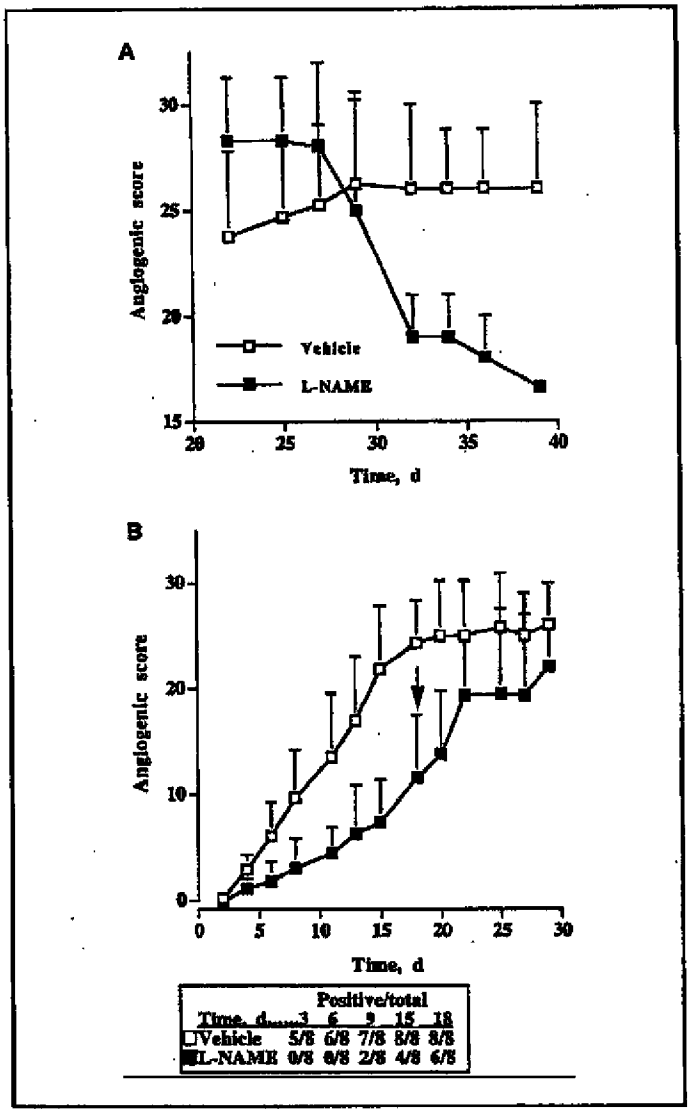

Fig. 6. Effect of the nitric oxide synthase (NOS) inhibitor N^{ω}-nitro-L-arginine-methyl ester (L-NAME) on angiogenesis induced by tumor samples from head and neck cancer patients in the rabbit cornea. A) Pattern of regression of tumor-induced angiogenesis by systemic NOS inhibition. L-NAME (1 g/L) was given to the animals in the drinking water for 1 week from day 26 after tumor implant (four fragments from two patients). B) Effect of systemic NOS inhibition in preventing tumor angiogenesis. Animals were treated with L-NAME for 1 week before surgery and for 12 days after corneal implant of tumor specimens. Neovascular growth in treated animals did not occur until up to 1 week after treatment discontinuation. The sample size was eight fragments from the tumor of four patients for both of the two experimental animal groups. The efficacy of L-NAME administration was evaluated during and at the end of the treatment as acetylcholine-induced relaxation in rabbit aortic rings preconstricted with phenylephrine as previously described *(27)*. Following 14 days from the beginning of the treatment, the vasorelaxation to 10 μ*M* acetylcholine was 11% (95% confidence interval [CI] = 5%–17%) in L-NAME-treated versus 68% (95% CI = 60%–76%) in aortic rings from untreated animals (10 for each group). After 5 days from the ending of L-NAME administration, vasorelaxation returned to normal levels (40% [95% CI = 34%–46%] relaxation, n = 8) (arrow in panel B). d = day.

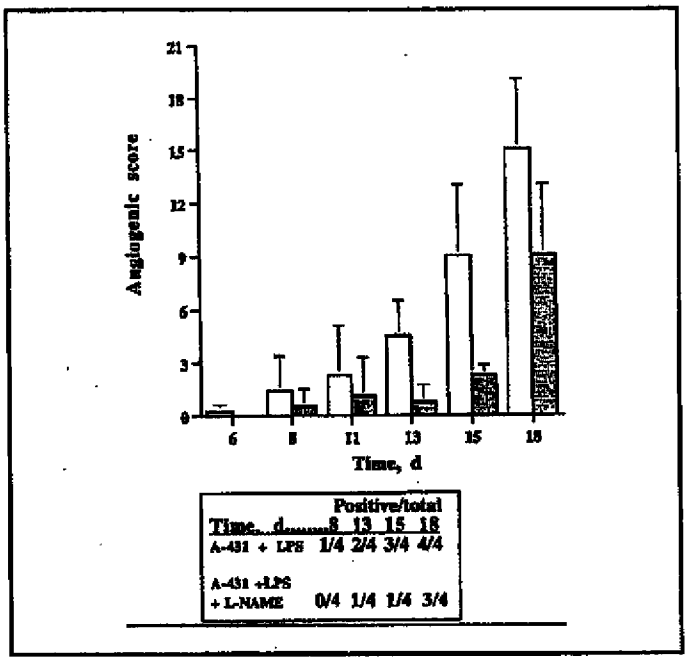

Fig. 7. Angiogenesis induced by A-431 cell line. Angiogenic response of A-431 cells stimulated for 24 hours before corneal implant with 10 μg/mL lipopolysaccharide (LPS) in control animals (open bars) and in rabbits pretreated with L-NAME (dotted bars). Systemic nitric oxide synthase (NOS) inhibition by L-NAME prevented and delayed angiogenesis. Data are expressed as angiogenic score over time (four implants for each experimental group). Table inset: *in vitro* treatment of the cells with 200 μM L-NAME reverted the angiogenic activity of LPS-stimulated A-431 cells. Data are expressed as positive implants over total implants performed (four implants for each experimental group). d = day.

defense mechanism and as a potential mediator of the inflammatory response *(36,37)*. Our results indicate that NOS activity in tumor tissue from patients with head and neck cancer is increased by threefold to fivefold. The rise in iNOS activity is differently distributed within the malignant tissue, being higher at the invasive tumor edge than in the tumor core. The detection of increased NOS/cGMP activity at the tumor front area discloses the heterogeneity of the metabolic demand/function of this signaling cascade within the tumor mass *(38)*. We demonstrate that increases in NOS activity, cGMP levels, and microvessel density are highly correlated with the metastatic phenotype of head and neck cancer at the tumor periphery.

At the interface between tumor and host normal tissue, remodeling of the extracellular matrix and increased angiogenesis take place *(39)*. Multivariate analysis confirms that the intensity of vascularity and cGMP levels at the invasive edge of the tumor correlate independently with the probability of metastasis from the other clinical and biologic features analyzed. Thus, a direct link between increased NOS/cGMP activity and angiogenesis with a more aggressive and metabolically active tumor cell subpopulation can be postulated, indicating a central role of NO production by head and neck cancer in influencing the risk of regional metastasis through neoangiogenesis.

The hypothesis that the increased NOS activity of tumor tissue is a key factor in promoting angiogenesis is demonstrated by the experiment in which tumor fragments are tested in the rabbit cornea. Consistent with angiogenesis being a risk factor for tumor spread, tumor samples from patients with lymph node metastases exhibit a higher angiogenic activity in rabbit corneas. Inhibition of angiogenesis is being proposed as a new approach to control tumor growth and prevent metastasis *(4)*. The angiogenesis induced by head and neck tumor fragments is sensitive to NOS inhibition. Persistent vasodilation is a specific feature in tumor vasculature that also appears to be unresponsive to vaso-

constrictor agents because of increased NOS activity *(40)*. The rapid regression of tumor angiogenesis under systemic NOS inhibition reported here proves that the tumor vasculature in the proliferative state of angiogenesis is highly susceptible to NOS inhibition and regresses. We recently documented that NO sustains endothelial proliferation by inducing the expression of endogenous basic fibroblast growth factor *(29)*. In the presence of NOS inhibition, endothelial cells do not produce basic fibroblast growth factor that can act as a survival factor, possibly modulating apoptosis. Therefore, while NOS inhibition can affect tumor growth by reducing blood flow via vasoconstriction *(41)*, it is also likely that this treatment induces apoptosis in proliferating endothelium by interfering with the autocrine survival mechanism of endothelial cells, ultimately leading to suppression of tumor blood supply. We have demonstrated that the NOS inhibitor L-NAME is able to prevent tumor angiogenesis. In fact, as long as NOS is inhibited in the host tissue, neovascularization is not promoted by the tumor tissue or by the epidermoid cell line. Once the NOS activity is re-established (i.e., released from inhibition) in the host, tumor angiogenesis starts again, suggesting that, like other antiangiogenic drugs, NOS inhibitors require long-term administration to control angiogenesis.

Although a body of evidence indicates a definite role for NO in tumor growth, the end point of increased NO production within the tumor mass is controversial *(42)*. In experimental models, NO facilitates tumor growth and vascularization *(14,43)*. Conversely, increased production of NO by tumor cells causes lysis of bystander cells *(44)*. Our findings suggest that the up-regulation of NOS is a crucial point in the multistep process of head and neck cancerogenesis, being associated with the acquisition of an angiogenic and metastatic phenotype. Although we cannot provide a definite explanation for the mechanism by which NO controls angiogenesis in head and neck cancer, there are suggestive observations. The involvement of the p53 tumor suppressor gene in the regulation of NOS expression *(45)* and angiogenesis *(46)* raises the possibility that the p53 mutation found in approximately 50% of head and neck cancers *(47)* could result in an increase in NO production and, thus, in NO-related angiogenesis, ultimately leading to tumor progression. The existence of a link between VEGF and NO in different biologic settings is also increasingly recognized *(18,19,48)*. VEGF expression correlates with increased vascularity and malignant progression, an event that is likely to occur in head and neck cancer patients *(49,50)*. We recently reported that breast carcinoma cells overexpressing VEGF require the NO pathway to induce angiogenesis *in vivo (19)* and that NO is an upstream signal in the molecular cascade following KDR (kinase domain region) receptor activation in vascular endothelium *(51)*. Thus, NO production by squamous cell carcinoma could possibly control VEGF expression and fate within the tumor.

In conclusion, this study documents that a strong correlation exists between the activity of the NOS pathway, angiogenesis, and metastatic behavior in head and neck cancer. Despite the evidence that assessment of microvessel counts correlates with prognosis in several solid tumors, the pathologic assessment of vascular density does not currently give information about the biochemical pathway involved in tumor angiogenesis and cannot be readily used for monitoring of therapeutic effects or give an overall assessment of angiogenesis. On the basis of the results reported here, we suggest that monitoring NOS activity might provide further information regarding the biologic behavior of head and neck cancer in relation to angiogenesis and tumor spread.

References

(1) Parker SL, Tong T, Bolden S, Wingo PA. Cancer statistics, 1996. CA Cancer J Clin 1996;46:5–27.

(2) Shah JP, Medina JE, Shaha AR, Schantz SP, Marti JR. Cervical lymph node metastasis. Curr Probl Surg 1993;30:1–335.

(3) Folkman J. Angiogenesis in cancer, vascular, rheumatoid and other disease. Nat Med 1995;1:27–31.

(4) Barinaga M. Designing therapies that target tumor blood vessels. Science 1997;275:482–4.

(5) Fidler IJ, Ellis LM. The implications of angiogenesis for the biology and therapy of cancer metastasis. Cell 1994;79:185–8.

(6) Petruzzelli GJ, Snyderman CH, Johnson JT, Myers EN. Angiogenesis induced by head and neck squamous cell carcinoma xenografts in the chick embryo chorioallantoic membrane model. Ann Otol Rhinol Laryngol 1993; 102:215–21.

(7) Lingen MW, Polverini PJ, Bouck NP. Retinoic acid induces cells cultured from oral squamous cell carcinomas to become anti-angiogenic. Am J Pathol 1996;149:247–58.

(8) Gasparini G, Weidner N, Maluta S, Pozza F, Boracchi P, Mezzetti M, et al. Intratumoral microvessel density and p53 protein: correlation with metastasis in head-and-neck squamous-cell carcinoma. Int J Cancer 1993;55: 739–44.

(9) Albo D, Granick MS, Jhala N, Atkinson B, Solomon MP. The relationship of angiogenesis to biological activity in human squamous cell carcinomas of the head and neck. Ann Plast Surg 1994;32;588–92.

(10) Klijanienko J, el-Naggar AK, de Braud F, Rodriguez-Peralto JL, Rodriguez R, Itzhaki M, et al. Tumor vascularization, mitotic index, histopathologic grade, and DNA ploidy in the assessment of 114 head and neck squamous cell carcinomas. Cancer 1995;75:1649–56.

(11) Thomsen LL, Lawton FG, Knowles RG, Beesley JE, Riveros-Moreno V, Moncada S. Nitric oxide synthase activity in human gynecological cancer. Cancer Res 1994;54:1352–4.

(12) Thomsen LL, Miles DW, Happerfield L, Bobrow LG, Knowles RG, Moncada S. Nitric oxide synthase activity in human breast cancer. Br J Cancer 1995;72:41–4.

(13) Rosbe KW, Prazma J, Petrusz P, Mims W, Ball SS, Weissler MC. Immunohistochemical characterization of nitric oxide synthase activity in squamous cell carcinoma of the head and neck. Otolaryngol Head Neck Surg 1995;113;541–9.

(14) Jenkins DC, Charles IG, Thomsen LL, Moss DW, Holmes LS, Baylis SA, et al. Roles of nitric oxide in tumor growth. Proc Natl Acad Sci U S A 1995;92:4392–6.

(15) Moncada S, Palmer RM, Higgs EA. Nitric oxide: physiology, pathophysiology, and pharmacology. Pharmacol Rev 1991;43;109–42.

(16) Nathan C, Xie QW. Nitric oxide synthases: roles, tolls, and controls. Cell 1994;78:915–8.

(17) Schmidt HH, Walter U. NO at work. Cell 1994;78:919–25.

(18) Morbidelli L, Chang CH, Douglas JG, Granger HJ, Ledda F, Ziche M. Nitric oxide mediates mitogenic effect of VEGF on coronary venular endothelium. Am J Physiol 1996;270:H411–5.

(19) Ziche M, Morbidelli L, Choudhuri R, Zhang HT, Donnini S, Granger HJ, et al. Nitric oxide synthase lies downstream from vascular endothelial growth factor-induced but not basic fibroblast growth factor-induced angiogenesis. J Clin Invest 1997;99:2625–34.

(20) International Union Against Cancer. TNM classification of malignant tumours. Berlin: Springer-Verlag, 1987.

(21) Michael L. Squamous cell carcinoma. In: Ferlito A, editor. Surgical pathology of laryngeal neoplasms. London: Chapman & Hall Medical, 1996: 123–42.

(22) Bani D, Masini E, Bello MG, Bigazzi M, Bani Sacchi TB. Relaxin activates the L-arginine-nitric oxide pathway in human breast cancer cells. Cancer Res 1995;55:5272–5.

(23) Ghigo D, Arese M, Todde R, Vecchi A, Silvagno F, Costamagna C, et al.

Middle T antigen-transformed endothelial cells exhibit an increased activity of nitric oxide synthase. J Exp Med 1995;181:9–19.
(24) Weidner N, Semple JP, Welch WR, Folkman J. Tumor angiogenesis and metastasis—correlation in invasive breast carcinoma. N Engl J Med 1991; 324:1–8.
(25) Ziche M, Gullino PM. Angiogenesis and neoplastic progression *in vitro*. J Natl Cancer Inst 1982;69:483–7.
(26) Ziche M, Alessandri G, Gullino PM. Gangliosides promote the angiogenic response. Lab Invest 1989;61:629–34.
(27) Ziche M, Morbidelli L, Masini E, Amerini S, Granger HJ, Maggi CA, et al. Nitric oxide mediates angiogenesis *in vivo* and endothelial cell growth and migration *in vitro* promoted by substance P. J Clin Invest 1994;94: 2036–44.
(28) Chomczynski P, Sacchi N. Single-step method of RNA isolation by acid guanidinium thiocyanate-phenol-chloroform extraction. Anal Biochem 1987;162:156–9.
(29) Ziche M, Parenti A, Ledda F, Dell'Era P, Granger HJ, Maggi CA, et al. Nitric oxide promotes proliferation and plasminogen activator production by coronary venular endothelium through endogenous bFGF. Circ Res 1997;80:845–52.
(30) Reiling N, Ulmer AJ, Duchrow M, Ernst M, Flad HD, Hauschildt S. Nitric oxide synthase: mRNA expression of different isoforms in human monocytes/macrophages. Eur J Immunol 1994;24:1941–4.
(31) Ignarro LJ. Signal transduction mechanisms involving nitric oxide. Biochem Pharmacol 1991;41:485–90.
(32) Franchi A, Gallo O, Boddi V, Santucci M. Prediction of occult neck metastases in laryngeal carcinoma: role of proliferating cell nuclear antigen, MIB-1, and E-cadherin immunohistochemical determination. Clin Cancer Res 1996;2:1801–8.
(33) Cobbs CS, Brenman JE, Aldape KD, Bredt DS, Israel MA. Expression of nitric oxide synthase in human central nervous system tumors. Cancer Res 1995;55:727–30.
(34) Villiotou V, Deliconstantinos G. Nitric oxide, peroxynitrite and nitrosocompounds formation by ultraviolet A (UVA) irradiated human squamous cell carcinoma: potential role of nitric oxide in cancer prognosis. Anticancer Res 1995;15:931–42.
(35) Jenkins DC, Charles IG, Baylis SA, Lelchuk R, Radomski MW, Moncada S. Human colon cancer cell lines show a diverse pattern of nitric oxide synthase gene and nitric oxide generation. Br J Cancer 1994;70: 847–9.
(36) Green SJ. Nitric oxide in mucosal immunity [published erratum appears in Nat Med 1995;1:717]. Nat Med 1995;1:515–7.
(37) Guo FH, De Raeve HR, Rice TW, Stuehr DJ, Thunnissen FB, Erzurum SC. Continuous nitric oxide synthesis by inducible nitric oxide synthase in normal human airway epithelium *in vivo*. Proc Natl Acad Sci U S A 1995; 92:7809–13.
(38) Heppner GH. Tumor heterogeneity. Cancer Res 1984;44:2259–65.
(39) Dunstan S, Powe DG, Wilkinson M, Pearson J, Hewitt RE. The tumour stroma of oral squamous cell carcinomas show increased vascularity compared with adjacent host tissue. Br J Cancer 1997;75:559–65.
(40) Andrade SP, Hart IR, Piper PJ. Inhibitors of nitric oxide synthase selectively reduce flow in tumor-associated neovasculature. Br J Pharmacol 1992;107:1092–5.
(41) Tozer GM, Prise VE, Chaplin DJ. Inhibition of nitric oxide synthase induces a selective reduction in tumor blood flow that is reversible with L-arginine. Cancer Res 1997;57:948–55.
(42) Vamvakas S, Schmidt HH. Just say NO to cancer? [editorial]. J Natl Cancer Inst 1997;89:406–7.
(43) Takahashi M, Fukuda K, Ohata T, Sugimura T, Wakabayashi K. Increased expression of inducible and endothelial constitutive nitric oxide synthases in rat colon tumors induced by azoxymethane. Cancer Res 1997;57: 1233–7.
(44) Xie K, Huang S, Dong Z, Juang SH, Wang Y, Fidler II. Destruction of bystander cells by tumor cells transfected with inducible nitric oxide (NO) synthase gene. J Natl Cancer Inst 1997;89:421–7.
(45) Forrester K, Ambs S, Lupold SE, Kapust RB, Spillare EA, Weinberg WC, et al. Nitric oxide-induced p53 accumulation and regulation of inducible nitric oxide synthase expression by wild-type p53. Proc Natl Acad Sci U S A 1996;93:2442–7.
(46) Dameron KM, Volpert OV, Tainsky MA, Bouck N. Control of angiogenesis in fibroblasts by p53 regulation of thrombospondin-1. Science 1994; 265:1582–4.
(47) Gallo O, Chiarelli I, Bianchi S, Calzolari A, Porfirio B. Loss of the p53 mutation after irradiation is associated with increased aggressiveness in recurred head and neck cancer. Clin Cancer Res 1996;2:1577–83.
(48) Tsurumi Y, Murohara T, Krasinski K, Chen D, Witzenbichler B, Kearney M, et al. Reciprocal relation between VEGF and NO in the regulation of endothelial integrity. Nat Med 1997;3:879–86.
(49) Sauter E, Nesbit M, Herlyn M. Vascular endothelial growth factor (VEGF) is a marker of disease progression in head and neck cancer [abstract]. Proc Am Assoc Cancer Res 1997;38:331.
(50) Inoue K, Ozeki Y, Saganuma T, Sugiura Y, Tanaka S. Vascular endothelial growth factor expression in primary esophageal squamous cell carcinoma. Association with angiogenesis and tumor progression. Cancer 1997; 79: 206–13.
(51) Parenti A, Morbidelli L, Cui XL, Douglas JG, Hood JD, Granger HJ, et al. Nitric oxide is an upstream signal of vascular endothelial growth factor-induced extracellular signal-regulated kinase$_{1/2}$ activation in postcapillary endothelium. J Biol Chem 1998;273:4220–6.

Notes

O. Gallo and E. Masini contributed equally to this work.

Supported by funds from the Italian Association for Cancer Research (Special Project "Angiogenesis") (M. Ziche), European Communities BIOMED-2("Angiogenesis and Cancer") (M. Ziche), the National Council of Research (M. Ziche and E. Masini), and the Italian Ministry of University, Scientific and Technological Research (M. Ziche).

We thank Professor D. Bani, University of Florence, for conducting the immunofluorescence analysis and Professor V. Boddi, University of Florence, for doing the statistical evaluation.

Manuscript received October 30, 1997; revised February 10, 1998; accepted February 13, 1998.

British Journal of Pharmacology (1996) 118, 829–838

Nitric oxide: a key mediator in the early and late phase of carrageenan-induced rat paw inflammation

[1]Daniela Salvemini, Zhi-Qiang Wang, Pamela S. Wyatt, David M. Bourdon, *Margaret H. Marino, Pamela T. Manning & Mark G. Currie

Inflammatory Diseases Research, G.D. Searle Co., 800 N. Lindbergh Boulevard, St Louis, Missouri 63167, U.S.A. and * Protein Biochemistry Department, G.D. Searle Co., 700 Chesterfield Parkway, St Louis, MO 63017, U.S.A.

1 The role of nitric oxide (NO) derived from constitutive and inducible nitric oxide synthase (cNOS and iNOS) and its relationship to oxygen-derived free radicals and prostaglandins (PG) was investigated in a carrageenan-induced model of acute hindpaw inflammation.

2 The intraplantar injection of carrageenan elicited an inflammatory response that was characterized by a time-dependent increase in paw oedema, neutrophil infiltration, and increased levels of nitrite/nitrate (NO_2^-/NO_3^-) and prostaglandin E_2(PGE_2) in the paw exudate.

3 Paw oedema was maximal by 6 h and remained elevated for 10 h following carrageenan administration. The non-selective cNOS/iNOS inhibitors, N^G- monomethyl-L-arginine (L-NMMA) and N^G-nitro-L-arginine methyl ester (L-NAME) given intravenously (30–300 mg kg^{-1}) 1 h before or after carrageenan administration, inhibited paw oedema at all time points.

4 The selective iNOS inhibitors, N-iminoethyl-L-lysine (L-NIL) or aminoguanidine (AG), failed to inhibit carrageenan-induced paw oedema during the first 4 h following carrageenan administration, but inhibited paw oedema at subsequent time points (from 5–10 h). iNOS mRNA was detected between 3 to 10 h following carrageenan administration using ribonuclease protection assays. iNOS protein was first detected 6 h and was maximal 10 h following carrageenan administration as shown by Western blot analysis. Administration of the iNOS inhibitors 5 h after carrageenan (a time point where iNOS was expressed) inhibited paw oedema at all subsequent time points. Infiltrating neutrophils were not the source of iNOS since pretreatment with colchicine (2 mg kg^{-1}) suppressed neutrophil infiltration, but did not inhibit the iNOS mRNA expression or the elevated NO_2^-/NO_3^- levels in the paw exudate.

5 Inhibition of paw oedema by the NOS inhibitors was associated with attenuation of both the NO_2^-/NO_3^- and PGE_2 levels in the paw exudate. These inhibitors also reduced the neutrophil infiltration at the site of inflammation.

6 Recombinant human Cu/Zn superoxide dismutase coupled to polyethyleneglycol (PEGrhSOD; 12×10^3 u kg^{-1}), administered intravenously either 30 min prior to or 1 h after carrageenan injection, inhibited paw oedema and neutrophil infiltration, but had no effect on NO_2^-/NO_3^- or PGE_2 production in the paw exudate. The administration of catalase (40×10^3 u kg^{-1}), given intraperitoneally 30 min before carrageenan administration, had no effect on paw oedema. Treatment with desferrioxamine (300 mg kg^{-1}), given subcutaneously 1 h before carrageenan, inhibited paw oedema during the first 2 h after carrageenan administration, but not at later times.

7 These results suggest that the NO produced by cNOS is involved in the development of inflammation at early time points following carrageenan administration and that NO produced by iNOS is involved in the maintenance of the inflammatory response at later time points. The potential interactions of NO with superoxide anion and PG is discussed.

Keywords: Acute inflammation; nitric oxide synthase inhibitors; superoxide anion; peroxynitrite; carrageenan

Introduction

Carrageenan-induced paw oedema is a useful model to assess the contribution of mediators involved in vascular changes associated with acute inflammation. The development of oedema in the rat hindpaw following the injection of carrageenan has been described as a biphasic event in which various mediators operate in sequence to produce this inflammatory response (Vinegar *et al.*, 1969). The initial phase of oedema (0–1 h), which is not inhibited by non-steroidal anti-inflammatory drugs such as indomethacin or aspirin, has been attributed to the release of histamine, 5-hydroxytryptamine (5-HT) and bradykinin (Di Rosa *et al.*, 1971). In contrast, the second accelerating phase of swelling (1–6 h), has been correlated with the elevated production of prostaglandins (PG, Di Rosa & Willoughby, 1971; Di Rosa *et al.*, 1971), and more recently has been attributed to the induction of inducible cyclo-oxygenase (COX-2) in the hindpaw (Seibert *et al.*, 1994). Local neutrophil infiltration and activation also contribute to this inflammatory response (Di Rosa & Sorrentino, 1968; Vinegar *et al.*, 1971; Boughton-Smith *et al.*, 1993) by producing, among other mediators, oxygen-derived free radicals such as superoxide anion (O_2^-) and hydroxyl radicals (see Fantone & Ward, 1982 for review).

Another important mediator in acute and chronic inflammation is nitric oxide (NO). NO is generated via the oxidation of the terminal guanidino nitrogen atom of L-arginine by the enzyme, nitric oxide synthase (NOS). Three major isoforms of NOS have been identified. Two expressed constitutively, are calcium/calmodulin-dependent and are classified together as constitutive NOS isoforms (cNOS). The third is a cytokine-inducible, calcium/calmodulin-independent isoform of NOS (iNOS) (see Moncada *et al.*, 1991; Moncada & Higgs, 1993 for reviews). NO is a potent vasodilator; its in-

[1] Author for correspondence.

volvement during an inflammatory response may be related to its ability to increase vascular permeability and oedema through changes in local blood flow (see Moncada *et al.*, 1991; Moncada & Higgs, 1993 for reviews). Furthermore, NO has been shown to increase the production of pro-inflammatory prostaglandins in *in vitro* (Rettori *et al.*, 1992; Salvemini *et al.*, 1993; Inoue *et al.*, 1993; Corbett *et al.*, 1993; Davidge *et al.*, 1995), *ex vivo* (Salvemini *et al.*, 1994; Sautebin & Di Rosa, 1994) and *in vivo* studies (Salvemini *et al.*, 1995a,b; Sautebin *et al.*, 1995), potentially by S-nitrosation of cysteine residues in the catalytic domain of cyclo-oxygenase (COX) enzymes (Hajjar *et al.*, 1995).

In addition, NO can also react with superoxide anion to form peroxynitrite ($ONOO^-$), a potent oxidizing molecule capable of eliciting lipid peroxidation and cellular damage (Beckman *et al.*, 1990; Radi *et al.*, 1991; Rubbo *et al.*, 1994). These findings suggest that NO has the ability to exert multiple cytotoxic effects during inflammatory responses including an increase PG production as well as the formation of $ONOO^-$.

The interactions between NO, free radicals and the COX pathway in acute inflammation are poorly defined. NO appears to be involved in the acute inflammatory response following the intraplantar injection of carrageenan into the rat hindpaw as non-selective cNOS/iNOS inhibitors such as N^G-monomethyl-L-arginine (L-NMMA) attenuate oedema at the early times (up to 3 h) following carrageenan administration (Ialenti *et al.*, 1992). However, the effects of NOS inhibitors at later times after the onset of the inflammatory response have not been investigated and the role of iNOS in this model of inflammation is not known. Therefore, we have used this model of acute inflammation induced by the injection of carrageenan into the rat hindpaw to assess the roles of constitutive and inducible nitric oxide synthase in the progression of the inflammatory response, as well as to study the relationship that may exist between NO, prostaglandins and oxygen-derived free radicals.

Methods

Carrageenan paw oedema

Male Sprague-Dawley rats (175–200 g, Harlan Sprague Dawley, Indianapolis, IN, U.S.A.) were housed and cared for under the guidelines of the institutional animal care and use committee. They received a subplantar injection of carrageenan (0.1 ml of a 1% suspension in 0.85% saline) into the right hind paw. Paw volume was measured with a plethysmometer (Ugo-Basile, Varese, Italy) immediately prior to the injection of carrageenan and thereafter at hourly intervals for 10 h. Oedema was expressed as the increase in paw volume (ml) after carrageenan injection relative to the pre-injection value for each animal. Unless specified, drugs were administered intravenously in a volume of 2.5 ml kg, either 1 h before or 1 h after carrageenan injection.

Determination of nitrite/nitrate and prostaglandin E_2 from carrageenan-injected rat paws

At specified times after the intraplantar injection of carrageenan, rats were killed and each paw was cut at the level of the calcaneus bone. Paws were gently centrifuged at 250 *g* for 20 min in order to recover a sample of the oedematous fluid. The volume of fluid that was recovered from each paw was measured. Blood was removed from the fluid sample by filtering through a 10,000 mol. wt. cut-off filter (Millipore, Bedford, MA, U.S.A.). Nitrite/nitrate (NO_2^-/NO_3^-) concentrations were measured by the diaminonapthalene (DAN) assay as described (Misko *et al.*, 1993b). Nitrate in the paw fluid samples (10 μl) was converted to nitrite by the incubation with nitrate reductase (14 mu) and the reduced form of nicotinamide adenine dinucleotide phosphate (1 nmol) for 10 min at room temperature. The reaction was terminated by dilution with water and addition of the DAN reagent. NO_2^-/NO_3^- concentrations were then determined fluorometrically (Misko *et al.*, 1993b). The PGE_2 concentration in each paw fluid sample was determined by specific ELISAs (Cayman Chemicals, Ann Arbor, MI, U.S.A.). All determinations were performed in duplicate. Total (T) NO_2^-/NO_3^- or PGE_2 present in the entire oedematous fluid of each paw was calculated as follows:

$$T = \frac{\text{pmol nitrate/nitrate or ng PGE2 in the sample} \times \text{paw oedema volume(ml)}}{\text{sample volume(ml)}}$$

Results are expressed as nmol NO_2^-/NO_3^- or ng PGE_2/paw.

Myeloperoxidase assay

Myeloperoxidase (MPO), a haemoprotein located in azurophil granules of neutrophils, has been used as a biochemical marker for neutrophil infiltration into tissues (Bradley *et al.*, 1982). In the present study, MPO was measured photometrically by a method similar to that described previously (Laight *et al.*, 1994). At the specified times following the intraplantar injection of carrageenan, tissue from the pads of the rat hindpaw was removed with a scalpel and 5 mm pieces were then obtained with a tissue punch (5 mm punch from Roboz, Rockville, MD, U.S.A.). Each piece of tissue was homogenized in 1 ml of 50 mM phosphate buffer, pH 6, containing 0.5% hexadecyltrimethylammonium bromide (HTAB). The homogenized rat paw tissues were frozen (on dry ice) and thawed (immersion in warm water, 37°C) three times. Following centrifugation at 35,000 *g* for 20 min, 7 μl aliquots of each of the supernatants were mixed in wells of a 96 well plate with 200 μl of assay buffer (50 mM phosphate buffer, pH 6, containing 0.5% HTAB, 0.167 mg ml^{-1} *O*-dianisidine hydrochloride and 0.0005% hydrogen peroxide). Changes in absorbance at 460 nm were measured spectrophotometrically over 5 min.

iNOS nuclease protection assay

At various times following the intraplantar injection of carrageenan, rats were killed and paws were removed, immediately frozen on dry ice and stored at −80°C. RNA was prepared from the paws by first pulverizing the frozen paws into a fine powder. The frozen powder was then partially solubilized in a denaturing solution containing 4 M guanidine thiocyanate (Fluka), 25 mM Na citrate, and 0.5% sarcosyl (Sigma, St. Louis, U.S.A.). The RNA was extracted by a series of phenol/chloroform extractions (Gibco BRL/Fisher, U.S.A.) and was then precipitated with ethanol. The purified RNA pellet was solubilized in water and stored at −80°C. RNA integrity was assessed by gel electrophoresis. A rat iNOS (riNOS) probe was prepared for use in the protection assay. Briefly, a 196 bp fragment corresponding to bases 3176 (Pst) to 3372 (EcoRV) of the rat iNOS DNA sequence (GenBank accession No. U03699.Gb_Ro) was amplified by RT-PCR using RNA isolated from inflamed rat granulomatous air pouch tissue expressing iNOS mRNA and protein (Salvemini *et al.*, 1995a). This fragment was purified and cloned into a pGEM 5Z transcription vector (Promega). A ^{32}P antisense RNA transcript was generated using Promega's Riboprobe Gemini System II Buffers to detect the riNOS mRNA isolated from the paw. The ribonuclease protection assay was performed using the RPA II kit (Ambion) essentially as described by the manufacturer. The radiolabelled riboprobe was purified on a 7 M urea, 8% polyacrylamide sequencing gel (Biorad). The gel slice containing the purified probe was eluted for 2 h at 37°C (buffer provided in the Ambion kit). Ten micrograms of paw RNA was evaporated to dryness in 1.5 ml microfuge tubes and reconstituted in 20 μl of the hybridization buffer provided. The labelled probe (200,000 c.p.m.) was then added and incubated at 85°C for 10 min, then overnight at 45°C. Following the overnight incubation, 200 μl of a 1:50 dilution of RNase A/T1

in RNase digestion buffer was added for 30 min in order to degrade all of the RNA which did not hybridize to the probe; 300 μl of the RNase inactivation/precipitation solution containing carrier was then added to each tube and allowed to precipitate for 30 min at −20°C. Following centrifugation, the protected RNA was mixed with 5 μl of gel loading buffer, heated to 90°C for 3 min, then separated on a 7 M urea, 8% polyacrylamide sequencing gel. The gel was then exposed to X-ray film for one to three days at −80°C.

Determination of iNOS protein by Western blot analysis

Soft tissue was removed from individual rat paws and homogenized in lysis buffer containing 10 mM N-[2-hydroxyethylpiperazine]-N'-[ethanesulphonic acid] (HEPES), pH 7.5, 100 μM ethylenediamine tetraacetic acid (EDTA), 1 mM dithiothreitol (DDT), 2 μM tetrahydrobiopterin (THB), 2 μM flavin adenine nucleotide (FAD), 25 nM calmodulin, 0.5 mM phenymethylsulphonyl fluoride (PMSF), 10 μM leupeptin, 1.5 μM pepstatin A, and 10 μg ml^{-1} soybean trypsin inhibitor (SBTI). The homogenates were centrifuged at 12,000 *g* for 1 h at 4°C, then supernatants were fractionated on a 1.0 mm, 8% polyacrylamide Tris glycine gel (Novex, San Diego, CA U.S.A.). Proteins were transferred to Hybond ECL Nitrocellulose (Amersham, Arlington Heights, IL, U.S.A.) for 2 h at 100V at 4°C in a Bio-Rad Mini Trans-Blot cell in 25 mM Tris, 192 mM glycine (Novex, San Diego, CA, U.S.A.). The transfer buffer was replaced after 1 h. Following transfer, the membrane was blocked for 1 h at room temperature with 10% nonfat dry milk in Tris buffered saline tween (TBST; 20 mM Tris, 500 mM NaCl, pH 7.5, 0.1% Tween 20). Polyclonal antisera 587 was obtained from New Zealand White rabbits immunized with a synthetic peptide corresponding to amino acids 1124–1144 of mouse iNOS conjugated to thyroglobulin. Primary antibody was diluted 1 : 2000 in 2.5% nonfat dry milk in TBST and incubated overnight with the membrane at 4°C. The blot was washed for 1–2 h with several changes of 2.5% nonfat dry milk in TBST, then incubated with a 1 : 2000 dilution of goat anti-rabbit IgG secondary antibody conjugated to horseradish peroxidase (Biorad, Melville, NY, U.S.A.) in 2.5% nonfat dry milk in TBST for 1 h at room temperature. The membrane was then washed twice for 15 min with 2.5% nonfat dry milk in TBST, then washed twice for 15 min with TBST (no milk, increasing the Tween concentration to 0.3%). The immunoreactive proteins were detected by enhanced chemiluminescence (ECL) using Hyperfilm and ECL reagent (Amersham, Arlington Heights, IL, U.S.A.).

Immunohistochemical localization of iNOS and nitrotyrosine

Immunohistochemical staining for iNOS and nitrotyrosine was performed on 8 μm frozen sections of hindpaws obtained from rats perfused with Hanks balanced salt solution containing 20 mM HEPES and 1% formaldehyde. Tissue sections were air dried for 5 min and were post-fixed with 1% formaldehyde for 5 min at room temperature. For single staining, non-specific staining was blocked with 3% normal goat serum in 0.5 M Tris-HCl, pH 7.4, containing 1% Triton X-100, 1 h at room temperature. All subsequent incubations were carried out in this buffer. For detection of iNOS immunoreactivity, tissue sections were incubated for 16 h at 4°C with a 1/1000 dilution of either preimmune rabbit sera, the anti-iNOS antiserum 587 described above, or antiserum 587 preadsorbed with rat inducible iNOS protein purified from inflamed air pouch. Endogenous peroxidase activity was then reduced with periodic acid (Zymed Laboratories, Inc. San Francisco, CA, U.S.A.) for 45 s at room temperature followed by sequential incubations with biotinylated anti-rabbit IgG and avidin-biotin-peroxidase complex (ABC, Vector Laboratories, Inc., Burlingame, CA, U.S.A.) for 2 h each. The reaction product was visualized using 3,3'-diaminobenzidine intensified with nickel chloride for 6 min. For detection of nitrotyrosine immunoreactivity, tissue sections were incubated for 16 h at 4°C with a 1/1000 dilution of either preimmune serum, an anti-nitrotyrosine polyclonal rabbit serum generated to nitrated keyhole limpet haemocyanin, or the anti-nitrotyrosine serum and excess nitrotyrosine (10 mM), followed by sequential incubations with biotinylated anti-rabbit IgG and avidin-biotin-glucose oxidase complex (ABC, Vector Laboratories, Inc., Burlingame, CA, U.S.A.) for 2 h each. The reaction product was visualized using tetranitroblue tetrazolium for 10 min. Sections were counterstained with Mayer's haematoxylin, mounted, and photographed using bright field microscopy. For double immunohistochemical localization of iNOS and nitrotyrosine, sections were post-fixed in 1% formaldehyde for 5 min and non-specific staining was blocked by incubating with PBS containing 10 mM tyrosine, 1% BSA, 0.2% powdered skim milk and 0.3% triton-X 100 (PBS-BB) for 30 min at room temperature. Sections were then incubated with a 1/500 dilution of antiserum 587 in PBS-BB at 4°C overnight. Staining for iNOS was localized using a 1/200 dilution of Cy3-conjugated donkey anti-rabbit IgG (Jackson ImmunoResearch, West Grove, PA, U.S.A.) in PBS-BB. Next, sections were incubated with a 1/500 dilution of the anti-nitrotyrosine serum in PBS-BB and staining was localized using a 1/200 dilution of DTSF-conjugated-goat anti-rabbit IgG (Jackson ImmunoResearch, West Grove, PA, U.S.A.) Specific staining was visualized with epifluorescence.

Materials

Male Sprague Dawley rats were purchased from Harlan Sprague-Dawley (Indianapolis, IN, U.S.A.) and were housed and cared for in accordance with the guidelines of the Institutional Animal Care and Use Committee and in accordance with NIH guidelines on laboratory animal welfare. 2,3-Diaminonaphthalene was purchased from Aldrich (Milwaukee, WI, U.S.A.). Human polymorphonuclear leukocyte myeloperoxidase was obtained from Calbiochem (La Jolla, CA, U.S.A.) and recombinant human Cu/Zn superoxide dismutase coupled to polyethyleneglycol (PEGrhSOD) was obtained from DDI Pharmaceuticals Inc. (Mountain View, CA, U.S.A.). All other chemicals and reagents were obtained from Sigma (St. Louis, MO, U.S.A.). N-iminoethyl-L-lysine (L-NIL) was synthesized in house as described previously (Connor *et al.*, 1995).

Statistical analysis

Results are expressed as mean ± s.e.mean for (*n*) rats. The results were analysed by Student's unpaired *t* test to determine the significant differences between means, or by a two-way ANOVA followed by a least significant procedure to determine the nature of this response. A P value of <0.05 was considered to be statistically significant.

Results

Time-dependent increase in paw volume, NO_2^-/NO_3^-, PGE_2 and neutrophil infiltration

The intraplantar injection of carrageenan in rats led to a time-dependent increase in paw volume that was maximal after 6 h and remained elevated thereafter for 10 h (Figure 1b). The increase in paw volume was associated with an elevated production of NO_2^-/NO_3^- in the paw exudates. This increase in NO_2^-/NO_3^- was observed within 30 min (from 0.5 ± 0.05 nmol/paw to 16.2 ± 4 nmol/paw, $n=6$), remained constant for the subsequent 3 h and then increased further at 6 and 10 h following carrageenan administration (Figure 2a). The increase in NO_2^-/NO_3^- at 6 h and thereafter is likely due to the activity of iNOS. iNOS mRNA was detected at 3 and 10 h by ribonuclease protection assays (Figure 1a) and iNOS protein was detected at 6 h and was maximal by 10 h following carrageenan administration by Western blot analysis (Figure 1a).

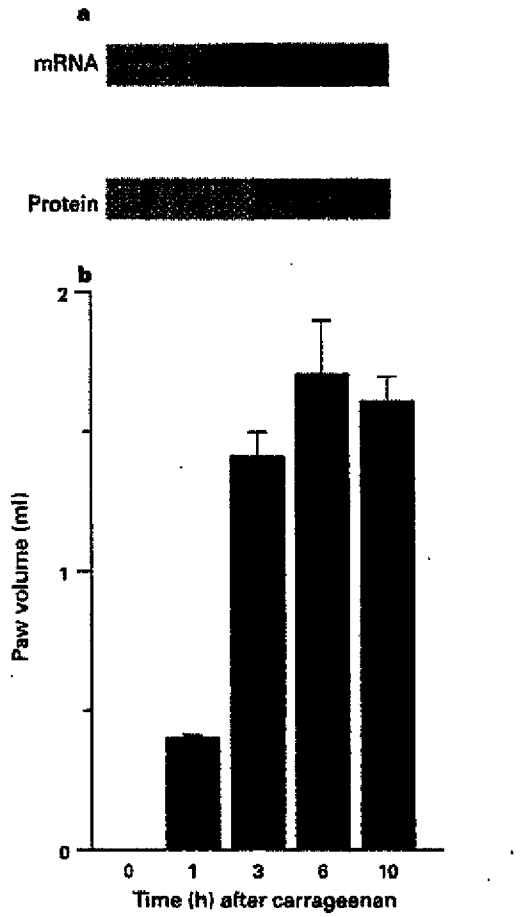

Figure 1 Time-dependent increase (0 to 10 h) in paw volume following carrageenan administration. The injection of carrageenan caused a time-dependent increase in paw volume that reached a maximum within 6–10 h (b; each point is the mean±s.e.mean for 6 experiments). iNOS mRNA was expressed in the paw tissue within 3 h after carrageenan and reached a maximum by 10 h (a). iNOS protein was detected by Western blot analysis at 6 h and also reached a maximum by 10 h after carrageenan administration (a).

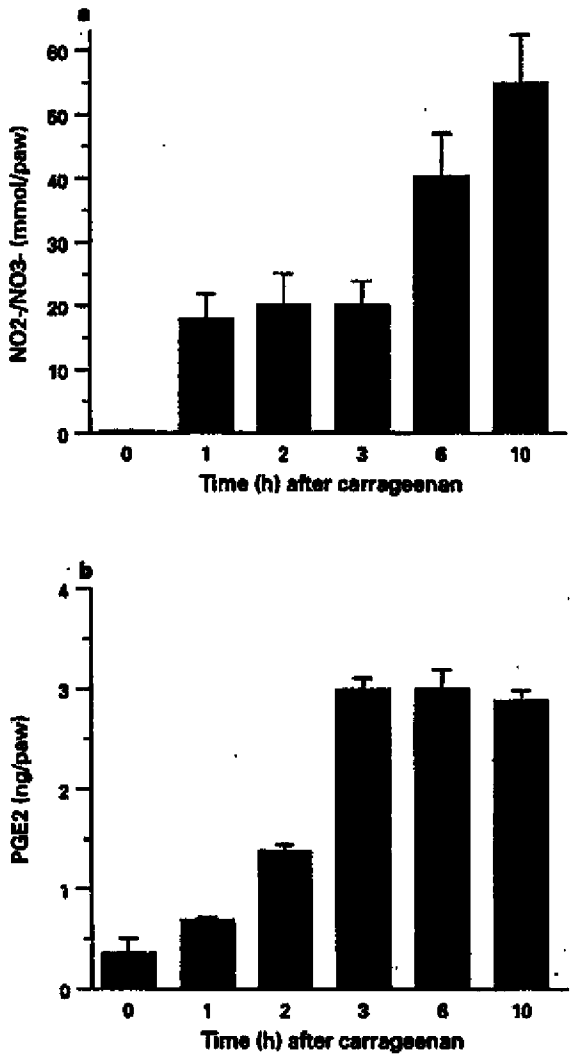

Figure 2 Time-dependent increase in NO_2^-/NO_3^- (a) and PGE_2 (b) following injection of carrageenan. Each point is the mean±s.e.mean for $n=6$ animals.

Six hours after carrageenan administration, the maximal increase in paw volume was also associated with neutrophil infiltration as measured by an increase in MPO activity in the paw tissue (from 214±12 to 3636±5 mu MPO/paw, $n=6$). Infiltrating neutrophils were found not to be the source of iNOS-derived NO. Treatment of rats with a subcutaneous injection of colchicine (2 mg kg^{-1}, 2 h before carrageenan administration; Boughton-Smith *et al.*, 1993), suppressed paw volume by at least 70% at all time points. Paw volume, measured 6 h after carrageenan administration, was decreased from 1.4±0.07 ml to 0.3±0.03 ml ($n=6$), and was associated with inhibition of neutrophil infiltration. MPO values decreased from 3636±5 mu/paw to 4±0.1 mu/paw ($n=6$). However, at the same time, ribonuclease protection assays demonstrated that the elevated expression of iNOS mRNA was unaltered by the colchicine treatment (not shown). In addition, this corresponded with a failure of colchicine to reduce the production of NO_2^-/NO_3^- in paw exudate (from 40±7 to 41±3 nmol/paw, $n=6$).

The paw tissues were also examined immunohistochemically for the presence of iNOS and nitrotyrosine (a marker for peroxynitrite formation). Immunohistochemical analysis of the paw tissues of control animals showed no iNOS or nitrotyrosine staining (Figure 3a and d). In contrast, 6 h following carrageenan administration, iNOS-like immunoreactivity was localized to discrete cells within the inflamed paw tissue (Figure 3b). This staining was specific for iNOS as it was completely eliminated by incubation of the iNOS antiserum with an excess of purified rat iNOS (Figure 3c). Based upon morphology and ED1 positive staining (not shown), the iNOS immunoreactivity was localized primarily to macrophage-like cells present in the inflamed paw tissue. Staining for nitrotyrosine was also found to be localized within discrete cells in the inflamed paw tissue (Figure 3e). This staining was almost completely eliminated by incubation of the primary anti-nitrotyrosine serum with 10 mM nitrotyrosine (Figure 3f). Using double immunofluorescence staining for iNOS (Figure 3g, red) and nitrotyrosine (Figure 3h, green), the staining for iNOS and nitrotyrosine was localized primarily to the same cells (Figure 3i, yellow-orange).

Carrageenan also elicited a time-dependent increase in PGE_2 production which increased after 2 h, reached a peak by 3 h and remained elevated thereafter (Figure 2b).

Effects of NOS inhibitors on paw volume, NO_2^-/NO_3^-, PGE_2 and neutrophil infiltration

The non-selective cNOS/iNOS inhibitor, N^G-nitro-L-arginine methyl ester (L-NAME) (30–300 mg kg^{-1}) administered intravenously 1 h before carrageenan ($n=6$), inhibited the paw oedema at all time points (Figure 4a). Complete inhibition of oedema formation was observed during the first hour. Paw volume measured after 1 h decreased from 0.4±0.01 ml in non-treated rats, to 0.3±0.01 ml, 0.08±0 ml and 0 ml in rats that received 30, 100 and 300 mg kg^{-1} L-NAME, respectively

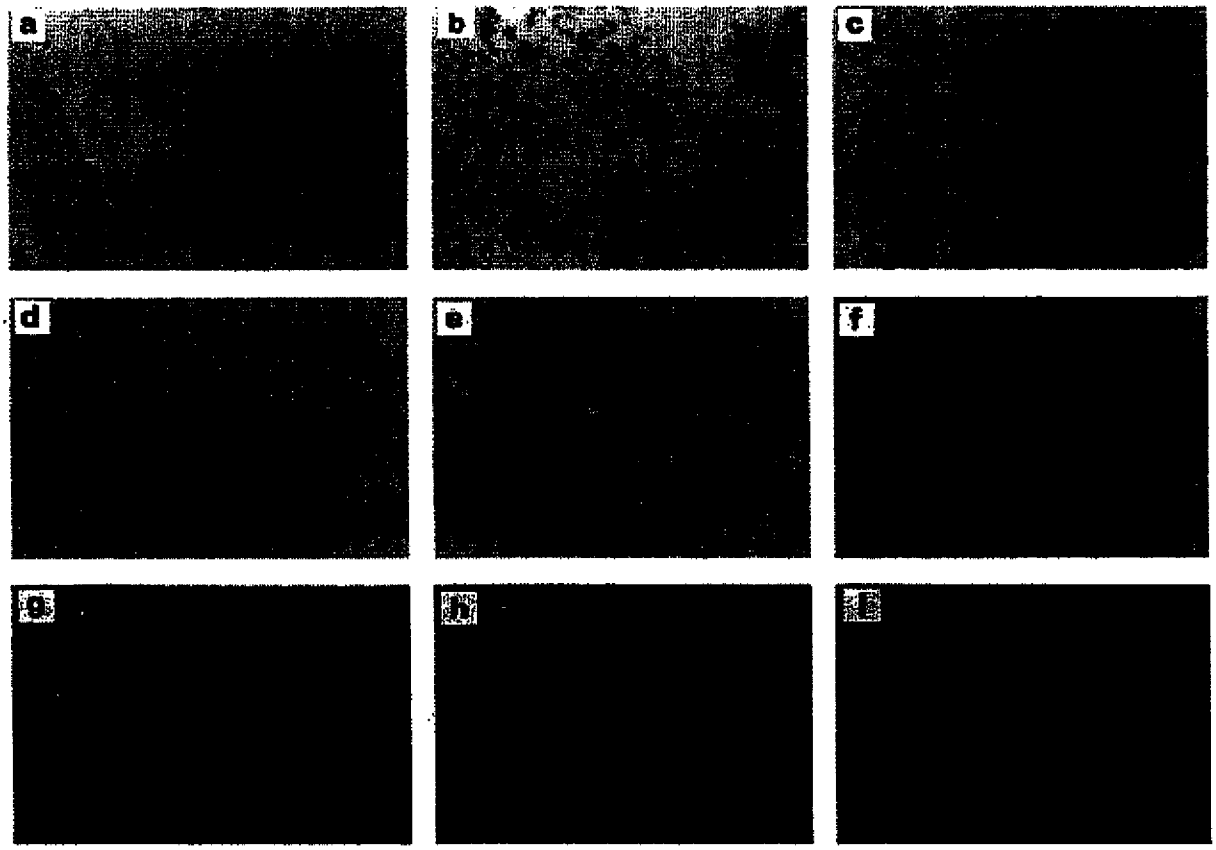

Figure 3 Immunohistochemical localization of iNOS and nitrotyrosine in the carrageenan-inflamed rat hindpaw. Control (a,d) and carrageenan-inflamed (all others) paw tissue sections were stained for iNOS or nitrotyrosine either using avidin-biotin-glucose oxidase (a–c), avidin-biotin-peroxidase (d–f) or indirect immunofluorescence (Cy3 or DFAP, g–i)-based detection. Six hours after the intraplantar injection of carrageenan, iNOS-like immunoreactivity was localized to discrete cells within the inflamed paw tissue (b,g). Based upon morphology and ED1 positive staining (not shown), iNOS was localized primarily to macrophage-like cells present in the inflamed paw tissue. Staining was absent in control tissue (a) or in inflamed tissue when the anti-iNOS antiserum was incubated with an excess of purified rat iNOS (c). Nitrotyrosine staining was also localized to discrete cells, similar in morphology to those expressing iNOS, within the inflamed paw tissue (e,h). Staining was absent in control paw tissue (d) or in inflamed tissue when the anti-initrotyrosine antiserum was incubated with 10 mM nitrotyrosine (f). Using double immunofluorescent staining, the iNOS (red, g) and nitrotyrosine (green, h) staining were co-localized primarily to the same cells as indicated by the yellow-orange colour (i) obtained when the photographs are double exposed.

($n=6$). At subsequent time points, L-NAME produced a partial, dose-dependent inhibition of paw oedema. In order to determine whether NO maintained the oedema following the injection of carrageenan, rats were given an intravenous injection of L-NAME 1 h after the intraplantar injection of carrageenan; paw swelling was assessed thereafter every hour for 10 h. Treatment with L-NAME (30–300 mg kg^{-1}, $n=6$) after the administration of carrageenan also reduced the increase in paw oedema in a dose-dependent manner (Figure 4b). Similar results were obtained with L-NMMA (30–300 mg kg^{-1}, $n=6$, Table 1A and B).

We next examined the role of iNOS by using two recently described selective iNOS inhibitors, L-NIL (Moore *et al.*, 1994; Connor *et al.*, 1995) and AG (Misko *et al.*, 1993a; Griffiths *et al.*, 1993; Wu *et al.*, 1995). We previously characterized both the potency and selectivity of these inhibitors *in vitro* using purified rat brain cNOS and mouse macrophage iNOS (Moore *et al.*, 1994). L-NIL and AG are approximately 30 fold more selective for the inducible than for the constitutive form of NOS, and L-NIL was approximately 10 fold more potent than AG at inhibiting iNOS activity (Moore *et al.*, 1994; Connor *et al.*, 1995). Neither L-NIL (30 mg kg^{-1}, i.v., $n=6$) nor AG (300 mg kg^{-1}, $n=6$) prevented the increase in paw volume observed from 0 to 4 h following carrageenan administration. However, these drugs inhibited the paw oedema observed at subsequent times (Figure 5). In addition, the administration of L-NIL (3–30 mg kg^{-1}, $n=6$) 5 h after the onset of inflammation, a time when iNOS was clearly expressed (Figure 1), inhibited paw oedema in a dose-dependent fashion (Figure 6). Similar results were obtained with AG, but higher doses were required to produce comparable effects (30–300 mg kg^{-1}, $n=6$, not shown).

The effects of both non-selective and selective NOS inhibitors on the production of NO_2^-/NO_3^- and PGE_2 in the paw exudate were also determined. Treatment with L-NMMA and L-NAME (300 mg kg^{-1}, $n=5$) inhibited the NO_2^-/NO_3^- and PGE_2 production in paw exudate at both 3 (Figure 7a and 8a) and 10 h (Figure 7b and 8b) after carrageenan administration. In contrast, L-NIL (30 mg kg^{-1}, $n=5$) and AG (300 mg kg^{-1}, $n=5$) inhibited NO_2^-/NO_3^- and PGE_2 release in paw exudate only at the 10 h time point (Figures 7b and 8b), but had no effect at 3 h following carrageenan administration (Figure 7a and 8a). Finally, treatment with the non-selective cyclo-oxygenase inhibitor, indomethacin (10 mg kg^{-1}, p.o., given 2 h before carrageenan, $n=6$), inhibited paw oedema at 2 h and at subsequent times ($n=6$, not shown), blocked PGE_2 production (Figure 8a and 8b), but had little effect on NO_2^-/NO_3^- production (Figure 7).

Both the non-selective cNOS/iNOS inhibitors as well as the more selective iNOS inhibitors attenuated neutrophil infiltration following carrageenan administration. Six hours after carrageenan treatment, MPO values decreased from 3636 ± 5 mu/paw in saline-treated rats to 150 ± 15 mu/paw, 138 ± 10 mu/paw, 500 ± 10 mu/paw and 570 ± 15 mu/paw in rats treated with L-NMMA, L-NAME (300 mg kg^{-1}, $n=6$), L-NIL (30 mg kg^{-1}, $n=6$) or AG (300 mg kg^{-1}, $n=6$), respectively.

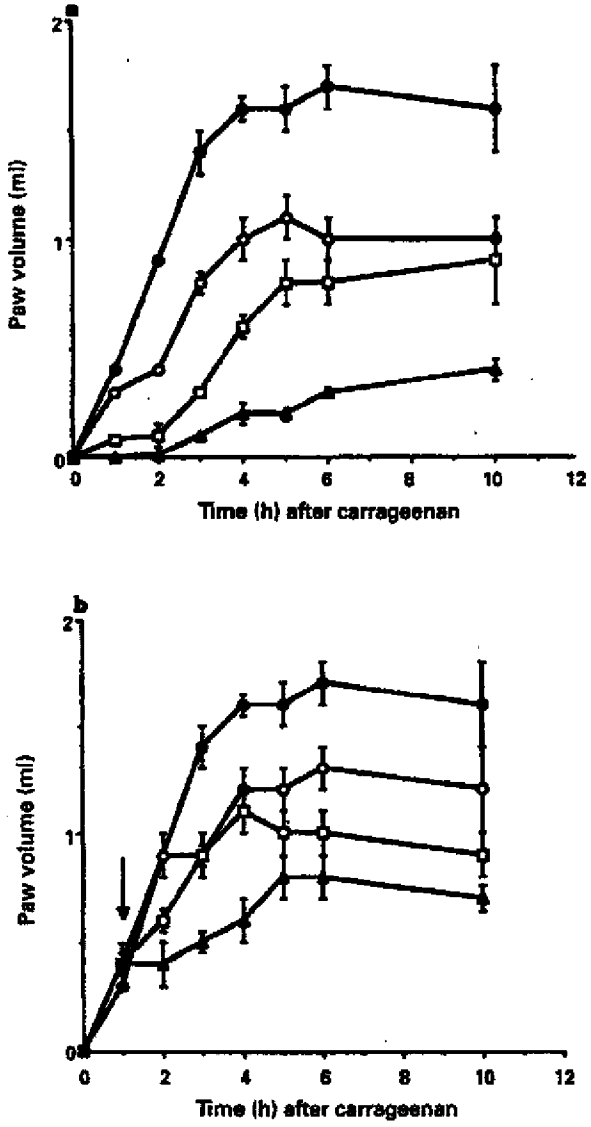

Figure 4 (a) Inhibition of carrageenan-induced paw oedema (●) by L-NAME at 30 (○), 100 (□) and 300 (▲) mg kg^{-1} when given 1 h before or (b) 1 h after as indicated by the arrow. Results are expressed as the increase in paw volume (ml). Each point is the mean ± s.e.mean for $n=6$ animals.

Effect of PEGrhSOD, catalase and desferrioxamine on paw volume, NO_2^-/NO_3^-, PGE_2 and neutrophil infiltration

To evaluate the roles of superoxide anions, rats were treated with PEGrhSOD. Treatment with PEGrhSOD (given at 12×10^3 u kg^{-1}, 30 min before carrageenan, $n=6$) inhibited the increase in paw oedema at all time points by at least 60% (Table 2). This anti-inflammatory effect was associated with inhibition of neutrophil infiltration. MPO values decreased from 3636 ± 5 mu/paw in saline-treated rats to 597 ± 20 mu/paw in rats treated with PEGrhSOD at 6 h after carrageenan ($n=6$). However, it did not affect the NO_2^-/NO_3^- or PGE_2 production in the paw exudate ($n=6$, not shown). The anti-inflammatory effects that occurred with PEGrhSOD were also observed when the drug was given 1 h after carrageenan (Table 2) supporting a previous study by Boughton-Smith *et al.* (1993).

To evaluate the roles of hydrogen peroxide and hydroxyl radicals, rats were treated with catalase and desferrioxamine respectively. Treatment with catalase (40×10^3 u kg^{-1}, i.p. 30 min before carrageenan; Hirschelmann & Bekemeir, 1981) had no effect on the formation of oedema ($n=4$, not shown). Treatment with desferrioxamine (300 mg kg^{-1}, s.c.) 1 h before carrageenan, Boughton-Smith *et al.*, 1993) inhibited paw oedema after the first hour by approximately 60% ($n=5$) and after the second hour by 38% ($n=5$). However, no inhibition occurred at subsequent times (Table 2).

Discussion

The anti-inflammatory effects of NOS inhibitors in acute and chronic models of inflammation have been and continue to be characterized. In view of the complex nature of the inflammatory response, the determination of possible mechanisms by which NO modulates this response will aid in designing novel and more efficacious NOS inhibitors. Two important discoveries have been made recently that may help to explain potential mechanisms of action of NO in inflammatory conditions. The first observation is that NO stimulates COX activity resulting in the exaggerated production of pro-inflammatory PG (Salvemini *et al.*, 1993). The second is that NO can react with O_2^- to form the cytotoxic radical peroxynitrite (Beckman *et al.*, 1990).

In the studies described here, we examined the significance of these interactions in acute inflammation induced by the injection of carrageenan into the rat hindpaw. For clarity, the oedema occurring from 0–4 h is termed the 'early phase' and that occurring at subsequent time points (4–10 h) the 'sustained phase'. The non-selective cNOS/iNOS inhibitors (L-NAME and L-NMMA), whether given 1 h before or after the onset of inflammation, attenuated the oedema at all points indicating a role for NO in this inflammatory response. The degree of inhibition obtained during the first 2 h was remarkable, achieving approximately 90%. The oedema that occurs during the first hour results from the concomitant release of histamine, 5-HT and kinins and is markedly inhibited (70–80%) by treatment with a combination of histamine, 5-HT and bradykinin receptor antagonists (Di Rosa *et al.*, 1971). However, single administration of these receptor antagonists inhibits oedema by only 30–40% (Di Rosa *et al.*, 1971). Thus the inhibitory effects of the non-selective NOS inhibitors is comparable to that achieved with a mixture of histamine, 5-HT and bradykinin receptor antagonists.

In our present study using both molecular and pharmacological tools, we have demonstrated that iNOS is expressed in this model within 4 h after injection of carrageenan and that its induction and the subsequent production of NO is involved in maintaining the oedema during the sustained phase of the inflammatory response. Both AG and L-NIL, two recently described iNOS inhibitors (Misko *et al.*, 1993a; Griffiths *et al.*, 1993; Moore *et al.*, 1994; Connor *et al.*, 1995; Wu *et al.*, 1995) failed to inhibit carrageenan-induced paw oedema during the first 4 h of the response but inhibited paw oedema at all subsequent times (from 4 to 10 h, Figure 5). In addition, iNOS mRNA was detected between 3 and 10 h after carrageenan administration by ribonuclease protection assays and iNOS protein was detected at 6 h, and was maximal at 10 h by Western blot analysis. iNOS-like immunoreactivity was also localized to macrophage-like cells within the inflamed paw tissue, but not in neutrophils, suggesting that resident macrophages in inflamed paw tissue and/or infiltrating monocytes are the source of iNOS-derived NO. The therapeutic administration of the selective iNOS inhibitors, L-NIL or AG, at a time when iNOS activity was initially detected, prevented the subsequent increase in oedema indicating that NO generated by iNOS maintains oedema during the later stages of the inflammatory response. When compared to L-NIL, higher doses of aminoguanidine were required to exert anti-inflammatory effects, consistent with the fact that L-NIL is a more potent inhibitor of iNOS in *in vitro* studies (Moore *et al.*, 1994). In addition, the detection of nitrotyrosine immunoreactivity within the inflamed tissue, primarily localized to the same cells as those expressing iNOS, suggests that peroxynitrite is formed during this re-

Table 1 Inhibition of carrageenan-induced paw oedema by L-NMMA (30–300 mg kg^{-1}) given either 1 h before (A) or 1 h after (B) carrageenan injection

	L-NMMA (mg kg^{-1})			
	0	30	100	300
A				
Time (h)				
0	0	0	0	0
1	0.4±0.01	0.3±0.01	0.08±0*	0
2	0.9±0.02	0.4±0.01*	0.1±0.05*	0.01±0.5*
3	1.4±0.1	0.8±0.05*	0.3±0.01*	0.1±0.01*
4	1.6±0.2	1.0±0.1*	0.6±0.05*	0.2±0.05*
5	1.6±0.3	1.0±0.1*	0.8±0.1*	0.2±0.03*
6	1.7±0.2	1.0±0.1*	0.8±0.1*	0.3±0.02*
10	1.6±0.2	1.0±0.2*	0.7±0.1*	0.3±0.05*
B				
Time (h)				
0	0	0	0	0
1	0.4±0.01	0.3±0.01	0.4±0.1	0.4±0.05
2	0.9±0.02	0.9±0.1	0.6±0.05*	0.4±0.1*
3	1.4±0.1	0.9±0.05*	0.9±0.1*	0.5±0.05*
4	1.6±0.2	1.2±0.1*	1.1±0.1*	0.6±0.1*
5	1.6±0.3	1.2±0.1*	1±0.1*	0.8±0.1*
6	1.7±0.2	1.3±0.1*	1±0.1*	0.8±0.1*
10	1.6±0.2	1.2±0.1*	0.9±0.1*	0.7±0.05*

Results are expressed as the increase in paw volume (ml). Each point is the mean±s.e.mean for $n=6$ animals. *$P<0.05$ compared to the corresponding control value.

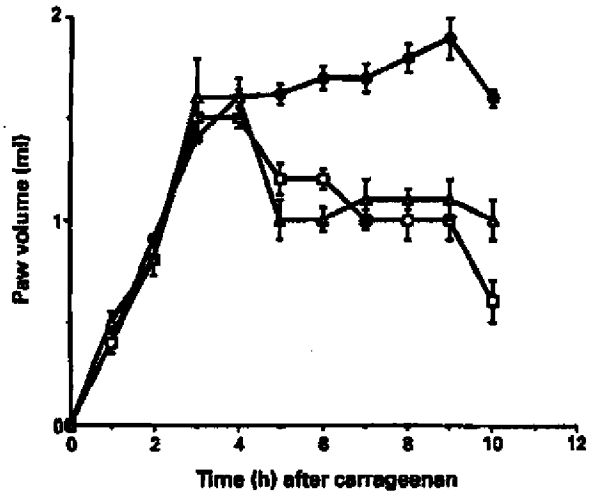

Figure 5 Inhibition of carrageenan-induced paw oedema (●) by L-NIL (30 mg kg^{-1}, □) or AG (300 mg kg^{-1}, △). Drugs were given i.v. 1 h before carrageenan. Results are expressed as the increase in paw volume (ml). Each point is the mean±s.e.mean for $n=6$ animals.

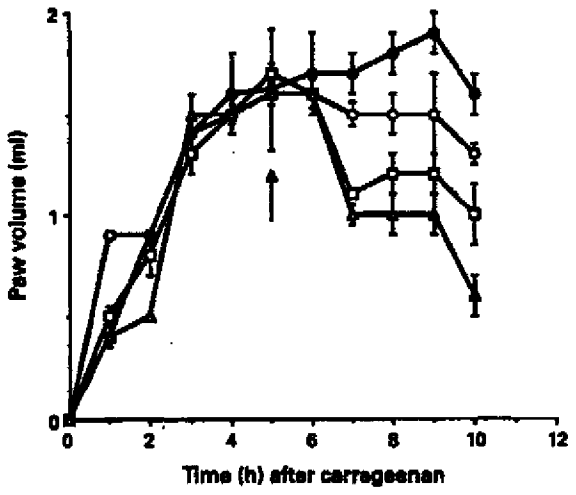

Figure 6 Inhibition of carrageenan-induced paw oedema (●) by L-NIL at 3 (○), 10 (□) or 30(△) mg kg^{-1}. L-NIL was given 5-h after the administration of carrageenan. Results are expressed as the increase in paw volume (ml). Each point is the mean±s.e.mean for $n=6$ animals.

sponse and may be responsible for inducing a portion of the tissue damage in the hindpaw. Importantly, the anti-inflammatory effects of the iNOS inhibitors were found to be independent of changes in arterial blood pressure. The non-selective NOS inhibitors on the other hand raise arterial blood pressure and this could account for some of their ability to attenuate the oedema response to carrageenan.

The involvement of cNOS in the early phase and of iNOS during the sustained phase of the oedematous response was also demonstrated by the differential ability of L-NMMA or L-NAME and L-NIL or AG to inhibit NO_2^-/NO_3^- production in the paw exudate. Three hours after carrageenan injection (a time point where iNOS was not expressed), NO_2^-/NO_3^- production was inhibited by L-NMMA or L-NAME, but not by L-NIL or AG suggesting that the NO generated in the early phase originated from cNOS activation. In contrast, the production of NO_2^-/NO_3^- in the paw exudate at the 10 h time point (when iNOS was expressed) was inhibited not only by L-NMMA or L-NAME, but also by L-NIL or AG, indicating that iNOS was responsible for the enhanced production of NO during the sustained phase of the response.

Prostaglandins are also important mediators of acute inflammation. Previous studies have demonstrated that although PGs do not contribute initially to the oedema occurring 1 h after carrageenan administration, their production does produce some of the inflammation within the second hour and at subsequent time points (Di Rosa *et al.*, 1971; Seibert *et al.*, 1994). The inducible isoform of cyclooxygenase (COX-2) appears to be responsible for PG production under these circumstances (Seibert *et al.*, 1994). Interestingly, as shown in Figure 8, the inhibition of NO generation by NOS inhibitors during both the early and sustained phase of oedema was associated with a reduction in PG production. We have recently reported that in both *in vitro* and *in vivo* studies, NO activates COX-1 and COX-2 resulting in an enhanced production of PG. In addition, NOS

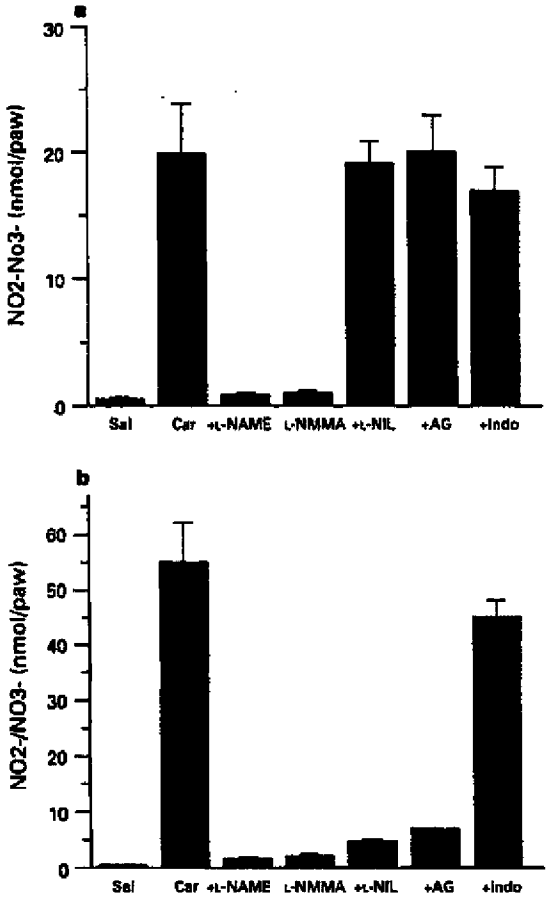

Figure 7 Effects of NOS inhibitors or indomethacin on NO_2^-/NO_3^- production at 3 (a) and 10 (b) h after carrageenan administration. The non-selective NOS inhibitors (L-NAME, L-NMMA) inhibited NO_2^-/NO_3^- production at 3 and 10 h (a and b), whereas the selective iNOS inhibitors (L-NIL or AG) inhibited NO_2^-/NO_3^- production only at the 10 h time point (b). Indomethacin had no effect (a and b). Each point is the mean ± s.e.mean for $n=6$ experiments.

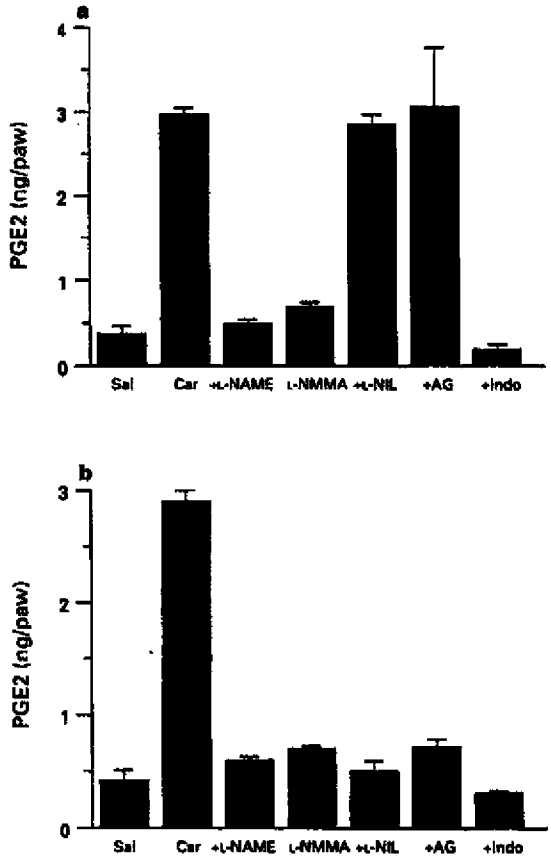

Figure 8 Effects of indomethacin or NOS inhibitors on PGE_2 production at 3(a) and 10(b) h after the administration of carrageenan. PGE_2 production at 3 and 10 h was completely inhibited by treatment with indomethacin (a and b). PGE_2 release at 3 and 10 h was also attenuated by the non-selective NOS inhibitors (L-NAME, L-NMMA), whereas the selective iNOS inhibitors (L-NIL, AG) attenuated PGE_2 production only at the 10 h time point (b). Each point is the mean ± s.e.mean for $n=6$ experiments.

inhibitors inhibit PG formation (Salvemini *et al.*, 1993; 1995a,b), a finding that has now been confirmed in a number of other studies (Inoue *et al.*, 1993; Corbett *et al.*, 1993; Sautebin & Di Rosa, 1994; Sautebin *et al.*, 1995). The inhibition of PG production by NOS inhibitors does not appear to be due to the direct inhibition of COX activity or PG isomerase activity (Salvemini *et al.*, 1993; 1994). It appears likely that NO derived from cNOS enhances PG formation at the early time points and NO derived from iNOS enhances PG production at the later times.

Carrageenan-induced paw oedema is neutrophil-dependent (this study; Di Rosa & Sorrentino, 1968; Vinegar *et al.*, 1971; Boughton-Smith *et al.*, 1993). As was observed previously in the carrageenan-induced air pouch model of inflammation (Salvemini *et al.*, 1995a), it seems that early in the inflammatory response in the hindpaw, infiltrating neutrophils are not the source of iNOS-derived NO since the anti-inflammatory effects of colchicine were not associated with inhibition of NO. Activated neutrophils, are an excellent source of oxygen-derived free radicals which have been implicated in many models of acute inflammation in which there is a neutrophil-dependent increase in vascular permeability (see Fantone & Ward, 1982 for review). As previously reported by others (Hirschelmann & Beckemein, 1981; Boughton-Smith *et al.*, 1993), we found that the removal of O_2^- by PEGrhSOD significantly inhibited the paw oedema. Furthermore, PEGrhSOD also inhibited neutrophil infiltration, a result that is consistent with a role for O_2^- in mediating neutrophil adhesion and infiltration (Schraufstatter *et al.*, 1987; Warren *et al.*, 1990). PEGrhSOD failed to affect NO and PG production, providing further evidence that infiltrating neutrophils do not contribute to the production of these mediators. Removal of hydrogen peroxide by catalase had no effect and removal of hydroxyl radicals by desferrioxamine inhibited oedema weakly only at the first hour. These results suggest that O_2^- rather than hydrogen peroxide or hydroxyl radicals are key players in the inflammatory response.

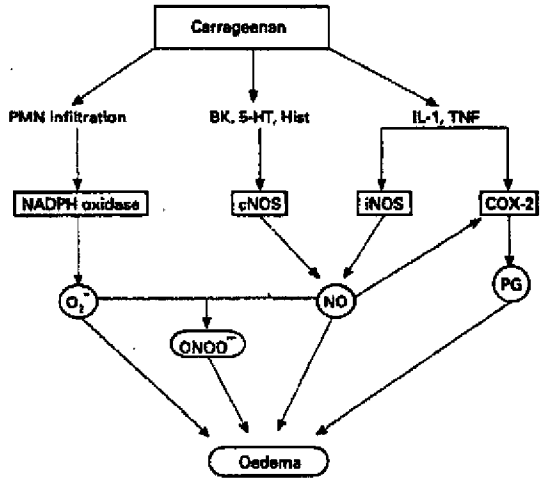

Figure 9 Proposed model of mechanism(s) of action of NO in carrageenan-induced acute inflammatory response in the rat hindpaw.

The interactions between NO, PG and O_2^- are summarized

Table 2 Inhibition of carrageenan-induced paw oedema by PEGrhSOG when given 30 min before (–30) or 1 h (+1) after carrageenan administration (A) and lack of effect of catalase (Cat) or desferrioxamine (Des) (B)

	0	–30	+1
A			
Time (h)			
0	0	0	0
1	0.4±0.01	0.1±0.01*	0.4±0.05
2	0.9±0.02	0.5±0.07*	0.6±0.01*
3	1.4±0.1	0.7±0.01*	0.7±0.02*
4	1.6±0.2	0.9±0.05*	0.8±0.07*
5	1.6±0.3	0.9±0.05*	0.8±0.07*
6	1.7±0.2	1±0.1*	0.8±0.05*
10	1.6±0.2	1.2±0.2*	1±0.1*
B			
Time (h)	*0*	*Cat*	*Des*
0	0	0	0
1	0.4±0.01	0.5±0.01	0.05±0.1*
2	0.9±0.02	0.9±0.1	0.6±0.03*
3	1.4±0.1	1.3±0.2	1.3±0.01
4	1.6±0.2	1.5±0.2	1.5±0.03
5	1.6±0.3	1.6±0.2	1.6±0.1
6	1.7±0.2	1.7±0.2	1.8±0.03
10	1.6±0.2	1.8±0.2	1.7±0.1

Results are expressed as the increase in paw volume (ml). Each point is the mean±s.e.mean for $n=6$ animals. *$P<0.05$ compared to corresponding control value.

in the model shown in Figure 9. Within the first hour following carrageenan injection, oedema is induced by the release of mediators such as histamine, bradykinin and 5-HT, but not by PG. These mediators, following activation of their receptors on endothelial cells, trigger cNOS activation resulting in the generation of NO. Since treatment with non-selective NOS inhibitors produced virtually complete inhibition of oedema formation at this time, we propose that NO released as a consequence of cNOS activation may be the final common mediator responsible for the early phase of the inflammatory response to carrageenan. Whether the cNOS efects are endothelial or neuronal NOS-mediated remains to be investigated in future studies. As the inflammatory response progresses, iNOS is induced and generates larger quantities of NO which appear to maintain the oedema during the sustained phase. Although the mechanism(s) involved in the regulation of iNOS induction in this model are not known, it is likely that cytokines are involved. In mice following the intraplantar injection of carrageenan, TNF-α, IFN-γ as well as cytokines such as IL-1 and IL-2 are produced (Ianaro *et al.*, 1994). These molecules have been shown to induce iNOS in a variety of cells including macrophages, smooth muscle cells and endothelial cells (see Moncada & Higgs, 1993 for review). COX-2 is also induced within 2 h after carrageenan administration (Seibert *et al.*, 1994). The NOS and COX pathways appear to operate together to amplify the inflammatory response. This is achieved by a synergistic interaction between NO and PG on blood flow and microvascular permeability (Warren *et al.*, 1992), as well as by a NO-driven COX activation leading to the exaggerated production of PG (Salvemini *et al.*, 1993; 1995a,b). The dual inhibition of NO and PG obtained with NOS inhibitors could account for their marked anti-inflammatory effect.

Neutrophil infiltration in response to carrageenan and following NADPH oxidase activation generates an oxygen-respiratory burst giving rise to oxygen-derived free radicals such as O_2^-. O_2^- promote lipid peroxidation, increase vascular permeability, elicit cellular recruitment and produce tissue damage (see Fantone & Ward, 1982 for review). Furthermore, the generation of O_2^- in the presence of NO forms the cytotoxic radical $ONOO^-$ (Beckman *et al.*, 1990). $ONOO^-$ can in turn decompose to form additional toxic molecules including nitrogen dioxide and OH (Beckman *et al.*, 1990; Radi *et al.*, 1991). The localization of nitrotyrosine immunoreactivity, a marker of peroxynitrite formation, within the inflamed paw tissue during the late phase of carrageenan-induced hindpaw inflammation suggests that $ONOO^-$ was generated and could be responsible in part for the production of tissue damage in this model. The precise biochemical nature of the role of $ONOO^-$ remains to be elucidated, but it appears not to involve to any great extent the formation of OH.

In summary, we propose that possible mechanisms by which NOS inhibitors exert their anti-inflammatory effects include the inhibition of: neutrophil infiltration, PG and NO production, and the generation of peroxynitrite. These findings also suggest that the inhibition of the sustained phase of the paw oedema following the intraplantar injection of carrageenan is suitable for the *in vivo* assessment of the anti-inflammatory actions of novel inhibitors of the inducible form of nitric oxide synthase.

We wish to thank Dr Thomas Misko for providing the antiserum to iNOS and nitrotyrosine and Drs Jaime Masferrer and Karen Seibert for critical evaluation of this manuscript.

References

BECKMAN, J.S., BECKMAN, T.W., CHEN, T.W., MARSHALL, P.A. & FREEMAN, B.A. (1990). Apparent hydroxyl radical production by peroxynitrite: implications for endothelial injury from nitric oxide and superoxide. *Proc. Natl. Acad. Sci. U.S.A.*, **87**, 1620–1624.

BOUGHTON-SMITH, N.K., DEAKIN, A.M., FOLLENFANT, R.L., WHITTLE, B.J.R. & GARLAND, L.G. (1993). Role of oxygen radicals and arachidonic acid metabolites in the reverse passive Arthus reaction and carrageenin paw oedema in the rat. *Br. J. Pharmacol.*, **110**, 896–902.

BRADLEY, P.P., PRIEBAT, D.A., CHRISTENSEN, R.D. & ROTHSTEIN, G. (1982). Measurement of cutaneous inflammation. Estimation of neutrophil content with an enzyme marker. *J. Invest. Dermatol.*, **78**, 206–209.

CONNOR, J., MANNING, P.T., SETTLE, S.L., MOORE, W.M., JEROME, G.M., WEBBER, R.K., TJOENG, F.S. & CURRIE, M.G. (1995). Suppression of adjuvant-induced arthritis by selective inhibition of inducible nitric oxide synthase. *Eur. J. Pharmacol.*, **273**, 15–24.

CORBETT, J.A., KWON, G., TURK, J. & MCDANIEL, M.L. (1993). IL-1β induces the coexpression of both nitric oxide synthase and cyclooxygenase by islets of langerhans: activation of cyclooxygenase by nitric oxide. *Biochemistry*, **32**, 13767–13770.

DAVIDGE, S.T., BAKER, P.N., MCLAUGHLIN, M.K. & ROBERTS, J.M. (1995). Nitric oxide produced by endothelial cells increases production of eicosanoids through activation of prostaglandin H synthase. *Circ. Res.*, **77**, 274–283.

DI ROSA, M., GIROUD, J.P. & WILLOUGHBY, D.A. (1971). Studies of mediators of the acute inflammatory response induced in rats in different sites by carrageenin and turpentine. *J. Pathol.*, **104**, 15–29.

DI ROSA, M. & SORRENTINO, L. (1968). The mechanism of the inflammatory effect of carrageenin. *Eur. J. Pharmacol.*, **4**, 340–343.

DI ROSA, M. & WILLOUGHBY, D.A. (1971). Screens for anti-inflammatory drugs. *J. Pharm. Pharmacol.*, **23**, 297–300.

FANTONE, J.C. & WARD, P.A. (1982). Role of oxygen-derived free radicals and metabolites in leukocyte-dependent inflammatory reactions. *Am. J. Pathol.*, **107**, 397–418.

GRIFFITHS, M.J.D., MESSENT, M., MACALLISTER, R.J. & EVANS, T.W. (1993). Aminoguanidine selectively inhibits inducible nitric oxide synthase. *Br. J. Pharmacol.*, **110**, 963–968.

HAJJAR, D.P., LANDER, H.M., PEARCE, F.S., UPMACIS, R.K. & POMERANTZ, K.B. (1995). Nitric oxide enhances prostaglandin-H synthase activity by a heme-independent mechanism: evidence implicating nitrosothiols. *J. Am. Chem. Soc.*, **117**, 3340–3346.

HIRSCHELMANN, R. & BEKEMEIR, H. (1981). Effects of catalase, peroxidase, superoxide dismutase and 10 scavengers of oxygen radicals in carrageenin edema and in adjuvant arthritis of rats. *Experientia*, **37**, 1313–1314.

IALENTI, A., IANARO, A., MONCADA, S. & DI ROSA, M. (1992). Modulation of acute inflammation by endogenous nitric oxide. *Eur. J. Pharmacol.*, **211**, 177–182.

IANARO, A., O'DONNELL, C.A., DI ROSA, M. & LIEW, F.Y. (1994). A nitric oxide synthase inhibitor reduces inflammation, down-regulates inflammatory cytokines and enhances interleukin-10 production in carrageenin-induced oedema in mice. *Immunol.*, **82**, 370–375.

INOUE, T., FUJUO, K., MORIMOTO, S., KOH, E. & OGIHARA, T. (1993). Nitric oxide mediates interleukin-1-induced prostaglandin E_2 production by vascular smooth muscle cells. *Biochem. Biophys. Res. Commun.*, **194**, 420–424.

LAIGHT, D.W., LAD, N., WOODWARD, B. & WATERFALL, J.F. (1994). Assessment of myeloperoxidase activity in renal tissue after ischaemia/reperfusion. *Eur. J. Pharmacol.*, **292**, 81–88.

MISKO, T.P., MOORE, W.M., KASTEN, T.P., NICKOLS, G.A., CORBETT, J.A., TILTON, R.G., MCDANIEL, M.L., WILLIAMSON, J.R. & CURRIE, M.G. (1993a). Selective inhibition of the inducible nitric oxide synthase by aminoguanidine. *Eur. J. Pharmacol.*, **233**, 119–225.

MISKO, T.P., SCHILLING, R.J., SALVEMINI, D., MOORE, W.M. & CURRIE, M.G. (1993b). A fluorometric assay for the measurements of nitrite in biological samples. *Anal. Biochem.* **214**, 11–16.

MONCADA, S. & HIGGS, A. (1993). The L-arginine-nitric oxide pathway. *N. Engl. J. Med.*, **329**, 2002–2012.

MONCADA, S., PALMER, R.M.J. & HIGGS, E.A. (1991). Nitric oxide: physiology, pathophysiology and pharmacology. *Pharmacol. Rev.*, **43**, 109–141.

MOORE, W.M., WEBBER, R.K., JEROME, G.M., TJOENG, F.S., MISKO, T.P. & CURRIE, M.G. (1994). L-N^6-(1-Iminoethyl)lysine: A selective inhibitor of inducible nitric oxide synthase. *J. Med. Chem.*, **37**, 3886–3888.

RADI, R., BECKMAN, J.S., BUSH, K.M. & FREEMAN, B.A. (1991). Peroxynitrite-induced membrane lipid peroxidation: the cytotoxic potential of superoxide and nitric oxide. *Arch. Biochem. Biophys.*, **288**, 481–487.

RETTORI, V., GIMENO, M., LYSON, K. & MCCANN, S.M. (1992). Nitric oxide mediates norepinephrine-induced prostaglandin E_2 release from the hypothalamus. *Proc. Natl. Acad. Sci. U.S.A.*, **89**, 11543–11546.

RUBBO, H., RADI, R., TRUJILLO, M., TELLERI, R., KALYANARAMAN, B., BARNES, S., KIRK, M. & FREEMAN, B.A. (1994). Nitric oxide regulation of superoxide and peroxynitrite-dependent lipid peroxidation. *J. Biol. Chem.*, **269**, 26066–26075.

SALVEMINI, D., MANNING, P.T., ZWEIFEL, B.S., SEIBERT, K., CONNOR, J., CURRIE, M.G., NEEDLEMAN, P. & MASFERRER, J.L. (1995a). Dual inhibition of nitric oxide and prostaglandin production contributes to the antiinflammatory properties of nitric oxide synthase inhibitors. *J. Clin. Invest.*, **96**, 301–308.

SALVEMINI, D., MISKO, T.P., SEIBERT, K., MASFERRER, J.L., CURRIE, M.G. & NEEDLEMAN, P. (1993). Nitric oxide activates cyclooxygenase enzymes. *Proc. Natl. Acad. Sci. U.S.A.*, **90**, 7240–7244.

SALVEMINI, D., SEIBERT, K., MASFERRER, J.L., MISKO, T.P., CURRIE, M.G. & NEEDLEMAN, P. (1994). Endogenous nitric oxide enhances prostaglandin production in a model of renal inflammation. *J. Clin. Invest.*, **93**, 1940–1947.

SALVEMINI, D., SETTLE, S.L., MASFERRER, J.L., SEIBERT, K., CURRIE, M.G. & NEEDLEMAN, P. (1995b). Regulation of prostaglandin production by nitric oxide; an in vivo analysis. *Br. J. Pharmacol.*, **114**, 1171–1178.

SAUTEBIN, L. & DI ROSA, M. (1994). Nitric oxide modulates prostacyclin biosynthesis in the lung of endotoxin-treated rats. *Eur. J. Pharmacol.*, **262**, 193–196.

SAUTEBIN, L., IALENTI, A., IANARO, A. & DI ROSA, M. (1995). Modulation by nitric oxide of prostaglandin biosynthesis in the rat. *Br. J. Pharmacol.*, **114**, 323–328.

SIEBERT, K., ZHANG, Y., LEAHY, K., HAUSER, S., MASFERRER, J., PERKINS, W., LEE, L. & ISAKSON, P. (1994). Pharmacological and biochemical demonstration of the role of cyclooxygenase 2 in inflammation and pain. *Proc. Natl. Acad. Sci. U.S.A.*, **91**, 12013–12017.

SCHRAUFSTATTER, I.U., HYSLOP, P.A., JACKSON, J. & COCHRANE, C.C. (1987). Oxidant injury of cells. *Int. J. Tissue React.*, **9**, 317–324.

VINEGAR, R., SCHREIBER, W. & HUGO, R. (1969). Biphasic development of carrageenan edema in rats. *J. Pharmacol. Exp. Ther.*, **166**, 96–103.

VINEGAR, R., MACKLIN, A.W., TRUAX, J.F. & SELPH, J.L. (1971). Histopathological and pharmacological study of carrageenin inflammation in the rat. *Pharmacologist.*, **13**, 284–290.

WARREN, J.B., COUGHLAN, M.L. & WILLIAMS, T.J. (1992). Endotoxin-induced vasodilation in anaesthetized rat skin involves nitric oxide and prostaglandin synthesis. *Br. J. Pharmacol.*, **106**, 953–957.

WARREN, J.S., YABROFF, K.R., MANDEL, D.M., JOHNSON, K.J. & WARD, P.A. (1990). Role of O_2^- in neutrophil recruitment into sites of dermal and pulmonary vasculitis. *Free Rad. Biol. Med.*, **8**, 163–172.

WU, C.C., CHEN, S.J., SZABO, C., THIEMERMANN, C. & VANE, J.R. (1995). Aminoguanidine attenuates the delayed circulatory failure and improves survival in rodent models of endotoxic shock. *Br. J. Pharmacol.*, **114**, 1666–1672.

(Received January 2, 1996
Revised February 1, 1996
Accepted March 1, 1996)

EXHIBIT D

WRITTEN OPINION OF THE INTERNATIONAL SEARCHING AUTHORITY

International application No.
PCT/JP2004/017887

Box No. V Reasoned statement under Rule 43bis.1(a)(i) with regard to novelty, inventive step or industrial applicability; citations and explanations supporting such statement

1. Statement

Novelty (N)	Claims	5-7	YES
	Claims	1-4	NO
Inventive step (IS)	Claims		YES
	Claims	1-7	NO
Industrial applicability (IA)	Claims	1-7	YES
	Claims		NO

2. Citations and explanations:

Document 1. JP, 64-13019, A (Tsumura Juntendo Co., Ltd.), 17 January, 1989 (17.01.89), Patent claims, working example 12)

Document 1 cited in the ISR describes a compound expressed in formula I, which is an active ingredient of a aldose reductase inhibitor, and the compound described in working example 12 as a concrete example is a reduction of the double bond of the compound expressed in formula (9) above and corresponds to the derivative of the compound expressed in formula (9). And formula (I) includes the compound expressed in formula (9) described in claim 1, and a compound where the portions x, y of the compound of working example 12 were joined, in other words, double-bonded, is also considered to be equal to being described.
Therefore, the inventions of claims 1-4 do not appear to be novel or to involve an inventive step in view of document 1.

And letting food, beverages or a feed contain the above aldose reductase inhibitor of document 1 is also something that a person skilled in the art could easily do.
Therefore, the inventions of claims 5-7 do not appear to involve an inventive step in view of document 1.